Louisiana Tech University
Louisiana Tech Digital Commons

Doctoral Dissertations | Graduate School

Spring 2002

A new long -term design model for rehabilitation pipe liners

Shanyun Wang

Follow this and additional works at: https://digitalcommons.latech.edu/dissertations

 Part of the Civil Engineering Commons

INFORMATION TO USERS

This manuscript has been reproduced from the microfilm master. UMI films the text directly from the original or copy submitted. Thus, some thesis and dissertation copies are in typewriter face, while others may be from any type of computer printer.

The quality of this reproduction is dependent upon the quality of the copy submitted. Broken or indistinct print, colored or poor quality illustrations and photographs, print bleedthrough, substandard margins, and improper alignment can adversely affect reproduction.

In the unlikely event that the author did not send UMI a complete manuscript and there are missing pages, these will be noted. Also, if unauthorized copyright material had to be removed, a note will indicate the deletion.

Oversize materials (e.g., maps, drawings, charts) are reproduced by sectioning the original, beginning at the upper left-hand corner and continuing from left to right in equal sections with small overlaps.

Photographs included in the original manuscript have been reproduced xerographically in this copy. Higher quality 6" x 9" black and white photographic prints are available for any photographs or illustrations appearing in this copy for an additional charge. Contact UMI directly to order.

ProQuest Information and Learning
300 North Zeeb Road, Ann Arbor, MI 48106-1346 USA
800-521-0600

UMI®

Reproduced with permission of the copyright owner. Further reproduction prohibited without permission.

Reproduced with permission of the copyright owner. Further reproduction prohibited without permission.

NOTE TO USERS

This reproduction is the best copy available.

UMI®

Reproduced with permission of the copyright owner. Further reproduction prohibited without permission.

Reproduced with permission of the copyright owner. Further reproduction prohibited without permission.

A NEW LONG-TERM DESIGN MODEL FOR REHABILITATION PIPE LINERS

by

Shanyun Wang, M.S.

A Dissertation Presented in Partial Fulfillment
of the Requirements for the Degree
Doctor of Philosophy

COLLEGE OF ENGINEERING AND SCIENCE
LOUISIANA TECH UNIVERSITY

March 2002

Reproduced with permission of the copyright owner. Further reproduction prohibited without permission.

UMI Number: 3036908

UMI®

UMI Microform 3036908
Copyright 2002 by ProQuest Information and Learning Company.
All rights reserved. This microform edition is protected against
unauthorized copying under Title 17, United States Code.

ProQuest Information and Learning Company
300 North Zeeb Road
P.O. Box 1346
Ann Arbor, MI 48106-1346

Reproduced with permission of the copyright owner. Further reproduction prohibited without permission.

LOUISIANA TECH UNIVERSITY

THE GRADUATE SCHOOL

February 21,2002
Date

We hereby recommend that the dissertation prepared under our supervision by Shanyun Wang entitled A New Long-term Design Model for Rehabilitation Pipe Liners be accepted in partial fulfillment of the requirements for the Degree of Doctor of Philosophy

Supervisor of Dissertation Research

Head of Department
Computational Analysis and Modeling
Department

Recommendation concurred in:

Advisory Committee

Approved:
Director of Graduate Studies

Approved:
Dean of the Graduate School

Dean of the College

GS Form 13
(1/00)

Reproduced with permission of the copyright owner. Further reproduction prohibited without permission.

ABSTRACT

Thin-walled plastic pipe liners are routinely used to rehabilitate structurally sound host pipes that have lost their hydraulic integrity. Such liners are often installed below the water table and are consequently subjected to external hydrostatic pressure which may lead to creep-induced radial deflections and eventual collapse of the liner within the host pipe. Most of the current liner design model is based on the extension of short-term model to a long-term buckling liner design method. The objective of this thesis is to examine and provide a correction factor C^* to allow short-term liner buckling models to be more accurately used in the prediction of long-term liner lifetime.

The long-term liner buckling models considered in this research include ASTM F1216, simple power law models, and models given by Li, Cohen, Straughan, Falter, and Zhao. And ASTM, Straughan, Falter and McAlpine's model are very similar. They all include the coefficient a and exponent m which account for the influence of host-pipe constrain and imperfections. The comparison between those design models and experimental data sets in Trenchless Technology Center had been performed by the author in 1999. In this research a new design model which considered the C^* as a function of linear and quadratic combinations of liner geometry, material properties, ground water pressure and a correction factor C^* will be presented. A simplified design approach which only considers the effect of creep constants and ground water pressure will also be presented in this research. These models are show good agreement to the

Reproduced with permission of the copyright owner. Further reproduction prohibited without permission.

experimental data and finite analysis results. In general, the C^* value was seen to be almost greater than 1.0, with C^* equal to 1.3 for a polyester material tested at the TTC when a 50 years is desired. And the simplify design model is proposed as a new design model for tight fitting sewer rehabilitation liners. The ASTM model design approach, which uses ½ of elastic modulus, is not a good design methodology in the liner design.

Reproduced with permission of the copyright owner. Further reproduction prohibited without permission.

TABLE OF CONTENTS

ABSTRACT iii
LIST OF TABLES viii
LIST OF FIGURES xi
ACKNOWLEDGMENTS xiv

CHAPTER 1. INTRODUCTION 1
1.1 Background and Research Need 2
1.2 Objectives and Scope 5

CHAPTER 2. LITERATURE REVIEW 7
2.1 Encased Buckling Theory of Free Rings 7
2.2 Elastic Buckling of Constrained Pipe Liners 9
2.3.1 Theory of Encased Ring Buckling 9
2.3.2 Modes for Encased Ring Buckling 15
2.3 Creep Behavior of Plastic Materials 17
2.4 Long-term Liner Buckling Models 20
2.4.1 Extension of Elastic Buckling Models Using a Creep Modulus 20
2.4.2 ASTM F1216 21
2.4.3 Power Law Model 23
2.4.4 Cohen and Arends Models 23
2.4.5 Straughan Model 24
2.4.6 Zhao's Model 25
2.4.7 Falter's Design Model 25
2.4.8 McAlpine's Design Model 28
2.5 Liner Buckling Experiments 29

CHAPTER 3. STATISTICAL ANALYSIS AND THEORY 32
3.1 Introduction 32
3.2 Statistical Approach 32
3.2.1 The method of Least Squares 36
3.2.2 Models and Factorial Effects 39
3.2.3 Estimation of Paramenters 40
3.3 The SAS Program and Sample Input File 41

CHAPTER 4. PROPOSED LINER DESIGN MODEL 44
4.1 Introduction 44
4.2 Extension of Short-term Models to Predict Long-term Response 44
4.2.1 ASTM F1216 45

Reproduced with permission of the copyright owner. Further reproduction prohibited without permission.

4.2.2 Straughan's Model....45
4.2.3 Falter's Model....46
4.2.4 McAlpine's Design Model....46
4.2.5 Summary of Model Comparison....47
4.3 Discussion of Other Long-term Models....48
4.4 Proposed Long-term Model....48
4.5 Importance of C^*....49

CHAPTER 5. FINITE ELEMENT MODELING FOR CONSTRINAED LINER BUCKLING....52
5.1 Introduction....52
5.2 Assumptions....52
5.2.1 Loading Condition....52
5.2.2 Material Properties....53
5.2.3 2-D Configuration....54
5.3 The FEA Model....54
5.3.1 Definition of Geometric Parameters....54
5.3.2 Constrained from the Host Pipe....56
5.3.3 Model Setups....57
5.3.4 Solution Procedures....57
5.4 Verification of Finite Element Model....58
5.4.1 Mesh Refinement....58
5.4.1 Verification of Finite Element Results....60

CHAPTER 6. FINITE ELEMENT RESULTS....62
6.1 Matrix of FEA Runs....62
6.2 Influence of Parameters on Buckling Time....63
6.2.1 Influence of DR....63
6.2.2 Influence of Gap....64
6.2.3 Influence of Ovality....64
6.2.4 Influence of Creep Constants....66
6.2.5 Influence of Ground Water Pressure....67

CHAPTER 7. DETERMINATION OF C* USING STATISTICAL METHODS....69
7.1 Statistical Modeling....70
7.1.1 C^* as a Function of A, n, Gap, Ovality, PR and DR....70
7.1.2 Simplification by Assuming C^* is a Quadratic Function of PR....70
7.1.3 Determination of Non-negligible Treatment Combinations....71
7.2 Formulation of the Long-term Model....74
7.3 Comparison of the Model with FEA Results....77

Reproduced with permission of the copyright owner. Further reproduction prohibited without permission.

CHAPTER 8. SIMPLIFCATION OF THE LONG-TERM DESIGN MODEL 79
8.1 Introduction 79
8.2 Examination of the Influence of Geometrical Parameters on C^* 79
8.3 Simplified Design Model 84
8.4 Comparison of the Simply Model with FEA Results 87

CHAPTER 9. EVALUATION OF THE DESIGN MODEL 89
9.1 Comparison with the Experimental Data 89
9.2 Comparison with Other Models 91
9.3 Discussion of the Proposed (Simplified) Model 92

CHAPTER 10. CONCLUSIONS AND RECOMMENDATIONS 96
10.1 Conclusion 96
10.2 Recommendations 98

APPENDIX A FINITE ELEMENT RESULTS 100

APPENDIX B C^* VALUES BASED ON THE FINITE ELEMENT RESULTS IN APPENDIX A 111

APPENDIX C LISTING OF y_0, y_1, AND y_2 VALUES CORRESPONDING TO APPENDIX B 121

APPENDIX D PORTION OF SAS INPUT DATA 131

APPENDIX E SAS PROGRAM 135

APPENDIX F MATERIAL PROPERTIES AND LINER BUCKLING EXPERIMENT RESULTS 143

APPENDIX G ABAQUS INPUT FILE 147

APPENDIX H MATHCAD IMPLEMENTATION OF THE DESIGN MODEL 150

REFERENCES 157

Reproduced with permission of the copyright owner. Further reproduction prohibited without permission.

LIST OF TABLES

Table		Page
2.1	Buckling Equation Parameters	13
2.2	Coefficients for Constant a (Zhu, 2000)	13
2.3	Coefficients for Constant m (Zhu, 2000)	14
3.1	Analysis of Variance for a 3^k Design	34
3.2	ANOVA Table	38
3.3	Coefficient C_i for Three-level Orthoginal Polynomial Trend Contrasts	41
4.1	Long-term Buckling Model Equation Parameters	47
5.1	Relative Change in Buckling Pressure as a Function of the Number of Elements	59
5.2	Buckling Pressure in psi for One-lobe Models with 4 and 8 layers of Elements	59
5.3	Relative Change in Buckling Time for Different Numbers of Elements	60
5.4	Comparison of Buckling Times in hours using the FEA Model Employed in this Thesis and the Model Used by Zhao(1999)	61
7.1a	Coefficient Used to Computer *D0*	75
7.1b	Coefficient Used to Computer *D1*	75
7.1c	Coefficient Used to Computer *D2*	75
7.1d	Coefficient Used to Computer *B0*	76
7.1e	Coefficient Used to Computer *B1*	76

Reproduced with permission of the copyright owner. Further reproduction prohibited without permission.

7.1f Coefficient Used to Computer *B2* 76

7.1g Coefficient Used to Computer *E0*..... 76

7.1h Coefficient Used to Computer *E1*..... 76

7.1i Coefficient Used to Computer *E2*..... 76

7.2 Comparison of the Results of the Model with the FEA Results..... 78

8.1 SigmaPlot Regression Results for the Lower Bound Model..... 85

8.2 Coefficient Used to Determine y_0 86

8.3 Coefficient Used to Determine y_1..... 86

8.4 Comparison of the Results of the Simplified Model with the FEA Results 89

9.1 Comparison of DR Values Computed Using Various Pressures for Time=438,000 hrs(50 years), Gap=0.4%, Ovality=3%, 0.5A (6.05e-8$psi^{-1}hr^{-n}$) and 0.75 n (0.18)..... 94

9.2 Comparison of DR Values Computed Using Various A Values for Time=438,000 hrs(50 years), Gap=0.4%, Ovality=3%, Pg = 15 psi and 1n (0.24)..... 95

9.3 Comparison of DR Values Computed Using Various n Values for Time=438,000 hrs(50 years), Gap=0.4%, Ovality=3%, Pg = 15 psi and 1A (1.21e-7$psi^{-1}hr^{-n}$)..... 95

9.4a Matrix of Creep Parameters 95

9.4b C^* for a 50 Years Life for the Material Combinations in Table 9.4a..... 95

A.1 FEA Results for Material Properties A=1.21e-7($psi^{-1}hr^{-n}$), n=0.24..... 101

A.2 FEA Results for Material Properties A=1.21e-7($psi^{-1}hr^{-n}$), n=0.36..... 102

A.3 FEA Results for Material Properties A=1.21e-7($psi^{-1}hr^{-n}$), n=0.12 103

Reproduced with permission of the copyright owner. Further reproduction prohibited without permission.

A.4 FEA Results for Material Properties A=1.21e-8($psi^{-1}hr^{-n}$), n=0.24 104

A.5 FEA Results for Material Properties A=1.21e-8($psi^{-1}hr^{-n}$), n=0.36 105

A.6 FEA Results for Material Properties A=1.21e-8($psi^{-1}hr^{-n}$), n=0.12 106

A.7 FEA Results for Material Properties A=1.21e-6($psi^{-1}hr^{-n}$), n=0.24 107

A.8 FEA Results for Material Properties A=1.21e-6($psi^{-1}hr^{-n}$), n=0.36 108

A.9 FEA Results for Material Properties A=1.21e-6($psi^{-1}hr^{-n}$), n=0.12 109

A.10 FEA Results for Ovality= 6%, Gap = 0.1%, DR= 70 110

B.1 C^* Values for Material Properties A=1.21e-7($psi^{-1}hr^{-n}$), n=0.24 112

B.2 C^* Values for Material Properties A=1.21e-7($psi^{-1}hr^{-n}$), n=0.36 113

B.3 C^* Values for Material Properties A=1.21e-7($psi^{-1}hr^{-n}$), n=0.12 114

B.4 C^* Values for Material Properties A=1.21e-8($psi^{-1}hr^{-n}$), n=0.24 115

B.5 C^* Values for Material Properties A=1.21e-8($psi^{-1}hr^{-n}$), n=0.36 116

B.6 C^* Values for Material Properties A=1.21e-8($psi^{-1}hr^{-n}$), n=0.12 117

B.7 C^* Values for Material Properties A=1.21e-6($psi^{-1}hr^{-n}$), n=0.24 118

B.8 C^* Values for Material Properties A=1.21e-6($psi^{-1}hr^{-n}$), n=0.36 119

B.9 C^* Values for Material Properties A=1.21e-6($psi^{-1}hr^{-n}$), n=0.12 120

Reproduced with permission of the copyright owner. Further reproduction prohibited without permission.

C.1 Values of y_0 for A=1.21e-8 ($psi^{-1}hr^{-n}$), and Three Levels of n 122

C.2 Values of y_0 for A=1.21e-7($psi^{-1}hr^{-n}$), and Three Levels of n 123

C.3 Values of y_0 for A=1.21e-6 ($psi^{-1}hr^{-n}$), and Three Levels of n 124

C.4 Values of y_1 for A=1.21e-8 ($psi^{-1}hr^{-n}$), and Three Levels of n 125

C.5 Values of y_1 for A=1.21e-7 ($psi^{-1}hr^{-n}$), and Three Levels of n..... 126

C.6 Values of y_1 for A=1.21e-6 ($psi^{-1}hr^{-n}$), and Three Levels of n 127

C.7 Values of y_2 for A=1.21e-8 ($psi^{-1}hr^{-n}$), and Three Levels of n..... 128

C.8 Values of y_2 for A=1.21e-7 ($psi^{-1}hr^{-n}$), and Three Levels of n 129

C.9 Values of y_2 for A=1.21e-6 ($psi^{-1}hr^{-n}$), and Three Levels of n 130

D.1 Portion of SAS Factorial Input Data Set for y_0 132

D.2 Portion of SAS Factorial Input Data Set for y_1..... 133

D.3 Portion of SAS Factorial Input Data Set for y_2 134

F.1 Creep Properties of Various Polymers..... 144

F.2 Material Properties for the Insituform Enhanced Product (Lin, 1994)..... 144

F.3 Long-term Buckling Test Results for the Insituform Enhanced Product (Guice et. al, 1994) 145

Reproduced with permission of the copyright owner. Further reproduction prohibited without permission.

LIST OF FIGURES

Figure		Page
1.1	Typical Deformation Mode of a Cracked Pipe	3
1.2	Pressure Verse Deflection Curve for an Unconstrained Pipe (Zhao, 1999)	3
2.1	Free Standing Pipe Buckling Mode (Zhao, 1999)	8
2.2	Glock's Predefined One Lobe Deflection Pattern	11
2.3	(a)Elliptically Shaped (b) Egg Shaped, and (c) Horseshoe Shaped Host Pipe	15
2.4	Typical Buckling Modes.	15
2.5	Steps in Non-liner Hydrostatic Buckling of Encased Circular Liner Pipe(Gumbel, 2001)	17
2.6	Data and Fit of Lin's (1995) Data	20
2.7	Reduction Factor K_v for Liners with Initial Deformations	27
2.8	Reduction Factor K_s for Initial Gap Between Host Pipe and Liner	28
2.9	Hydraulic System Used for Long-term Testing in TTC	31
3.1	The Short-term SAS Factorial Analysis Input File	42
5.1	Schematic Which Defines the Ovality and Gap Parameters	55
5.2	A One-lobe FEA Model Which Employs Half-symmetry	57
5.3	A Portion of the 1280 Element Results Showing the CPE4 Elements	60
6.1	Effect of DR on Critical Time as a Function of Pressure	64

Reproduced with permission of the copyright owner. Further reproduction prohibited without permission.

6.2 Effect of Gap on Critical Time as a Function of Pressure 65

6.3 Effect of Ovality on Critical Time as a Function of Pressure.....65

6.4 Effect of n on Critical Time as a Function of Pressure 66

6.5 Effect of A on Critical Time as a Function of Pressure.....67

6.6 Effect of PR on Critical Time as a Function of Pressure 68

7.1 Sigmaplot Regression Output for A=1.21e-7($psi^{-1}hr^{-n}$), n =0.24, DR=30, Ovality=0.0%, Gap=0.1.....73

8.1 Graph of C^* Verse PR for Each Combination of A and n (the Results of 81 FEA Runs are Plotted on Each Graph).....84

8.2 C^* Verse PR for A = 1.21e-7 ($psi^{-1}hr^{-n}$), and n =0.24 with a Liner Fit to the Lower Data Points Shown 88

9.1 Comparison of Long-term Models with Experimental Data.....90

F.1 Strain Verse Time for the Material in Table F.1 and for the Extreme Values of A and n Simulated in the Finite Element Analysis.....146

H.1 MathCAD Implementation of the Long-term Liner Design Models for DR 154

H.2 MathCAD Implementation of the Simplify Long-term Liner Design Model for DR 155

H.3 MathCAD Implementation of the Long-term Liner Design Models for Buckling Time.....156

H.4 MathCAD Implementation of the Simplify Long-term Liner Design Model for Buckling Time.....156

Reproduced with permission of the copyright owner. Further reproduction prohibited without permission.

ACKNOWLEDGMENTS

I would like to express my deepest appreciation to my advisor Dr. David Hall for his advice and continuous guidance through the completion of this thesis. In particular, I express my heartfelt thanks for his unbounded patience in correcting my Chinese/English difficulties. Also, special thanks goes to my committee member Dr. Raja Nassar for his explanations of statistical theory and methods, as well as for his technical comments on my research topics. Also, special thanks to Dr. Ben Choi and Dr. Aziz Saber for their input and service on my advisory committee and for their contribution in correcting drafts of this thesis.

Thanks to Dr. Terry McConathy for her generous financial support in my last quarter study, as well as to College of Engineering and Science of Louisiana Tech University and Trenchless Technology Center for providing financial support through my study.

I also would like to thank Ms. Martha Stevens for her kindness and assistance whenever needed during my graduate study in Louisiana Tech University. This research would not have been possible without the Trenchless Technology Center and Dr. Raymond Sterling.

Further gratitude goes to Dr. Qiang Zhao, Dr. Meihuan Zhu, Mr. Jian Zhao, Mr. Hong Lin, and Mr. Wei Zhao who performed research in liner buckling before and during the time that I conducted my research. Their help was invaluable. I'd like to thank

Reproduced with permission of the copyright owner. Further reproduction prohibited without permission.

all the faculty, staff and friends I met in Louisiana Tech University for their affection and kindness during my days in Ruston.

I would also like to thank my husband, Mr. Yongge Wu, for his continual encourage, support and tolerance of my long length study in Ruston. The last but not the least thanks go to my parents, parents-in-law, grandmother, brother, and sister, whose support, encouragement and love led me to complete this thesis.

Reproduced with permission of the copyright owner. Further reproduction prohibited without permission.

CHAPTER 1

INTRODUCTION

Piping systems constructed of concrete, clay and cast iron have been in use for more than a century. Many of these systems have deteriorated significantly and are in need of repair. Rehabilitation of existing sewer-pipe systems in the United States using "trenchless" methods has become popular over the past 20 years. Trenchless methods, which replace or repair existing pipelines with little or no soil excavation, can reduce damage to existing services and structures, disruption of business, loss of environmental quality, traffic delays and damage to other facilities. Trenchless methods are especially attractive for pipelines located in congested areas.

One method of trenchless repair involves insertion of a tight fitting, polymeric liner into a deteriorated host pipe. Insertion of this liner stops the infiltration of groundwater into the sewer system and stabilizes the soil around the host pipe. Although there are clear advantages of using such liners, the lack of accurate structural design equations to size these liners based on the external groundwater pressure has in some cases impeded the acceptance of this technique. Finding appropriate design equations for tight fit pipe liners which could produce safe and economical designs is a challenging problem that has received the attention of those in both industry and academia.

Reproduced with permission of the copyright owner. Further reproduction prohibited without permission.

1.1 Background and Research Need

The structural deterioration of an underground infrastructure system such as a pipeline consists of two typical situations. The damaged pipeline is either partially deteriorated (structurally safe) and can carry the soil and surcharge loads for a considerable time, or it is fully deteriorated and unable to support the soil load above it. Most of the time the damaged pipelines are structurally safe, but with passing time the soil pressure and/or the removal of soil around the pipe by infiltration into the pipe can lead to pipe collapse. This research focuses on partially deteriorated host pipes.

The loads to which a buried pipe is subjected are mainly soil, traffic, and external groundwater pressure. The traffic and related loads (mainly carried by the original pipe) act on the pipe through interaction with the soil. When a rigid sewer pipe is subjected to excessive vertical force caused by ground and traffic loading, it is likely to crack, as shown in Figure 1.1. If the deformation of a rigid pipe exceeds 10% of the vertical diameter, it is customary to replace the pipe. For deformations less than 10%, rehabilitation is an attractive option. For rehabilitation applications, the only active load applied to the pipe liner is the hydrostatic pressure induced by the underground water that infiltrates through the cracks in the host pipe.

It is well known that thin-walled structural elements are susceptible to instability (or buckling) when they are exposed to in-plane compressive stresses. Since the external groundwater pressure induces a compressive hoop stress in the wall of the liner, a liner that has been incorrectly sized (is too thin) may buckle within the host pipe before the expected service life is exhausted. A typical load-deflection curve is shown is Figure 1.2.

Reproduced with permission of the copyright owner. Further reproduction prohibited without permission.

Notice that a small increase in loading causes a large increase in deflection as the buckling pressure is approached.

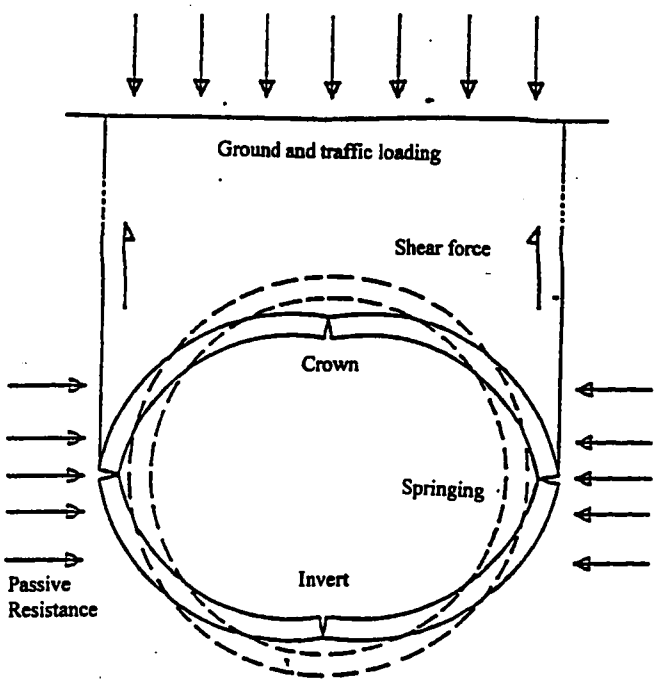

Figure 1.1 Typical Deformation Mode of a Cracked Pipe

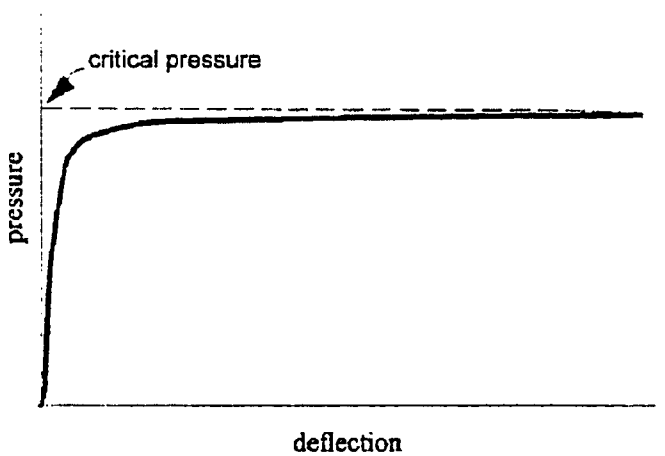

Figure 1.2 Pressure Versus Deflection Curve for an Unconstrained Pipe (Zhao, 1999)

Reproduced with permission of the copyright owner. Further reproduction prohibited without permission.

For long-term design applications, the liner must be able to withstand the groundwater pressure for the desired design life. Although the liner may not buckle immediatly after it is installed, the groundwater pressure will cause the polymeric liner material to slowly deform over time. If these accumulated deformations become too great, the liner will collapse. Thus, the time-dependent creep deformation of the liner should be accounted for during the design process.

The current design equations (ATSM F1216-93) used for the buckling pressure of constrained liners are based on Timoshenko's model for short-term buckling of an unconstrained ring (Timoshenko and Gere, 1961). The unconstrained ring model has been modified by a factor (termed the "enhancement factor") that accounts for the deviation between experimental results for constrained liners and the theory for unconstrained rings. The effect of creep deforation is accounted for using a long-term modulus in place of the short-term elastic modulus. The long-term modulus is typically taken as ½ of the short-term flexural modulus. Thus, short-term and not long-term material properties are currently used to design pipeline rehabilitation liners. Clearly, liner design should be based on both the short-term AND the long-term properties of the liner material since the primary cause of failue is accumulating creep deformation.

During the last past 10 years, the Trenchless Technology Center (TTC) at Louisiana Tech University has been actively involved in liner buckling research. The TTC has carried out a variety of experimental, computational and statistical studies to provide utility owners and designers with important information to help them in designing and specifying polymeric liner products. A significant amount of finite element analysis of short-term (linear-elastic) and long-term buckling has been completed

Reproduced with permission of the copyright owner. Further reproduction prohibited without permission.

at the TTC. Zhu (2000) extended the work of Zhao (1999) to generate a short-term model that simultaneously accounts for the effects of several geometry parameters on liner buckling. The research presented in this thesis aims to extend the work of Zhu to long-term design applications.

1.2 Objectives and Scope

The primary goal of the proposed work is to develop a long-term buckling model which is based on liner geometry parameters, the short-term elastic modulus, creep properties of the liner material, and the ground water pressure. This research will systematically isolate and quantify the influence of each of these parameters on long-term liner buckling. The objective for this research is to develop a liner buckling model that is based on the short-term as well as the long-term properties of a liner material.

To fulfill this objective, this research program is comprised the following activities:

- Conduct a literature review of the design equations used for sewer rehabilitation liner applications.
- Explore the similarity between existing liner design models.
- Use the ABAQUS finite element software to simulate the response of pipe liners subjected to long-term pressure loading for a range of geometries and material properties typical in sewer rehabilitation applications.
- Develop a new long-term liner design model based on statistical analysis of the finite element simulations. This will involve development of a factor, C^*, to

Reproduced with permission of the copyright owner. Further reproduction prohibited without permission.

quantify the influence of geometrical and material parameters on the long-term performance of liners.

- Simplify the design model discussed above to facilitate its use in design applications.
- Explore the ability of the design model to represent experimental data and to reproduce the finite element results on which the model is based.
- Compare the design model resulting from this research to models that do not provide a correction factor for long-term behavior so that the potential impact of this research may be quantified.

Reproduced with permission of the copyright owner. Further reproduction prohibited without permission.

CHAPTER 2

LITERATURE REVIEW

Tight fitting liners installed in deteriorated sewer pipes are susceptible to buckling under external ground water pressure. The relevant literature on the subject of buckling can be categorized as buckling of unconstrained liners, buckling of constrained liners, and creep induced buckling of liners. The current ASTM design guideline is based on buckling of free standing liners (Figure 2.1). This approach is generally considered to be overly conservative.

The primary concern of the present study is focused on the long-term buckling behavior of encased liners subjected to sustained pressure in which the time-dependent deformation of the polymeric materials is the main reason for the final collapse. This chapter is intended to present the fundamental buckling theories for thin-walled cylinders encased in rigid cavities, the behavior of liner materials, and the relevant experiment work that is available in the literature.

2.1 Elastic Buckling Theory of Free Rings

Research on the elastic stability of free circular and cylindrical tubes began as far back as 1858. Fairbarn's research (Fairbarn, 1858) on cylindrical tubes under external

Reproduced with permission of the copyright owner. Further reproduction prohibited without permission.

pressure concluded that the length of the pipe and the ratio of diameter-to-wall thickness of the pipe were important parameters in establishing the external buckling pressure.

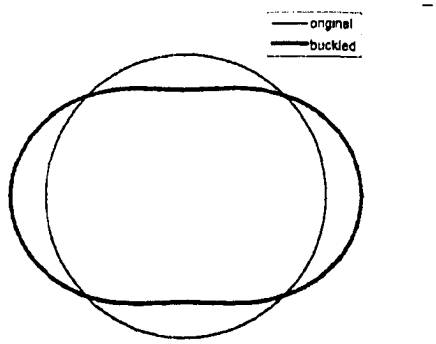

Figure 2.1 Free Standing Pipe Buckling Mode (Zhao, 1999)

Bryan (1884) derived the critical external pressure P_{cr} that can be applied hydrostatically on a thin ring. The critical external pressure P_{cr} can be expressed as follows:

$$P_{cr} = \frac{3EI}{r^3} \tag{2-1}$$

In 1888, G.H. Bryan analyzed an infinitely long pipe under external pressure through the minimum potential energy criterion of stability. When the moment of inertia $I = t^3/12$, an equivalent equation for long pipes can be written as

$$P_{cr} = \frac{2E}{1-\nu^2} \times (\frac{t}{D})^3 \tag{2-2}$$

where D is the mean diameter of the pipe, t is the thickness, and ν is Poisson's ratio.

If Equation (2-2) is modified to use the dimension ratio SDR (frequently used by the industry to describe the pipe thickness), this equation can be written as:

$$P_{cr} = \frac{2E}{1-\nu^2} \times \frac{1}{(SDR-1)^3} \tag{2-3}$$

Reproduced with permission of the copyright owner. Further reproduction prohibited without permission.

where SDR is the Standard Dimension Ratio which is defined as the outside pipe diameter divided by the mean pipe wall thickness of the pipe.

Equation (2-3) was summarized by Timoshenko and Gere in *Theory of Elastic Stability* (1961) and has been used widely as a basis for the design of underground pipes. This expression has been adopted in the U.S. as a basis for CIPP design. However, this equation is based on the buckling phenomenon of a free ring without outside constraint. It neglects the existence of the host pipe as a rigid constraint which confines the liner and significantly inhibits its buckling.

2.2 Elastic Buckling of Constrained Pipe Liners

The tight fit liner buckling problem is often idealized by considering the response of a thin ring encased in a rigid host pipe. For thin rings, the primary failure mode is buckling, which is related to the geometry of a structure and the modulus of elasticity of a material. The prevention of buckling of a liner under external hydrostatic pressure is one of the primary criteria typically used in the design of these liners.

2.2.1 Theory of Encased Ring Buckling

Amstutz (1969) stated that under practical conditions the plastic behavior of steel would cause liner failure at a lower load than that needed to cause elastic snap-through buckling. Chicurel (1968) dealt with a "shrink buckling" phenomenon which he described as follows: "If a thin elastic circular ring is compressed by being inserted into an opening of a smaller diameter than the outside diameter of the free ring, the ring may be collapsed inwardly over a small arc." The shrink buckling phenomenon is not the same as the buckling phenomenon of a pipe liner because shrink buckling is caused by

Reproduced with permission of the copyright owner. Further reproduction prohibited without permission.

hoop compression, while the buckling of a CIPP liners is due to external uniform pressure. When a thin ring buckles, the hoop compressive force will disappear immediately in the case of shrink buckling, whereas the external uniform pressure in the other case will continue to act on the ring as it deforms during buckling. This "post-buckling" behavior can be important in understanding CIPP behavior.

Cheney (1971) used small-deflection theory to study the stability of a circular ring encased in a rigid cavity under the effect of external uniform pressure. The constraint effect from the surrounding soil was modeled as an elastic support with a modulus expressed as a function of the physical parameters of the soil.

Glock (1977), who gave the first theoretically sound model for the constrained liner buckling, also adopted the one-lobe deformation mode which was widely accepted at his time by researchers of liners and of buried pipes. In his analysis, the radial deflection for the buckled portion was assumed to have the functional form

$$u = u_0 \cdot \cos^2\left(\frac{\pi \cdot \theta}{2 \cdot \phi}\right) \tag{2-4}$$

in which 2ϕ represented the deflected region (Figure 2.2). By using a non-linear deformation theory and the principle of minimum potential energy, Glock developed a similar form to Timoshenko's equation

$$P_{cr} = \frac{E}{1-\nu^2} \cdot \left(\frac{t}{D}\right)^{2.2} \tag{2-5}$$

This model does not take into consideration any initial imperfections of the liner wall, does not account for gap between the liner and its host pipe, and is applies to a perfectly circular host pipe (does not account for ovality). Consequently, it may overestimate the buckling resistance of imperfect liners.

Reproduced with permission of the copyright owner. Further reproduction prohibited without permission.

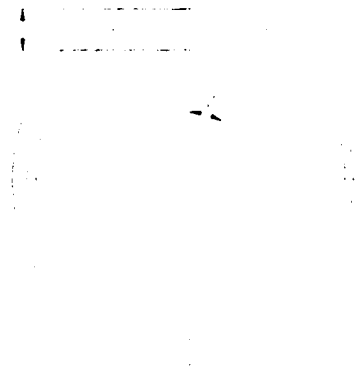

Figure 2.2 Glock's Predefined One Lobe Deflection Pattern

Boot(1998) extended the range of the application of Glock's analysis for the elastic buckling of rigidly constrained pipe linings subject to annular pressure to cover systems incorporating symmetrical (two-lobe) and asymmetrical annular (one-lobe) (Figure 2.4) gaps between liners and their host pipes. Boot's solution is for a plane stress condition. In his paper "Elastic buckling of cylindrical pipe linings with small imperfections subject to external pressure," the equation for geometrically imperfect single lobe buckling is as follows:

$$\frac{P_{cr}}{E} = (\frac{D}{t})^{-2.2} \tag{2-6}$$

The corresponding equation for a tight fitting liner (no gap and imperfect two lobe buckling) is

$$\frac{P_{cr}}{E} = 1.323(\frac{D}{t})^{-2.2} \tag{2-7}$$

Moore (1989) used single-wave theories (one-lobe) to examine the buckling of a ring encased in a rigid cavity. The critical pressure value is given as:

Reproduced with permission of the copyright owner. Further reproduction prohibited without permission.

$$P_{cr} = 2.5 \cdot (\frac{t}{D})^{2.2} \cdot E \tag{2-8}$$

Equation (2-8) also can be expressed as

$$P_{cr} = \frac{2.275E}{1-\nu^2}(\frac{1}{SDR-1)^{2.2}}$$

After the analysis of experimental buckling pressure data obtained by Aggarwal and Cooper (1984), Lo et al. (1993), Guice et al. (1994), and Omara et al. (1997) suggested that the critical pressure of a constrained liner can be expressed as

$$P_{cr} = \frac{aE}{(1-\nu^2)(SDR-1)^m} \tag{2-9}$$

where a is a coefficient and m is an exponent that varies depending on the liner geometry or model assumptions. These coefficients and exponents for each model (Timosenko, Chicurel, Cheney, Moore and Glock) are summarized in Table 2.1. It should be noted that there are consistencies in the exponents for the different models. Models which impose a constraint around the liner surface use solutions with an exponent of 2.2. However, the coefficients can vary significantly depend upon the types of assumptions made. To accurately predict these coefficients and exponents, Zhao (1999) and Zhu (2000) determined the constants for a and m based on 81 series of finite element runs to develop a model that could simultaneously account for mean liner diameter to thickness ratio DR, the gap between a liner and its host pipe, the host pipe ovality and the local imperfection on the buckling pressure. Their expression is identical to Equation (2-9) except that it is based on DR, not on SDR:

$$P_{cr} = \frac{aE}{(1-\nu^2)(DR-1)^m} \tag{2-10}$$

Reproduced with permission of the copyright owner. Further reproduction prohibited without permission.

The coefficient a as a function of gap, ovality, and longitudinal instruction is expressed as

$$a = b_1 + b_2x + b_3y + b_4z + b_5xy + b_6xz + b_7yz + b_8x^2 + b_9y^2 + b_{10}z^2 + b_{11}x^2y + b_{12}x^2z + b_{13}y^2x + b_{14}y^2z + b_{15}z^2x + b_{16}z^2y + b_{17}xyz + b_{18}x^2y^2 + b_{19}x^2z^2 + b_{20}y^2z^2 + b_{21}x^2yz + b_{22}y^2xz + b_{23}z^2xy + b_{24}x^2y^2z + b_{25}x^2z^2y + b_{26}y^2z^2x + b_{27}x^2y^2z^2 \quad (2\text{-}11)$$

where b_i (i = 1,..27) is given in Table 2.2. Here x = gap ratio, y = ovality, and z = longitudinal intrusion. Similarly, the exponent m is given as

$$m = c_1 + c_2x + c_3y + c_4z + c_5xy + c_6xz + c_7yz + c_8x^2 + c_9y^2 + c_{10}z^2 + c_{11}x^2y + c_{12}x^2z + c_{13}y^2x + c_{14}y^2z + c_{15}z^2x + c_{16}z^2y + c_{17}xyz + c_{18}x^2y^2 + c_{19}x^2z^2 + c_{20}y^2z^2 + c_{21}x^2yz + c_{22}y^2xz + c_{23}z^2xy + c_{24}x^2y^2z + c_{25}x^2z^2y + c_{26}y^2z^2x + c_{27}x^2y^2z^2 \quad (2\text{-}12)$$

where c_i (i = 1,..27) is given in Table 2.3. Equations (2-11) and (2-12) are only valid for $30 < DR < 70$, $0.1\% < gap < 0.7\%$, $0\% < ovality < 6\%$, and $0\% <$ longitudinal intrusion $< 2.25\%$.

Table 2.1 Buckling Equation Parameters

Model	Coefficient, *a*	Exponent, *m*
Timoshenko unconstrained	2.0	3.0
Chicurel's shrink buckling	2.76	2.2
Moore's encased ring	2.275	2.2
Cheney's encased ring	2.55	2.2
Glock's encased ring	1.0	2.2

Table 2.2 Coefficients for Constant a (Zhu, 2000)

$x^2y^2z^2$	x^2y^2z	x^2y^2	x^2z^2y	x^2yz	x^2y	x^2z^2	x^2z	x^2
-0.012498	-0.007202	-0.013519	0.0616369	0.107695	0.0433333	0.616516	-0.851605	-2.73111
xy^2z^2	xy^2z	$x\,y^2$	xyz^2	xyz	xy	xz^2	xz	X
0.0086706	-0.004621	0.0119815	0.0075684	-0.086169	-0.191778	-0.802743	0.0564691	6.49522
y^2z^2	y^2z	y^2	yz^2	yz	y	z^2	z	1
-0.004649	0.0099268	-0.00298	0.0245297	-0.095319	-0.030172	0.0286771	1.0946	1.06019

Reproduced with permission of the copyright owner. Further reproduction prohibited without permission.

Table 2.3 Coefficient for Constant m (Zhu, 2000)

$x^2y^2z^2$	x^2y^2z	x^2y^2	x^2z^2y	x^2yz	x^2y	x^2z^2	x^2z	x^2
-0.001183	0.001797	-0.002901	0.0050114	-0.000123	-0.001296	-0.021509	0.271605	-0.66
xy^2z^2	xy^2z	$x\,y^2$	xyz^2	xyz	xy	xz^2	xz	x
0.0011986	-0.003063	0.0027469	-0.002967	0.0038395	0.000537	0.03538	-0.441728	1.14667
y^2z^2	y^2z	y^2	yz^2	yz	y	z^2	z	1
-0.000474	0.0012883	-0.000673	0.0025972	-0.007398	0.0061093	-0.028409	0.255457	2.25553

Thépot (2001) extended the range of Glock's analysis for the elastic buckling of non-circular lining with annular gap. He presented an analytically based model that accounts for the effect of gap and ovality, and provides a way to move between one-lobe and two-lobe buckling modes. His method can also be used to analyze egg-shaped and horseshoe-shaped host pipes (Figure 2.3). The Glock-Thépot model is presented as:

$$P_{cr} = 0.455 \cdot E_L \cdot k^{\frac{2}{5}} \cdot \Gamma_{p,g} \cdot \frac{t^{11/5}}{P^{2/5} \cdot R^{9/5}} \tag{2-13}$$

where $\Gamma_{p,g}$ is the reduction factor of the critical pressure due to the initial gap, E_L is the long-term modulus, k=1 for one-lobe and 2 for two-lobe deformation modes, R is the average radius where the lobe is expected, p is the perimeter of the liner, and $\Gamma_{p,g}$ is the reduction factor of the critical pressure due to the initial gap. If the initial gap is equal to zero for the case of a two-lobe deformation mode, Equation (2-13) can be expressed as

$$P_{cr} = 0.6 \cdot \frac{t^{2.2}}{P^{0.4} \cdot R^{1.8}} \tag{2-14}$$

For a circular lining using R=D/2 and $P = \pi D$, Equation (2-14) can be simplified as follows:

$$P_{cr} = 1.323\left(\frac{t}{D}\right)^{2.2} \cdot E \tag{2-15}$$

Reproduced with permission of the copyright owner. Further reproduction prohibited without permission.

This formula is same as Equation (2-7). It also can be expressed as

$$P_{cr} = \frac{1.204E}{1-\nu^2} \cdot \left(\frac{1}{SDR-1}\right)^{2.2} \qquad (2\text{-}16)$$

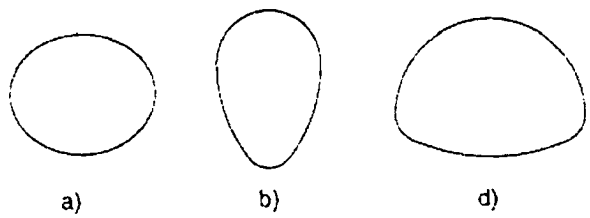

Figure 2.3 (a) Elliptically Shaped, (b) Egg Shaped, and (c) Horseshoe Shaped Host Pipes

2.2.2 Models for Encased Ring Buckling

Typically, a constrained cylindrical shell tends to deform in a symmetric two-lobe mode when the annular gap is evenly distributed along the circumference as shown in Figure 2.4a. On the other hand, if the gap is unevenly distributed, the liner occasionally deforms in an asymmetric one-lobe mode as shown in Figure 2.4b. Final collapse always tends to occur in a one-lobe mode.

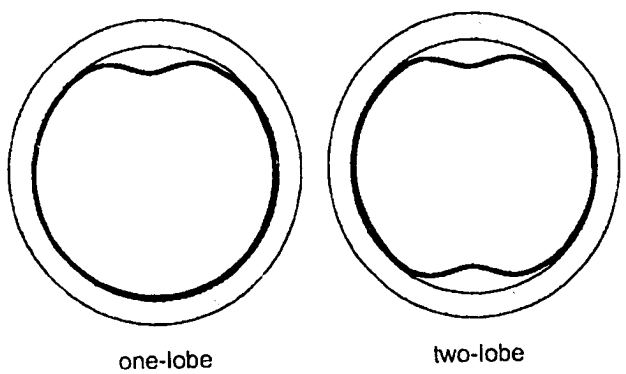

Figure 2.4 Typical Buckling Modes

Reproduced with permission of the copyright owner. Further reproduction prohibited without permission.

Previous investigations (e.g. Yamamoto & Mastubara, 1981) showed that the two-lobe model associates with higher critical pressures than one-lobe mode. Most liner buckling tests conducted at the TTC at Louisiana Tech University reveal a roughly symmetric two-lobe deflection pattern during pressurization followed by a single lobe collapse. The observed two-lobe deformation histories can be further divided into symmetrical and asymmetrical. Figure 2.5 illustrates the steps leading to buckling failure of an encased circular liner pipe subjected to external hydrostatic pressure.

Generally speaking, however, experimental results indicate that a restrained liner with an even surrounding gap will usually deform into a roughly symmetrical two-lobe shape and will contact the host pipe at diametrically opposite points and have maximum deflections at 90^{o} to these contact points. Seemann *et al.* (2000) revealed that the degree of symmetry of the lobes increases with increasing host pipe ovality. Zhao (1999) simulated the lobe transitions from two-lobe to one-lobe using the finite element method and found that the conventional one- and two-lobe buckling modes correspond to the lower and upper bound critical pressures. Hence in this research the one-lobe model is used for long-term buckling simulations.

Reproduced with permission of the copyright owner. Further reproduction prohibited without permission.

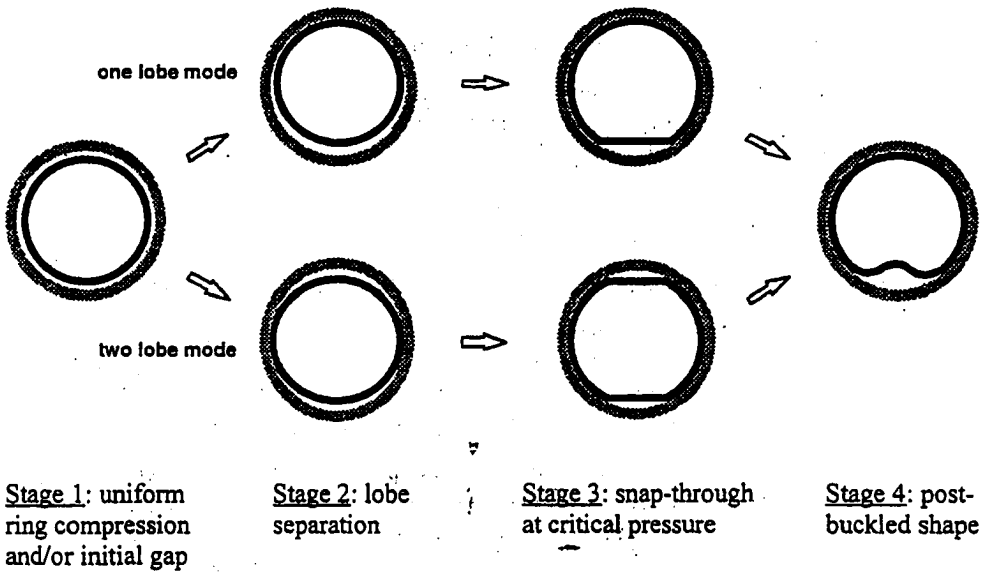

Figure 2.5 Steps in Non-linear Hydrostatic Buckling of Encased Circular Liner Pipes (Gumbel, 2001)

2.3 Creep Behavior of Plastic Materials

Plastic materials are susceptible to time-dependent deformation even when the stress is kept constant. This time-dependent deformation is also referred to as viscoelastic behavior or creep (the progressive deformation of a material under a constant load). When a plastic or reinforced plastic is held under sustained stress, its strain continues to increase with time, and the magnitude of stress needed to produce failure diminishes with time. In ASTM D2990-95, the creep modulus is described as "the ratio of initial applied stress to creep strain." The creep modulus is not a true modulus of elasticity. It is a parameter that describes the rate of movement or flow of the material over time.

The total strain is often partitioned into elastic (recoverable) and creep (permanent) parts as

$$\varepsilon^T = \varepsilon^E + \varepsilon^{CR} \tag{2-17}$$

Reproduced with permission of the copyright owner. Further reproduction prohibited without permission.

where ε^T represents the total strain, ε^E is the elastic strain, and ε^{CR} is the creep strain. The elastic strain can be expressed as

$$\varepsilon^E = \frac{\sigma}{E} \tag{2-18}$$

Much research involving creep behavior of plastics has been conducted, and many theories have been developed. Generally, the research approaches can be divided into theoretical methods and experimental methods. Theoretical methods include mechanical and physical chemistry approaches. The Maxwell creep model, Kelvin model, and combined model (Jaeger and Cook, 1976) are typical mechanical approaches. A physical chemistry approach was used by Goldfein (1960) in which the energy of action and temperature were taken into account.

As early as 1944, Findley published 2,000 hour tensile creep data for several reinforced thermosetting plastics. Since then, many investigators, including Pao and Marin (1952) and Kinney (1972), have reported the results of long-term creep tests for plastics. Those works included tensile, compressive, flexural and combined loading conditions.

Findley(1944) found that tensile creep of several reinforced thermosetting materials could be illustrated as follows:

$$\varepsilon = \varepsilon_0 + \varepsilon_t t^n \tag{2-19}$$

where

ε = total elastic plus time-dependent strain;

ε_0 = stress-dependent, time-independent initial elastic strain;

ε_t = stress-dependent, time-dependent coefficient of time-dependent strain;

Reproduced with permission of the copyright owner. Further reproduction prohibited without permission.

n = material exponent, substantially independent of stress magnitude (dimensionless);

t = time after loading (given in hours).

Although the equation was developed from tensile creep tests, it is often used to describe material behavior under compression and flexure, as well as for combined loading states (such as combined tensile and shear stress).

A number of other forms of this model exist, as outlined by Zhao (1999). A Norton type creep law (Norton, 1929) is a time-hardening formula where the strain rate is a nonlinear function of stress:

$$\varepsilon^{CR} = A\sigma^{l}t^{n} \tag{2-20}$$

The Norton model above is known as a time-hardening model, since time is explicitly given in the constitutive relation. A strain-hardening form of this expression can be written as follow

$$\tilde{\varepsilon}^{CR} = (A \cdot \sigma^{n} \cdot [(n+1)\varepsilon]^{n})^{\frac{1}{n+1}} \tag{2-21}$$

This strain-hardening form is often employed in computational analyses because it gives better results that the time hardening form.

When the exponent on stress (l) is equal to 1.0, Equation (2-20) can be expressed as

$$\varepsilon^{CR} = A\sigma t^{n} \tag{2-22}$$

Combining Equations (2-18) and (2-22), the total strain can be expressed as

$$\varepsilon = \frac{\sigma}{E} + A\sigma t^{n} \tag{2-23}$$

Reproduced with permission of the copyright owner. Further reproduction prohibited without permission.

The Norton type creep model in Equation (2-23) is used in fitting Lin's (1995) data. The fit curves and test data are shown in Figure 2.6, and the creep constants corresponding to these fits are A=1.21e-7 psi^{-1} hr^{-n} and n=0.24.

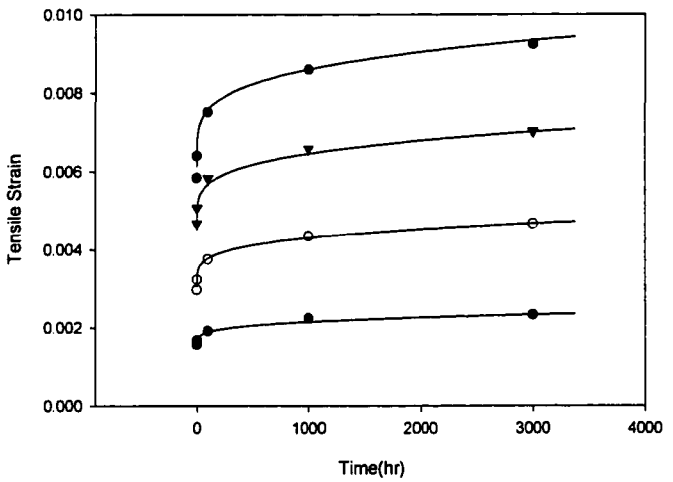

Figure 2.6 Data and Fit of Lin's (1995) Data

2.4 Long-term Liner Buckling Models

2.4.1 Extension of Elastic Buckling Models Using a Creep Modulus

The creep phenomenon applies to all polymeric pipe liners and plays an important role in liner design. In the traditional pipe buckling model (Timoshenko, Chicurel, Cheney and Glock), the creep behavior is not taken into consideration. Many models dealing with long-term buckling behavior are based on direct substitution of the creep modulus for the elastic modulus. Mengens and Gaube (1969) indicated that buckling is a

Reproduced with permission of the copyright owner. Further reproduction prohibited without permission.

deformation-related phenomenon and that the buckling pressure at any time can be determined by replacing the elastic modulus with the creep modulus of material. Welch (1989) used an equivalent elastic modulus in a computational approach to predict creep-induced buckling of liners installed in round and oval pipes. Hucks (1972) cautioned that although the creep modulus does decrease as creep accumulates and time passes, the true elastic modulus is at least equal to its original value.

Some researchers, such as Falter (1996), have already applied test data gained from conducting tests according to ASTM Standard D2990-95, "Test Method for Tensile, Compressive, Flexural Creep and Creep-Rupture of Plastics," for use as a creep modulus in the buckling expression for liner design.

2.4.2 ASTM F1216

Since the publication of ASTM F1216, many in the industry have used it as the primary design basis for selecting polymeric pipe liners. There are two levels of deterioration that must be considered in the design of liners: 1) partially deteriorated host pipes, and 2) fully deteriorated host pipes. For partially deteriorated host pipes, the original host pipe can support the soil and traffic loading, and thus, in this case, only hydrostatic pressure by groundwater is taken into account for liner design. For the fully deteriorated pipe, the original host pipe is not structurally sound and cannot support soil and live traffic load. In this case the CIPP must carry the hydraulic, soil and live loads. The design criterion for partially deteriorated gravity pipes is stated as follows:

Partially Deteriorated Gravity Pipe Condition: The CIPP is designed to support hydraulic loads due to groundwater since the original pipe can support the soil and surcharge loads. The purchaser should determine the groundwater level, and the thickness

Reproduced with permission of the copyright owner. Further reproduction prohibited without permission.

of the CIPP should be sufficient enough to withstand this hydrostatic pressure without collapsing. The following equation may be used to determine the thickness required:

$$P = \frac{2KE_L}{(1-\nu^2)}\frac{1}{(SDR-1)^3}\frac{C}{N} \qquad (2\text{-}24)$$

where E_L represents the long-term (time-corrected) modulus of elasticity for CIPP; it is chosen as 50% of the short-term modulus of elasticity; K is the enhancement factor of the soil and existing pipe adjacent to the new pipe (a minimum value of 7.0 is recommended where there is full support of the existing pipe); N is the factor of safety; q is the percent ovality of original pipe; C is the ovality reduction factor which can be expressed as

$$C = ([1-\frac{q}{100}]/[1+\frac{q}{100}]^2)^3 \qquad (2\text{-}25)$$

and $q = 100 * (\text{mean inside diameter - minimum inside diameter})/\text{mean inside diameter}$.

ASTM F1216 employs Timoshenko's equation (1961) with an enhancement factor K to estimate the buckling pressure of CIPP liners. There are several questions about this design criterion:

(1) Is E_L = ½ E appropriate for all CIPP liners at 50 years of service life? It is a common industry practice to set the long-term modulus of elasticity at 50% of the initial value of the modulus of elasticity. The long-term modulus of the material over 50 years may be reduced more than 50% for some products and less for others.

(2) How is buckling pressure estimated at different service lives? Because the long-term buckling pressures are affected by many known and unknown factors that need be considered in the design equation, what is the probability of the CIPP liner failing at a certain pressure and service life?

Reproduced with permission of the copyright owner. Further reproduction prohibited without permission.

(3) The enhancement factor K represents a means of adjusting for the deviation of the experimental results from the theoretical results. The experimental analysis by Aggarwal and Cooper (1984) indicates that the value of K varies from 6.5 to 25.8 when the dimension ratio (DR) varies from 30 to 90. So, they concluded that 7.0 could be the minimum value of K used for the design. Is this value suitable for design purposes?

(4) This model does not appropriately account for the gap between the host pipe and the liner, the support provided by the host pipe, and the creep response of different liner materials.

2.4.3 Power Law Model

A two-parameter power function was used by Guice *et al.* (1994) to fit the CPAR long-term test data. The critical pressure can be expressed as a function of time as

$$P = at^{-b} \tag{2-26}$$

where a, b are constants determined from regression analysis of the long-term pipe buckling data. Transferring the original power law model so that time becomes the dependent variable yields following equation:

$$t = (P/a)^{(-1/b)} \tag{2-27}$$

2.4.4 Cohen and Arends Models

Cohen and Arends (1988) suggested an exponential function for the creep buckling of thermoplastic bars. In their experiments, the recorded times to failure were averaged and correlated with the applied loads, and an exponential dependence between the critical time and the load was established. Their test specimens were carefully machined from high-density polyethylene (HDPE), and there were no uncertainties

Reproduced with permission of the copyright owner. Further reproduction prohibited without permission.

induced by gap and external rigid constrains. The creep buckling effect was observed by monitoring the top displacements of thermoplastic bars as a function of time under static loading conditions. The relationship between the applied dead load P and the buckling time is:

$$T_{cr} = T_0 \exp(\frac{-P}{P_0}) \tag{2-28}$$

where T_0 and P_0 are fitting constants, P is the applied axial load, and T_{cr} is the critical buckling time. After a qualitative analysis of fitting their data, the empirical relationship of Equation (2-28) was revised as (Cohen and Arends, 1988):

$$T_{cr} = T_0(\frac{P_0}{P})\exp(\frac{-P}{P_0}) \tag{2-29}$$

This equation has a more reasonable physical meaning: when $P \rightarrow 0$, for infinitely small values of the load, the critical time becomes infinitely large ($T_{cr} \rightarrow \infty$) as opposed to Equation (2-29), which predicts that the critical time can not be larger than T_0 when $P \rightarrow 0$.

2.4.5 Straughan Model

Straughan (1998) suggested a long-term design model, a generalized version of Timoshenko's and Glock's short-term models as:

$$P = C_1 \times \frac{E}{1-\nu^2} \times \frac{1}{(SDR-1)^{C_2}} \times t^{C_3} \tag{2-30}$$

where C_1, C_2, C_3 are constants determined from regression analysis using experimental liner buckling data. Using statistics, the concept of dependencies can be used to determine whether or not a mathematical model is "over-parameterized." If a mathematical model contains too many parameters, then a less complex model may be

Reproduced with permission of the copyright owner. Further reproduction prohibited without permission.

found that adequately describes the data. Wang (1999) determined that the model was over-parameterized and that either C_1 or C_2 should be eliminated from the model.

In the previous Straughan model, the time-to-failure had been treated as an independent variable. As discussed earlier with the Power Law Model, the buckling time is really the dependent variable and the applied pressure is the independent variable. Rewriting the Straughan model to reflect this yields following equation:

$$t = \left[P \times (SDR - 1)^{C_2} \times \frac{1 - \nu^2}{C_1 E} \right]^{\frac{1}{C_3}} \tag{2-31}$$

2.4.6 Zhao's Model

Based on numerical simulation of liner buckling using ABAQUS, Zhao (1999) developed a model which predicts the time required for buckling T_{cr}, based on the external pressure P and the short-term critical pressure P_{cr} as

$$T_{cr} = T_0 \left(\frac{P_{cr}}{P} - 1 \right)^n \tag{2-32}$$

where T_0 and n are fitting constants determined from regression analysis using experimental data. These parameters depend on material properties and on the liner-pipe configuration. This equation has a clear physical meaning:

(1) When $P_{cr}/P = 1$, the critical pressure is applied, the liner will buckle instantaneously;

(2) A liner will not buckle if no external pressure is applied (when $P_{cr}/P \rightarrow 0$, $T_{cr} = \infty$).

2.4.7 Falter's Design Model

Falter (1996) provided a liner buckling formula as

$$P_{a,v,s} = k_{v,s} \times \alpha_D \times S_L \tag{2-33}$$

Reproduced with permission of the copyright owner. Further reproduction prohibited without permission.

where α_D is the snap through factor of the rigidly bedded pipe without initial deflections and without gaps. It can be expressed as

$$\alpha_D = 2.62 \times (r_L / s_L)^{0.8}$$

S_L is the stiffness of liner, which can be expressed as

$$S_L = \frac{(EI)_L}{r_L^3} = \frac{E}{12} \bullet (\frac{s_L}{r_L})^3$$

where r_L is the average liner radius, s_L is the liner wall thickness, $K_{v,s}$ is the reduction factor for the simultaneous existence of initial deflections and gaps, (on the safe side $K_{v,s} \cong K_v \times K_s$ is valid), K_v is the reduction factor for initial deformation (see Figure 2.7), and K_s is the reduction factor for initial gap (see Figure 2.8).

If Equation (2-33) is modified to include the standard dimension ratio SDR, which is defined as the outside liner diameter over the liner thickness, this equation can be changed to the following form:

$$P_{a,v,s} = k_{v,s} \times E \times \frac{1}{(SDR-1)^{2.2}} \qquad (2\text{-}34)$$

with $\frac{r_L}{s_L} = \frac{SDR-1}{2}$

Equation (2-34) is identical to Glock's model with gap effects and initial deformations added. Falter expressed the long-term elastic modulus as

$$E(t) = \frac{E_{0.1h}}{(10t)^{0.0453}} \qquad (2\text{-}35)$$

Combining Equation (2-34) and (2-35), the long-term buckling model can be expressed as:

Reproduced with permission of the copyright owner. Further reproduction prohibited without permission.

$$P_{a,v,s} = k_{v,s} \times \alpha_D \times S_L = k_v \times k_s \times \frac{E}{(10t)^{0.0453}} \times \frac{1}{(SDR-1)^{2.2}} \qquad (2\text{-}36)$$

The calculated 50-year critical pressure is less than the value using Glock's model. Because of differences between plane stress and plane strain, gap and initial deformation effects and long-term modulus, Boot and Gumbel (1996) point out that Falter inappropriately combines imperfections by multiplying the reduction factors associated with the individual imperfections and initial gap as $K_{v,s} \cong K_v \times K_s$.

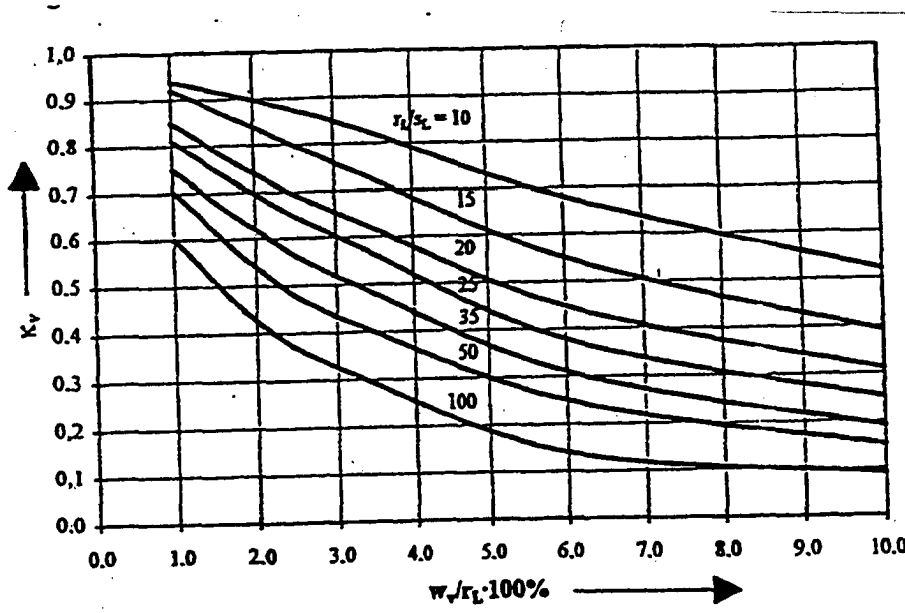

Figure 2.7 Reduction Factor K_v for Liners with Initial Deformations

Reproduced with permission of the copyright owner. Further reproduction prohibited without permission.

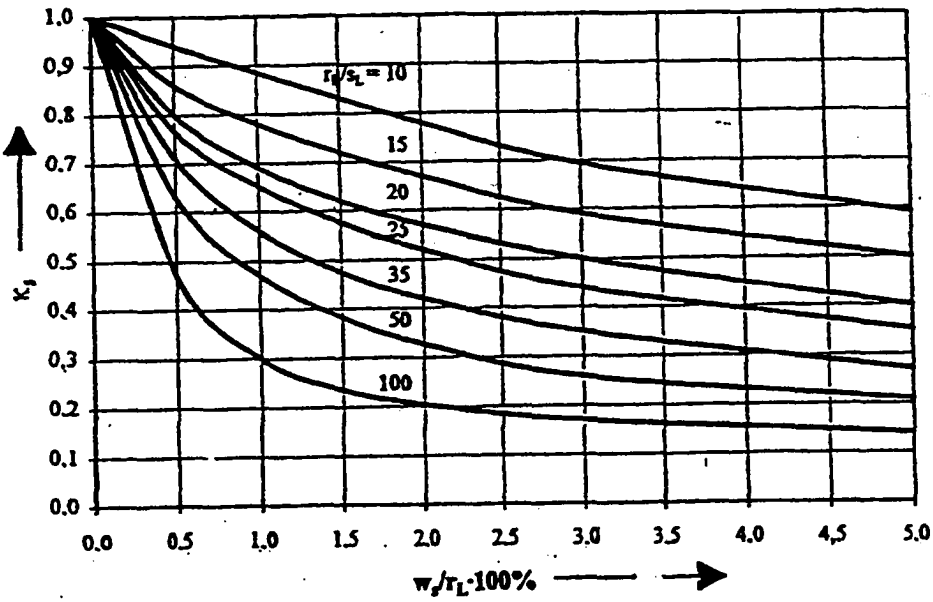

Figure 2.8 Reduction Factor K_s for Initial Gap Between Host Pipe and Liner

2.4.8 McAlpine's Design Model

Due to compressive creep, the circumference of the liner will continue to decrease and the gap size will continue increase resulting in lowering of the pressure required to cause the buckling of liner. McAlpine (1996) extended the short-term model given in Equation (2-9) as

$$P = c(t) \cdot E(t) \cdot \left(\frac{1}{1-\nu^2} \cdot \frac{1}{(SDR-1)^b}\right) \tag{2-37}$$

He gave the creep modulus as a function of time as

$$E(t) = E_s \cdot E_l / (E_l + E_s t^n) = E_s / ((1 + E_s / E_l) t^n) \tag{2-38}$$

Reproduced with permission of the copyright owner. Further reproduction prohibited without permission.

where E_s is the compressive time-independent modulus, E_t is a constant which characterizes the time-dependent stiffness, t is the time after loading, and n is a dimensionless material constant which characterizes time-dependent behavior.

2.5 Liner Buckling Experiments

A number of time dependent material characterization studies on liner materials have been carried out since the late 1980s. Welch (1989) was the first to study the time-dependent behavior of polymeric materials used in liner applications. Similar tests for were conducted by Lin(1995) under tension, compression, and flexural loading conditions for 3,000 hours.

The instantaneous buckling of CIPP was first studied by Aggarwal and Cooper (1984) who conducted external pressure tests of Insituform liners. In these tests, the liners were inserted in steel pipes. Then pressure was increased between the liner and casing in increments of approximately $1/10^{th}$ of the expected failure pressure until failure. The experimental failure pressure was much larger than the theoretical buckling pressure. The enhancement factor was first defined in their report as the test pressure divided by the theoretical buckling pressure (ASTM F1216-93).

Cohen (1988) conducted buckling tests for a number of thermoplastic materials by monitoring the top displacement of a test bar. Based on their tests, they established an exponential dependence between the critical time and the load.

Watkin (1989) conducted tests for the structural performance of a PVC liner at Utah State University. In these tests, the ratio of the experimental pressure over the theoretical buckling pressure was greater than 7.

Reproduced with permission of the copyright owner. Further reproduction prohibited without permission.

Shell Development Company conducted an experimental program to evaluate the collapse resistance of CIPP liners made with various epoxy resins (Lo et al., 1994). The test specimens had a constant diameter and different thicknesses. The results of these tests were also analyzed to determine the enhanced factor K, resulting in values ranging from 9.66 to 15.1.

The Trenchless Technology Center at Louisiana Tech University (1994 and 1998) had also conducted two sets of experiments in this area. Two distinct sets of long-term liner buckling experiments have been conducted at the TTC. The first set of experiments is known as the CPAR study (1994) and involved the testing of seven products. The second set of experiments (1999) is known as the BORSF study and only involved the testing of the one CIPP product.

In the CPAR tests (Guice *et al.* 1994), six CIPP products and one PVC product from five companies were evaluated. The primary control variables were pressure, time and DR. Test specimens were installed in 12-inch diameter host pipes, and DR ranged from 30 to 60. The longest buckling time allowed was 10,000 hours. In the BORSF tests (Hall et al., 1999), 180 specimens of the Insituform Enhanced polyester resin were subjected to long- and short-term tests. The full array of samples is represented by 6 groups, two diameters (8 and 12 inch diameter), and 6 different DRs. The six groups of 30 specimens are represented by nominal thickness of 4.5, 5.0 and 5.5 mm in the 8 inch diameter host pipes and nominal thickness of 5.5, 6.5 and 7.5 mm in the 12 inch diameter host pipes. DR ranges from 40 to 70 for these tests. In the BORSF tests, the liners were allowed to carry the external pressure for 10,000 hours, although some liners were

Reproduced with permission of the copyright owner. Further reproduction prohibited without permission.

allowed to survive longer. A schematic of the hydraulic test system is provided in Figure 2.9.

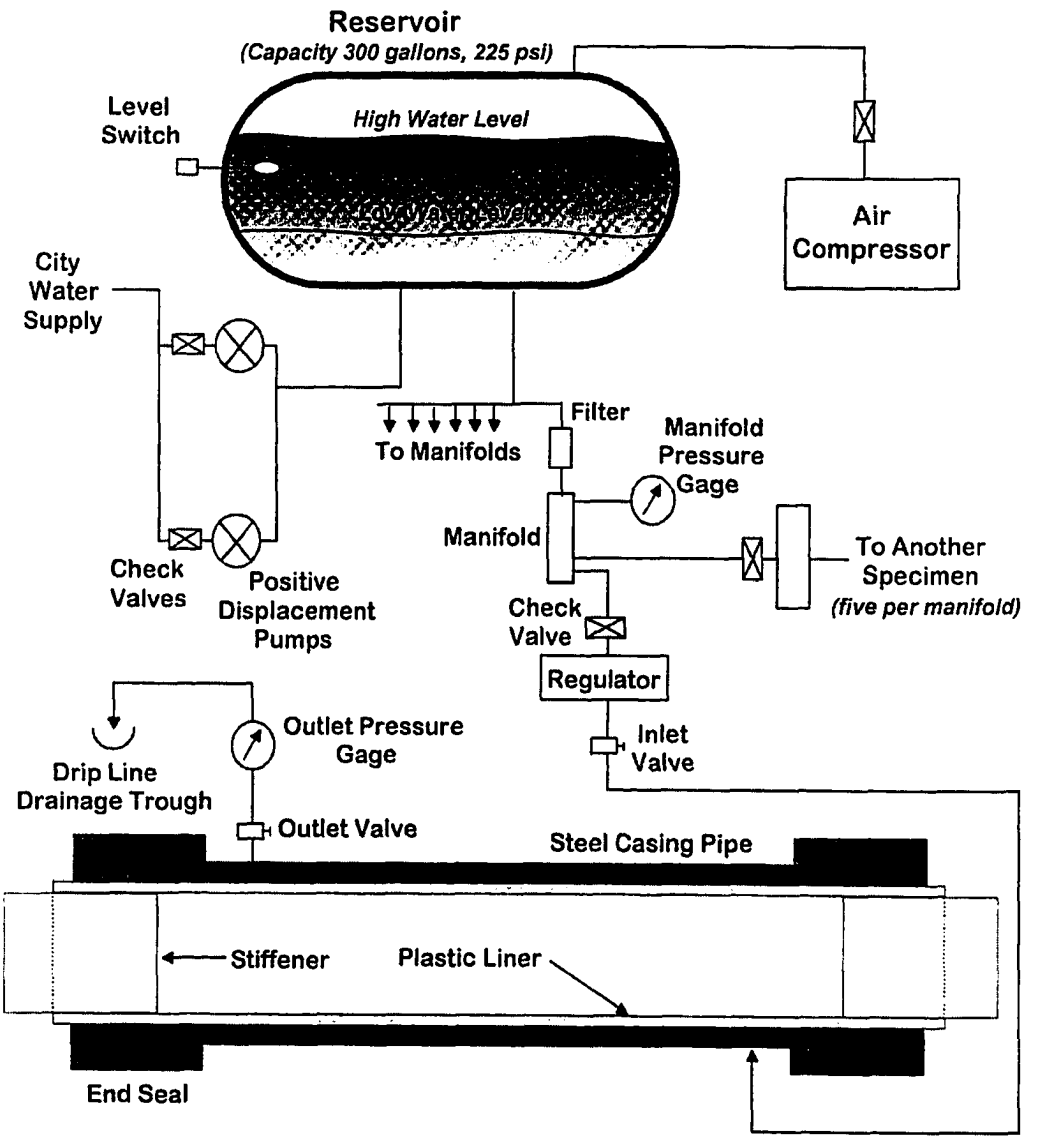

Figure 2.9 Hydraulic System Used for Long-term Testing in TTC

Reproduced with permission of the copyright owner. Further reproduction prohibited without permission.

CHAPTER 3

STATISTICAL ANALYSIS AND THEORY

3.1 Introduction

Statistical methods are widely used in engineering analysis. The ability of liner buckling models to predict liner collapse can be systematically analyzed using statistical techniques. This chapter introduces factorial designs and nonlinear regression theory. SAS and Sigmaplot was chosen as the statistical analysis tool. This chapter provides a basis for the following chapters.

3.2 Statistical Approach

Statistics, in a narrow sense, is a branch of science that deals with making inferences about populations based on samples. One important role in statistical analysis is to obtain a mathematical model. The discovery of associations and the ability to express such associations in a precise mathematical form may enable one to predict the unknown value of a variable based on the known value of one or more associated or related variables. The analyst's job is to use proper statistical methods to analyze the data in order to find the simplest form of the model. Simple graphical methods, Residual analysis and model adequacy checking play an important role in data interpretation.

A source of variation is anything that could cause an observation to have a

Reproduced with permission of the copyright owner. Further reproduction prohibited without permission.

different numerical value from another observation. Some sources of variation are minor, producing only small differences in the data. Others are major. Those are of particular interest called "treatment factors". The levels are specific types or amounts of the treatment that will be used in the experiment. The combinations of their levels are called treatment combinations and these methods which involve two or more treatment factors is called a factorial design. By a factorial design, all possible combinations of the levels of the factors are investigated. This design allows the effects of a factor to be estimated at several levels of the other factors, yielding conclusion that are valid over a range area.

If an experiment that involves four factors (A, B, C, D) have a, b, c, d levels, then the experiment is known as an "a × b × c × d factorial experiment" and has a total of v=abcd treatment combinations. This experiment is referred to as a 3^4 factorial design.

A 3^k factorial design is a factorial arrangement with k factors each at three levels. If all the factors have the same number of levels, the design is symmetric. Without loss of generality, we may refer to the three levels of the factors as low, intermediate and high. These levels will be designated by the digits 0 (low), 1(intermediate), and 2 (high). Each treatment combination in the 3^k design will be denoted by k digits, where the first digit indicates the level of factor A, the second digit indicate the level of factor B,..., and the kth digit indicates the level of factor K. For example, 0120 represents a treatment combination ABCD in a 3^4 design with AD at the low levels, B at the intermediate level, and C at the high level. Usually there are $3^k - 1$ degrees of freedom between 3^k treatment combinations. These treatment combinations allow sums of squares to be determined for k main effects, each with two degrees of freedom; two-factor interactions, each with four

Reproduced with permission of the copyright owner. Further reproduction prohibited without permission.

degrees of freedom. In general , an h-factor interaction has 2^h degree of freedom. The analysis of variance for this design is outlined in Table 3.1.

Table 3.1 Analysis of Variance for a 3^k Design

Source of Variation	Sum of Squares	Degrees of Freedom
K main effects		
A	SS_A	2
B	SS_B	2
.	.	.
.	.	.
.	.	.
K	SS_K	2
two-factor interactions $\binom{k}{2}$		
AB	$SS_{A\,B}$	4
AC	$SS_{A\,C}$	4
.	.	.
.	.	.
.	.	.
JK	SS_{JK}	4
three-factor interactions $\binom{k}{3}$		
ABC	$SS_{A\,BC}$	8
ABD	$SS_{A\,BD}$	8
.	.	.
.	.	.
.	.	.
IJK	SS_{IJK}	8
.	.	.
.	.	.
1 k-factor interactions		
ABC…K	$SS_{A\,BC\ldots K}$	2^k
Error	SS_E	$2^k(n-1)$
Total	SS_T	$n3^k-1$

Reproduced with permission of the copyright owner. Further reproduction prohibited without permission.

For example, the four-factor interaction ABCD has $2^4 - 1 = 8$ orthogonal two-degrees–of-freedom components, denoted by $ABCD^2$, ABC^2D, AB^2CD, $ABCD$, ABC^2D^2, AB^2C^2D, AB^2CD^2, and $AB^2C^2D^2$. The size of the design increases rapidly with k, such as: a 3^3 design has 27 treatment combinations per replication, a 3^4 has 81, a 3^5 has 243 and so on. The sum of squares for any main effect may be partitioned into a linear and quadratic component, each with a single degree of freedom, using the orthogonal contrasts. The two-factor interaction AB may be partitioned into four single-degree-of-freedom components corresponding to $AB_{L\times L}$, $AB_{L\times Q}$, $AB_{Q\times L}$, $AB_{Q\times Q}$. Similarly the three-factor interaction ABC may be partitioned into eight single-degrees-of-freedom components corresponding to $ABC_{L\times L\times L}$, $ABC_{L\times L\times Q}$, $ABC_{L\times Q\times L}$ and so on. Similar methods can be used for four-factor and five-factor interaction and so on.

A single replicate of a 3^k design is sometimes called a single replicate factorial. It can be analyzed when the number of treatment combinations is large and only a few contrasts are likely to be nonnegligible (Dean, 1999). Because in this particular case, some high-order interaction is nonegligible, the complete model must be used. With only one replicate, there is no estimated error. One approach to the analysis of an unreplicated factorial design is to assume that certain high-order interactions are negligible and combine their mean squares to estimate the error.

In order to split the interaction sum of squares into parts corresponding to negligible and nonnegligible orthogonal contrasts, first enter the data in the usual manner and obtain the sums of squares for all of the contrasts via CONTRAST statements in the procedure PROC GLM. Then, choose the highest interaction effects that are known to be negligible. The corresponding parameters can be removed from the complete model to

Reproduced with permission of the copyright owner. Further reproduction prohibited without permission.

give a submodel. The analysis of variance table can then be constructed with the error sum of squares being the sum of the contrast sums of squares for the negligible contrasts. The regression analysis method will be used via PROC REG. The least squares method has been used in the factorial designs and in regression analysis. Detail methodology will be presented in the following section.

3.2.1 The Method of Least Squares

A function $F(x_1, x_2 .... x_k; \theta_1, \theta_2, ..., \theta_p)$ is specified which relates the value of k input variables $x_1, x_2, ..., x_k$, to the expected values of k output variables y. This function depends upon a set of unknown parameters $2_1, 2_2, ...2_p$, which are estimated by fitting the model to a data set.

The method of least squares chooses the estimator that minimizes the sum of squares errors (SSE). With a data set

$(y_1, x_{11}, x_{21}, ... x_{k1})$

.....

$(y_n, x_{1n}, x_{2n}, ... x_{kn})$,

consisting of n sets of values of the response variables and k input variables, the parameter estimates

$\theta_1, ... \theta_p$

are therefore chosen to minimize the sum of squares, where SSE is written as:

$$SSE = \sum_{i=1}^{n} e_i^2 = \sum_{i=1}^{n} (y_i - f(x_{1i}, x_{2i}, ... x_{ki}; \theta_1, ... \theta_p))^2 \qquad (3\text{-}1)$$

SSE is the sum of the prediction errors squared where the sample regression function of Y on X is used to predict the Y values of the sample items.

So, the mean squared error is

Reproduced with permission of the copyright owner. Further reproduction prohibited without permission.

$$MSE = \frac{SSE}{(n-p)} \tag{3-2}$$

and

$$\hat{\sigma} = \sqrt{\frac{SSE}{n-p}} = \sqrt{MSE} \tag{3-3}$$

where p is the number of estimated parameters and $\hat{\sigma}$ is the common standard deviation of the populations of y values determined by the distinct x values.

The correlation coefficient, which is written as:

$$r = \frac{SXY}{\sqrt{SSX}\sqrt{SSY}} = \frac{\sum_{i=1}^{n}(x_i - \bar{x})(y_i - \bar{y})}{\sqrt{\sum_{i=1}^{n} x_i^2 - n\bar{x}^2}\sqrt{\sum_{i=1}^{n} y_i^2 - n\bar{y}^2}} \tag{3-4}$$

where $\bar{x} = \frac{1}{n}\sum_{i=1}^{n} x_i$ and the sample correlation coefficient r takes a value from -1 to 1. The closer the sample correlation coefficient is to either -1 or 1, the stronger is the relation between the two variables(x, y).

Another way to measure the contribution of X in predicting Y is to consider how much the errors of the predicted Y were reduced by using the information provided by X. The square of the coefficient of correlation is called the coefficient of determination. It is the most common measure of how well a regression model describes the data. When r^2 is equal to 0, it means that the values of the independent variable do not allow any prediction of the dependent variables. Likewise, when r^2 is equal to 1, it can perfectly predict the dependent variables from the independence variables.

$$r^2 = \frac{SSY - SSE}{SSY} \tag{3-5}$$

where:

Reproduced with permission of the copyright owner. Further reproduction prohibited without permission.

SSY = corrected total sum of squares for Y which can be written as:

$$SSY = \sum (y_i - \bar{y})^2; \tag{3-6}$$

SSE = sum of square error,

$$SSE = \sum (y_i - \hat{y}_i)^2; \tag{3-7}$$

SSR = sum of squares due to regression, which can be written as:

SSR = SSY-SSE; (3-8)

and

$$\hat{y} = f(x_1, x_2, \ldots x_i, \theta_1, \ldots \theta_p) \tag{3-9}$$

$$\bar{y} = \frac{\sum_{1}^{n} y_i}{n} \tag{3-10}$$

The process of calculating, tabulating, and examining some key numerical quantities are summarized in the ANOVA (analysis of variance) table. Table 3.2 is an example, which explains how to use an ANOVA table for regression

Table 3.2 ANOVA Table

Source	Degree of Freedom(df)	Sum of Squares (SS)	Mean Square (MS)	Computed F-Value	Computed P-Value
Regression	p	SSR	MSR	Fc=MSR/MSE	<0.05
Error	n-p-1	SSE	MSE		
Total	n-1	SSY	MSY		

SSY (sum of squares) term is measure of the variability of the dependent variable. The mean square (MS) terms provide two estimates of the population variances.

Reproduced with permission of the copyright owner. Further reproduction prohibited without permission.

$$MSR = \frac{\text{sum of squares due to regression}}{\text{regression degrees of freedom}} = \frac{SSR}{p} \tag{3-11}$$

$$MSE = \frac{\text{residual sum of squares}}{\text{residual degree of freedom}} = \frac{SSE}{n-1} \tag{3-12}$$

The F value gauges the contribution of the independent variables in predicting the dependent variable. It is the ratio

$$\frac{\text{regression variation from the dependent variable mean}}{\text{residual variation about the regression}} = \frac{MS_{reg}}{MS_{res}} = F \tag{3-13}$$

When F is a large number, one can conclude that the independent variables contribute to the prediction of the dependent variable. If the F ratio is around 1, one can conclude that there is no association between the variables.

The P value is the probability of being wrong in concluding that there is an association between the dependent variable and independent variables. The smaller the P values, the greater the probability that there is an association. Traditionally we conclude that the independent variables can be used to predict the dependent variable when $P < 0.05$.

3.2.2 Models and Factorial Effects

There are several models that may be appropriate for describing the data with several treatment factors. The selection of a suitable model depends on which factors do or do not interact. For three factors effects, it can have the following models.

The cell-means model for three treatment factors is

$$Y_{ijkl} = \mu + \tau_{ijk} + \varepsilon_{ijkl} \tag{3-14}$$

where $\varepsilon_{ijkl} \sim N(0,\sigma^2)$; $i = 1,...a$; $j = 1,..b$; $k = 1,...c$

Reproduced with permission of the copyright owner. Further reproduction prohibited without permission.

Alternatively, a model with mean effects and interactions is given as

$$Y_{ijk} = \mu + \alpha_i + \beta_j + \gamma_k + (\alpha\beta)_{ij} + (\alpha\gamma)_{ik} + (\beta\gamma)_{jk} + (\alpha\beta\gamma)_{ijk} + \varepsilon_{ijk} \quad (3\text{-}15)$$

$$\varepsilon_{ijkt} \sim N(0,\sigma^2);\ i = 1,...,a; j = 1,...,b; k = 1,...c.$$

where α_i, β_j, γ_k are the effects of the response of factors A, B, C at levels i, j, k, respectively, $(\alpha\beta)_{ij}$, $(\alpha\gamma)_{ik}$, $(\beta\gamma)_{jk}$ are the additional effects of the pairs of factors together at the specified levels, and $(\alpha\beta\gamma)_{ijk}$ is the additional effects of all three factors together at levels i, j, k. The three sets of factorial effects are called the main-effect parameters, the two-factor interaction parameters and the three-factors interaction parameter, respectively. If there are more than three factors, these equations have correspondingly more subscripts.

In an experiment involving v treatments, one way to check whether or not the treatments differ at all in terms of their effects on the response variable is using the null hypothesis test:

$H_0 : \{\tau_1 = \tau_2 = ... = \tau_v\}$

that the treatment effects are all equal against the alternative hypothesis

H_A : { at least two of them are not equal}

3.2.3 Estimation of Parameters

A function of the parameters of any model is said to be estimable if and only if it can be written as the expected value of a linear combination of the response variables. For the one-way analysis of variance model (Equation 3-14), every estimable model is of the form

$$E[\sum_i \sum_l a_{il} E[Y_{il}]] = \sum\sum a_{il}(\mu + \tau_i) = \sum_i b_i(\mu + \tau_i) \quad (3\text{-}16)$$

Reproduced with permission of the copyright owner. Further reproduction prohibited without permission.

where $b_i = \sum_{ii} a_{ii}$ and the a_{ii} 's are real numbers.

Clearly, $\mu + \tau_i$ is estimable, since it can be obtained by setting $b_i = 1$ and $b_2 = b_3 = ... = b_v = 0$. Similarly, if we choose $b_i = c_i$, then $\sum c_i = 0$ is called a contrast. The corresponding coefficients c_i s for orthogonal polynomial contrasts, c_i for different treatment levels can be found in statistical books. In this research the maximum level is three, the coefficient for three levels is shown in Table 3.3.

Table 3.3 Coefficients c_i for Three-level Orthogonal Polynomial Trend Contrasts

Trend	C_1	C_2	C_3
Linear	-1	0	1
Quadratic	1	-2	1

3.3 The SAS Program and Sample Input File

SAS is a commercially available statistical software program. It is one of the most powerful data analysis tools in the world. In this research, the GLM procedure and the REG procedure are used in the analysis. The GLM and REG procedures use the method of least squares to fit a given model to data. Each procedure has its syntax information in a User' Manual.

To illustrate the method that SAS uses to solve the analysis of a factorial design, the simple short-term factorial analysis method will be presented in this section. Each line in the input file corresponds to a digit number which needs to be eliminated in a real SAS run. The input file is in Figure 3.1.

Reproduced with permission of the copyright owner. Further reproduction prohibited without permission.

SAS INPUT FILE

```
1       Title 'Analysis 3-3 Factorial Design';
2       DATA SHORT;
3       INPUT A  A2 B B2 C C2 Y;
4       AB=A*B;
5       AB2=A*B2;
6       AC=A*C;
7       AC2=A*C2;
8       A2B=A2*B;
9       A2B2=A2*B2;
10      A2C=A2*C;
11      A2C2=A2*C2;
12      BC=B*C;
13      BC2=B*C2;
14      B2C=B2*C;
15      B2C2=B2*C2;
16      ABC=AB*C;
17      ABC2=AB*C2;
18      AB2C=AB2*C;
19      AB2C2=AB2*C2;
20      A2BC=A2B*C;
21      A2BC2=A2B*C2;
22      A2B2C=A2B2*C;
23      A2B2C2=A2B2*C2;
24      LINES;
25      * input data file, see Appendix D-1
26      .
        .
        .
28      ;
29      PROC PRINT;
30      PROC GLM;
31      MODEL Y=A B C A2 B2 C2  AB AB2 AC AC2  A2B A2B2
32                A2C A2C2 BC BC2  B2C B2C2 ABC  ABC2  AB2C
33                 AB2C2 A2BC A2BC2 A2B2C A2B2C2;
34      OUTPUT OUT= NEW P=YHAT R=RESID STDR=ERESID;
35      RUN;
```

Figure 3.1 The Short-term SAS Factorial Analysis Input File

Line 1 is the keywords '**Title**' which informs the program that all information until next keywords '**DATA**' are the title of the output program. It can be changed by user in order to separate different runs.

Line 2 (DATA option) begins the definition of the initial input data name.

Reproduced with permission of the copyright owner. Further reproduction prohibited without permission.

Line 3 (INPUT option) lists all the independent variables A, B, C, A2, B2, C2, in this case, they represent Gap, Ovality and Local imperfection and the dependent variable Y represents the corresponding constants a or m. The order of variables need match with the order of data file.

Lines 4-23 define all main, two-factor interaction, and three-way interactions following the INPUT statement in the complete model.

Lines 24-28 list input data file (contrast coefficients for all the contrasts). It is also shown in Appendix D-1.

Line 30 (PROCEDURE option) the statement starts the GLM procedure. The statement can also be expressed as

Proc glm;

Model dependent =independents</options>;

Line 31 defines the model to be fit in the PROC GLM procedure. This model needs to be updated with a new submodel by eliminating the negligible interactions.

Lines 32 (OUTPUT option) names an output data set which contains sums of squares, degrees of freedom, F statistics, and probability levels, predicted value, residuals, and standard residual for each effect in this model. The statement also can be expressed as:

Output<out=SAS-data-set> keywords = names <...keywords=names>

The REG procedure is similar to the GLM procedure. The only difference is:

PROC REG<options>.

dependents=<regressors></option>.

Reproduced with permission of the copyright owner. Further reproduction prohibited without permission.

CHAPTER 4

PROPOSED LINER DESIGN MODEL

4.1 Introduction

The similarities between different long-term design models will be presented in this chapter. This chapter provides a basis for developing a new long-term liner design model.

4.2 Extension of Short-term Models to Predict Long-term Response

It is common practice to predict the long-term response of plastics by substituting a creep modulus in place of the elastic modulus in deflection and strain relationships. This practice has been carried over to the buckling of thin walled pipe liners, as evidenced by the fact that most of the long-term liner design models are direct extensions of the analogous short-term liner design models. Close examination of these models leads to a generalized equation for groundwater pressure as a function of the critical pressure, the creep modulus, E_L, and the short-term modulus, E. Adding an additional correction factor C^* to the generalized equation provides a mechanism for more accurate long-term predictions. The importance C^* will be discussed in section 4.4. The generalized form can be expressed as

Reproduced with permission of the copyright owner. Further reproduction prohibited without permission.

$$P = C^* \cdot P_{cr} \cdot \frac{E_L}{E} \tag{4-1}$$

where E is the short-term elastic modulus and E_L is the long-term or creep modulus. The critical pressure, P_{cr}, accounts for the effects of geometry and material properties on the short-term response. As presented in chapter 2, Omara et al. (1996) gave a generalized form of the short-term buckling response as

$$P_{cr} = \frac{aE}{(1-\nu^2)(SDR-1)^m} \tag{4-2}$$

The similarities between existing long-term models and the generalized form for long-term models given in Equation (4-1) are presented below.

4.2.1 ASTM F1216

The ASTM F1216 model Equation (2-22) is restated here for convenience as

$$P = \frac{2KE_L}{1-\nu^2} \cdot \frac{1}{(SDR-1)^3} \cdot \frac{C}{N} \tag{4-3}$$

where E_L is typically taken as $E_s/2$. Substituting $P_{cr} = \frac{2KE}{1-\nu^2} \cdot \frac{1}{(SDR-1)^3} \cdot \frac{C}{N}$ and $C^* = 1$ into Equation (4-3) allows the ASTM F1216 model to be expressed as given in Equation (4-1). P_{cr} also has the same form as Equation (4-2), with $a = 2KC/N$ and $m = 3$.

4.2.2 Straughan's Model

Straughan's model Equation (2-28) is restated here for convenience as

$$P = C_1 \times \frac{E}{1-\nu^2} \times \frac{1}{(DR-1)^{C_2}} \times t^{C_3} \tag{4-4}$$

Reproduced with permission of the copyright owner. Further reproduction prohibited without permission.

Taking $P_{cr} = \frac{C_1 E}{1-\nu^2} \cdot \frac{1}{(SDR-1)^{C_2}}$, $E_L = t^{-C3}$, and $C^* = 1$ allows Straughan's model to be expressed as given in Equation (4-1). Note that C_1 is a combined constant that contains a constant applied to P_{cr} and a constant applied to E_L. P_{cr} also has the same form as Equation (4-2), with $a = C_1$ and $m = C_2$.

4.2.3 Falter's Model

Falter's model (Equation 2-34) is restated here for convenience as

$$P_{a,v,s} = k_v \cdot k_s \cdot \frac{E}{(10t)^{0.0453}} \cdot \frac{1}{(SDR-1)^{2.2}} \tag{4-5}$$

Taking $P_{cr} = \frac{k_v \cdot k_s \cdot E}{1-\nu^2} \cdot \frac{1}{(SDR-1)^{2.2}}$, $E_L = \frac{E}{(10t)^{0.045}}$, and $C^* = 1$ allows Falter's model to be expressed as given in Equation (4-1). P_{cr} also has the same form as Equation (4-2), with $a = k_V \cdot k_S$ and $m = 2.2$.

4.2.4 McAlpine's Design Model

McAlpine's model Equation (2-35) is restated here for convenience as

$$P = \frac{c(t)}{1-\nu^2} \cdot \frac{1}{(SDR-1)^b} \cdot \frac{E}{1+\frac{E}{E_t} \cdot t^n} \tag{4-6}$$

Taking $P_{cr} = \frac{c(t) \cdot E}{1-\nu^2} \cdot \frac{1}{(SDR-1)^b}$, $E_L = \frac{E}{1+\frac{E}{E_t} \cdot t^n}$, and $C^* = 1$ allows McAlpine's model to be expressed as given in Equation (4-1). P_{cr} also has the same form as Equation (4-2), with $a = c(t)$ and $m = b$.

Reproduced with permission of the copyright owner. Further reproduction prohibited without permission.

4.2.5 Summary of Model Comparison

Table 4.1 summarizes the results of the previous discussion. This comparison shows that the parameters used in the buckling models are very similar. For example, all models include both a coefficient *a* and an exponent *m* which account for the influence of host-pipe constraint and imperfections (which may or may not include ovality, gap and longitudinal imperfections). The expressions for the long-term modulus, E_L, are quite different for the models. Three of the models include time explicitly (Straughan, Falter, and McAlpine), whereas the ASTM F1216 estimates E_L only for a 50 year design life. Regardless of how long-term material behavior is incorporated, all of the models assume that the initial resistance to buckling, as predicted by a short-term model, decays with time. Notice also that C^* is 1 for all of the models.

Table 4.1 Long-term Buckling Model Equation Parameters

Original Long-term Buckling Form	Short-term Models		E_L	C^*
	a	m		
ASTM F1216	2KC/N	3	E / 2	1
Straughan's Model*	C_1	C_2	t^{-C3}	1
Falter's Model	$k_v \cdot k_s$	2.2	$\frac{E}{(10t)^{0.045}}$	1
McAlpine's Model	c(t)	b	$\frac{E}{1+\frac{E}{E_l}\cdot t^n}$	1

* C_1 is a combination of two constants, on applied to P_{cr} and one applied to E_L.

Reproduced with permission of the copyright owner. Further reproduction prohibited without permission.

4.3 Discussion of Other Long-term Models

Several of the long-term models presented in Chapter 2 are not extensions of short-term models to predict long-term response. These models include the power law model, Cohen's model (1989) and Zhao's model (2001). Such models are based on fitting experimental data or finite element results to determine values for the constants used in the models. The aim of the research presented in this thesis is to develop a long-term model that is based on creep properties of materials as determined from material characterization tests, not full scale liner tests or finite element simulation.

4.4 Proposed Long-term Model

The proposed design model is the generalized model given in Equation (4-1). The long-term creep modulus E_L is the stress level divided by the time dependent strain as

$$E_L = \frac{\sigma}{\varepsilon(t)} = \frac{1}{At^n + \frac{1}{E}} = \frac{E}{AEt^n + 1} \tag{4-14}$$

which is identical to the form for E_L given by McAlpine. Here, a Norton-type creep law as given in Equation (2-21) is used, where the exponent on stress is taken as 1.0. Substituting Equation (4-14) into Equation (4-1) leads to

$$P_l = C^* \frac{1}{AEt^n + 1} P_{cr} \tag{4-15}$$

Here, P_{cr} is based entirely on a short-term buckling analysis, E is the short-term elastic modulus, and A and n are material parameters which are determined by fitting data from creep deformation testing. Determination of C^*, which provides a correction factor to

Reproduced with permission of the copyright owner. Further reproduction prohibited without permission.

allow long-term response to be predicted from short-term models, is the focus of this thesis.

4.5 Importance of C^*

Substitution of a creep modulus into a short-term liner buckling model is not theoretically valid, although this has become common practice because of its simplicity. The purpose of this thesis is to provide a bridge to allow short-term liner buckling models to more accurately predict the lifetime of liners. The constant C^*, which will prove to be a function of the geometry of the liner / host pipe system and of the liner material properties, will provide a correction constant for predicting long-term response of liners.

Reasons for inaccuracies in the extension of short-term models to predict long-term response are summarized below.

1. Linear viscoelasticity versus non-linear viscoelasticity. If the exponent on stress in Equation (2-18) is equal to 1.0, then the material is called a linear viscoelastic material. This means that the long-term modulus, as given in Equation (4-14), is not a function of stress. Thus, in a body where stresses are constant, the stress will have a linear relationship with strain over time, even though strains are increasing with time. That is, if the stress at a given point is doubled, then the amount of strain that accumulates over time at that point will also double. Deviation in material response from linear viscoelastic behavior(l in Equation (2-18) becomes significantly different than 1.0) will result in stress redistribution when stress gradients are present in a body. The design model presented in this thesis assumes that the material is linear viscoelastic.

Reproduced with permission of the copyright owner. Further reproduction prohibited without permission.

2. Effect of evolving stresses and contact conditions. The use of elastic models to compute long-term stress-strain behavior assumes that the stresses at every point in the body are constant over time. Only the strains are allowed to change with time. For liners subjected to external pressure loading, the liner has an initial elastic deformation which is assumed to occur instantaneously when the pressure is applied. As time passes, the liner deforms within the host pipe due to creep, and the contact area between the liner and host pipe increase as time passes. This results in a decreased span for the lobe and a change in the stress levels at a given point. Hence, some error in the predicted long-term stress-strain analysis will be introduced, since the changing stresses and loading conditions are not considered in the elastic solution.

Also, as deformations become large, the stresses in the wall of the liner will not be as high as predicted from an elastic analysis due to stress relaxation across the wall of the liner. In this case, the liner will eventually experience deformations that are in excess of those that are elastically possible. A short-term model using a long-term elastic modulus does not account for this type of behavior. This relaxation should act to extend the lifetime of the liner since the stresses will be lower than those predicted elastically, especially in the case of materials that creep more easily.

3. Effect of using a creep modulus for buckling calculations. The buckling pressure is proportional to the short-term elastic modulus in all short-term models currently being considered for liner design. Although the creep-modulus decreases with time, the short-term elastic modulus may not change with time (in some cases it may actually increase). At any point in time, the stability of the liner will be governed by the current short-term elastic modulus, the current stress distribution, and the current geometry.

Reproduced with permission of the copyright owner. Further reproduction prohibited without permission.

The above discussion shows that short-term buckling models cannot be blindly extended to predict long-term response. The factor, C^*, is needed to correct the predictions of liner design models that are derived based on the assumption of linear elastic material behavior. The focus of this thesis is use statistical and finite element methods to analyze the influence of gap, ovality, DR, material properties, and groundwater pressure on the value of C^*.

Reproduced with permission of the copyright owner. Further reproduction prohibited without permission.

CHAPTER 5

FINITE ELEMENT MODELING FOR CONSTRAINED LINER BUCKLING

5.1 Introduction

In this study, a general purpose ABAQUS/Standard finite element analysis software (HKS, 1998) was used to simulate two dimensional long-term behavior of the encased liners. The assumptions made in constructing the numerical analysis are presented first in this chapter and are followed by a description of the implementation of the finite element model. The ABAQUS features used in this research are described where necessary.

5.2 Assumptions

The assumptions used in setting up the encased liner buckling finite element models are addressed as follow.

5.2.1 Loading Condition

According to ASTM F1216, the liner is designed to withstand only the hydrostatic pressure caused by the underground water which infiltrates through the cracks in the host pipe. The original pipe-soil system is assumed to be strong enough to resist all the loads transferred from the surrounding soils. And, the liner is assumed to interact only with the

Reproduced with permission of the copyright owner. Further reproduction prohibited without permission.

host pipe. Therefore, the only loads acting on the liner are the external groundwater pressure and the contact forces from the host pipe.

5.2.2 Material Properties

There are a variety of pipe liner materials on the market corresponding to a wide range of mechanical properties. One of the CIPP products, the Insituform Enhanced resin, a thermosetting plastic, is chosen as the object of this study because both short-term and long-term mechanical properties have been previously determined for this material at the TTC. Several material properties test (Guice et al., 1994, and Lin, 1995; Boot and Javadi, 1998) have shown similar elastic modulus and Poisson's ratio for tension and compression. In this research, the tensile elastic modulus is chosen as 538,621 psi, the compressive elastic modulus as 652,400 psi, and Poisson's ratio as 0.3.

The computational results presented here inherently assume that the liner materials are homogeneous and isotropic. These assumptions are typical for unreinforced thermoplastic products (such as PVC and polyethylene). The assumptions are believed to also apply to CIPP products made from non-woven fabrics injected with a thermosetting resin. The non-woven nature of the felt results in mechanical properties that show little difference in the longitudinal and circumferential directions. And, the stresses in the radial direction are very small compared to the in-plane stresses.

Even at room temperature, liner materials may exhibit significant creep deformation, especially at stress levels that are a significant fraction of the material yield strength. In this research, the flexural properties will be used for the short-term buckling simulations, while the compressive properties will be used for the long-term buckling simulations.

Reproduced with permission of the copyright owner. Further reproduction prohibited without permission.

5.2.3 2-D Configuration

Compared with the diameter of the liner, the liner thickness is very small and the liner system can be simplified as a thin-walled circular cylinder. Along the longitudinal direction, the contact conditions between the liner segment and the sewer pipe are assumed to be unchanging. To simplify the solution procedure, the original problem can be viewed as a ring configuration with the plane strain assumption, and the assumption of a single cross-section of the liner (with a length of unity) can be used to represent the entire liner. A plane-strain element (denoted as CPE4 in ABAQUS) is used to model the liner wall. After the mesh refinement study, 320x4 elements, or a total of 1280 elements in four layers were been used to simulate one-lobe buckling. Because of symmetry, only one-half of the circular liner was modeled.

5.3 The FEA Model

The ABAQUS finite element software will be used in the computational analysis. ABAQUS can solve a wide range of linear and nonlinear problems involving geometric nonlinearity, material nonlinearity, and boundary nonlinearity. It provides an extensive element library including contact elements and built-in creep constitutive models. And, the ABAQUS post processor can be used for visualization of results.

5.3.1 Definition of Geometric Parameters

The geometry of the pipe-liner system can be characterized by the liner dimension ratio, the annular gap between the liner and host pipe, and the ovality of the host pipe. These parameters are defined below.

Reproduced with permission of the copyright owner. Further reproduction prohibited without permission.

DR: DR is defined as the ratio of the mean liner diameter D (measured halfway between the liner inner diameter, ID, and outer diameter, OD) to the thickness of a liner t as

$$DR = \frac{D}{t} \tag{5-1}$$

This equation is different from the definition of SDR (SDR= OD/t where OD is the outside diameter of the liner) used in the current CIPP design equation.

DR levels of 30, 50 and 70 were chosen for this study because these values encompass the most common DRs used in field applications.

Gap: Accurately simulating the gap between the pipe liner and the host pipe is very important and helps us to understand contact-force evolution between the pipe liner and the host pipe (Figure 5.1). A uniformly distributed gap g was used for two-lobe models, while the total gap Δ was used for one-lobe models. The gap ratio, defined as the percentage of the gap size g to the liner mean diameter D in Equation (5-1), was varied from 0.0% to 0.7% for this study.

$$G\% = \frac{g}{D} \cdot 100\% \tag{5-2}$$

Note that the uniform gap is half of the total gap Δ, as expressed in Equation (5-3).

$$g = \frac{\Delta}{2} \tag{5-3}$$

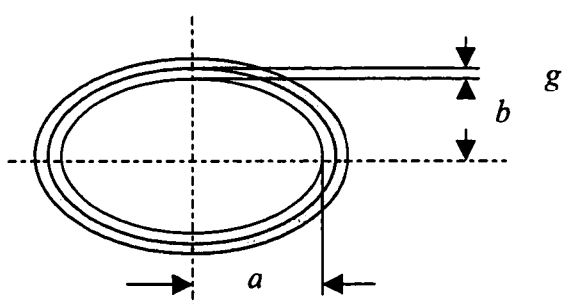

Figure 5.1 Schematic Which Defines the Ovality and Gap Parameters

Reproduced with permission of the copyright owner. Further reproduction prohibited without permission.

Ovality: As discussed in the literature review chapter, the elliptical shape of the host pipe will affect the liner's ability to resist collapse. In the present study, the initial ovality of the liner is always assumed to be the same as that of its host pipe.

$$\%Ovality = \frac{D_{max} - D_{min}}{D_{max} + D_{min}} \cdot 100\% \qquad (5\text{-}4)$$

As with Zhu's (2000) short term buckling model, when simulating the response of perfectly circular liners (0% ovality), a very small ovality is imposed to initiate the formation of a deformation lobe. The ovality ratio of 0.17% was found to be satisfactory in this study. Different levels of ovality (0%, 3%, 6%) were simulated for developing an improved long-term buckling model.

5.3.2 Constraint from the Host Pipe

ABAQUS offers an approach to defining contact interaction based on defining pairs of surfaces that may interact with each other. The surfaces of the contact area for the liner and host pipe are defined by the SURFACE DEFINITION command and the potential for contact is set up using CONTACT PAIR command. The friction coefficient is usually defined as zero for the current study by assuming both surfaces are smooth.

In this finite element model, the host pipe, which is assumed to be rigid, is modeled with a set of R2D2 (2-node two-dimensional rigid body) elements for the two-dimensional models. The set is defined as fixed without any transition or rotation relative to a reference node. All the degrees of freedom of the reference node are inhibited to fully constrain the host pipe against any motion.

Reproduced with permission of the copyright owner. Further reproduction prohibited without permission.

5.3.3 Model Setups

Zhao (1999) found that a one-lobe model is used to determine the buckling pressures for the short-term design model since it gives the lower bound for the critical pressure or time. A one lobe model is shown in Figure 5.2. Zhao's finite element results show excellent agreement with experimental data.

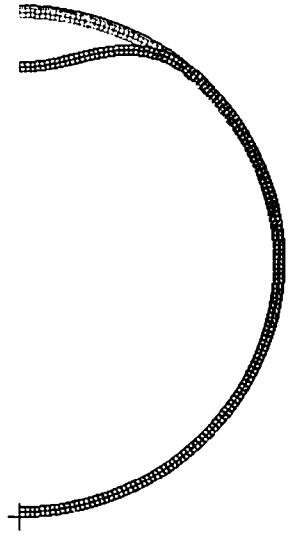

Figure 5.2 A One-lobe FEA Model Which Employs Half-symmetry

In a one-lobe model the gap is assumed to be unevenly distributed, as in Figure 2.2(b). The radial displacement at the bottom node where the liner touches the host pipe is constrained for simplicity. One-half of the liner and host pipe is modeled due to its symmetric configuration.

5.3.4 Solution Procedures

Short-term buckling will be modeled assuming rate-independent elastic material behavior with a pressure that increases monotonically from zero to the buckling pressure. For long-term buckling analyses, the FEA model must account for creep deformation that accumulates over time under the constant external pressure. ABAQUS uses the *creep

Reproduced with permission of the copyright owner. Further reproduction prohibited without permission.

option to model this behavior according to a Notron-Bailey's strain-hardening form (Equation 2-20).

Two different solution procedures in ABAQUS can be used to simulate these two different processes: STATIC for time-independent loading, and VISCO for time-dependent creeping behavior. Both procedures can deal with the geometrical nonlinearity resulting from finite displacements of the liner during liner buckling.

Finite element analysis of the short-term buckling of an encased liner includes one *STATIC* step. Here, the uniformly distributed external pressure is applied on the liner and is increased until the liner buckles.

In the long-term buckling analyses, an additional VISCO step applied in addition to a STATIC step which applies a pressure which is less than the critical pressure (the groundwater pressure). The VISCO step is included to incorporate the effects of creep deformation. Automatic time-stepping is governed by an accuracy tolerance parameter which is specified by the user. Creep behavior is defined through the *CREEP* option, where a strain hardening form of the constitutive relation is employed in this thesis.

5.4 Verification of Finite Element Model

5.4.1 Mesh Refinement

The liner was analyzed as a two-dimensional problem using a bi-linear, four-node, plane-strain element, as given by Zhu (2000). To validate the short-term model, the relative change in the critical buckling pressure for a liner with a DR of 50, an ovality of 3% and a gap of 0.4% for models with differing mesh discretizations was studied, as summarized in Table 5.1. Notice that the relative change between a model with 1280

Reproduced with permission of the copyright owner. Further reproduction prohibited without permission.

elements and 5120 elements is 1.27% for the one-lobe buckling model, which is employed in this thesis to develop an improved long-term buckling model. Two-lobe results are included here to illustrate that the one-lobe model is more conservative than the two-lobe model. Table 5.2 shows a comparison of the buckling pressures for the 1280 element and 5120 element models. Notice that there is very little difference in the buckling pressures determined using these two levels of mesh refinement.

Table 5.1 Relative Change in Buckling Pressure as a Function of the Number of Elements

DR=50 Oval=3%, Gap=0.4%					
		One-lobe		Two-lobes	
	Number of Elements	P_{cr} (psi)	Relative Change	P_{cr} (psi)	Relative Change
2 layers (160x2)	320	58.9	6.51%	78.1	11.05%
4 layers (320x4)	1280	62.2	1.27%	85.9	2.16%
8 layers (640x8)	5120	63.0	---	87.8	---

Table 5.2 Buckling Pressures in psi for One-lobe Models with 4 and 8 Layers of Elements

	Regular Mesh (340 x 4 layers)			Dense Mesh (640 x 8 layers)		
	OV=6%			OV=6%		
	G=0.1%	G=0.4%	G=0.7%	G=0.1%	G=0.4%	G=0.7%
DR=30	253.00	206.00	177.00	252.80	206.00	176.40
DR=50	71.90	51.20	41.20	71.80	51.20	41.20
DR=70	31.30	20.10	15.60	31.20	20.00	15.54

It is also necessary to evaluate the mesh refinement in terms of the buckling times predicted from the long-term model. Table 5.3 shows the relative change in buckling times for a DR of 50, an ovality of 3%, a gap of 0.4% and a PR of 0.5. Notice that the relative change in the buckling time between the model with 1280 elements and 5120 elements is 2.38%, indicating that the model with 1280 elements is sufficient to

Reproduced with permission of the copyright owner. Further reproduction prohibited without permission.

accurately predict buckling times. A portion of the mesh used for the analyses in this thesis is shown in Figure 5.3.

Table 5.3 Relative Change in Buckling Time for Different Numbers of Elements

	Insituform Enhanced Product (one-lobe)				
	Number of Elements	**P_{cr} (psi)**	**Relative Change**	**Buckling Time(hr)**	**Relative Change**
1 layer (80x1)	80	51.8	12.06%	5.943E05	14.6%
2 layers (160x2)	320	58.9	6.51%	6.959E05	8.26%
4 layers (320x4)	1280	62.2	1.27%	7.586E05	2.38%
8 layers (640x8)	5120	63.0	---	7.771E05	---

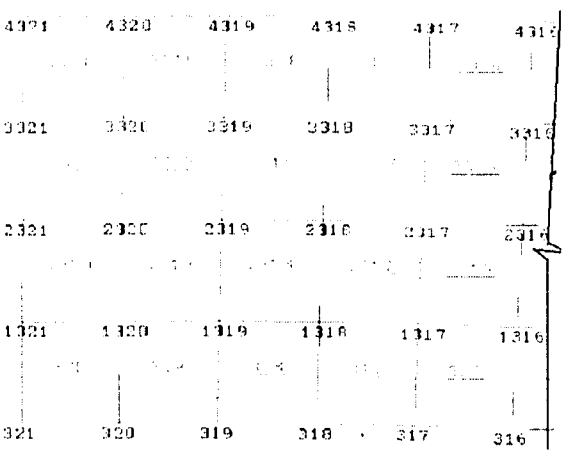

Figure 5.3 A Portion of the 1280 Element Mesh Showing the CPE4 Elements

5.4.2 Verification of Finite Element Results

The finite element model used in this thesis is identical to that of Zhu (2000). To verify that the results obtained using this model are consistent with the results of Zhao (1999), finite element runs were completed using the same material properties used by

Reproduced with permission of the copyright owner. Further reproduction prohibited without permission.

Zhao. A comparison of these models for an ovality of 3%, a gap of 0.7% and a DR of 50 is summarized in Table 5.4.

Table 5.4 Comparison of Buckling Times in hours Using the FEA Model Employed in this Thesis and the Model Used by Zhao (1999)

OV=3%, G=0.7%, DR=50,			
	Present's Results	**Zhao's Results**	**Relative Change**
PR=0.50	726200	680600	0.07
PR=0.70	6200	5979	0.04
PR=0.90	245	221	0.10

Note that Zhao (1999) used a dual beam element model, while the model used here is a 2D plane strain element model.

The model described in this chapter is utilized in the following chapter to generate a virtual test bed covering a wide range of gaps, ovalties, DRs, material property combinations, and groundwater pressure levels. The results of this test bed will provide the basis for developing an improved long-term design model.

Reproduced with permission of the copyright owner. Further reproduction prohibited without permission.

CHAPTER 6

FINITE ELEMENT RESULTS

The finite element model presented in the previous chapter is employed in this chapter to examine the effect of geometric parameters, material properties and ground water pressure on long-term buckling. The results presented in this chapter are carefully examined in Chapters 7 and 8 to generate new long-term buckling models.

6.1 Matrix of FEA Runs

The ABAQUS results for a matrix of 27 x 27 finite element runs will be described in this section. These 729 runs will include combinations of three levels of gap (0.1%, 0.4%, 0.7%), ovality (0%, 3%, 6%), DR (30, 50, 70), pressure level (0.1, 0.3, 0.5 P_{cr}), creep coefficient A (0.1A, 1A, 10A) and creep exponent n (0.5n, 1n, 1.5n). The buckling times resulting for each of these combinations is given in Appendix A. A total of nine tables are given, one for each A and n combination. Each of these 9 tables contains 3 groups of 27 finite element runs, with each group representing P/ P_{cr} values of 0.1, 0.3 and 0.5.

The parameter values given above were chosen to cover values, which are common in the pipeline rehabilitation industry. The results given and the models developed are not intended to be used outside the bounds of these parameters. For

Reproduced with permission of the copyright owner. Further reproduction prohibited without permission.

example, the variation of the creep properties, A and n, allow the model to easily cover the response of polymeric materials ranging from PVC to polyester, as seen in Table F.1 in Appendix F. The range is also expected to cover some modern polyethylene materials, although the polyethylene material given in Table F.1 would fall slightly outside the bounds of the analysis presented here, as depicted in Figure F.1 in Appendix F.

6.2 Influence of Parameters on Buckling Time

The influence of gap, DR, ovality, creep properties, and groundwater pressure on the buckling time is presented in this section. The results presented here are for a liner / host pipe system with a gap of 0.1%, an ovality of 6%, a DR of 70, creep coefficient of 1A, creep exponent of 1n, and a groundwater pressure which is 30% of the critical pressure. These parameters remain constant throughout this section except when the influence of a parameter is being explored.

6.2.1 Influence of DR

The dimension ratio DR is the fundamental design parameter in pipeline rehabilitation applications. The expected life of a liner depends on the DR value selected for a given external ground water pressure. The effect of DR on liner life is shown in Figure 6.1. For a given lifetime, a lower DR (a thicker liner) can withstand a higher groundwater pressure, as expected. Also, notice that the curves become steeper as pressure is increased. This increasing slope occurs because the critical time approaches zero as the groundwater pressure approaches the critical pressure.

Reproduced with permission of the copyright owner. Further reproduction prohibited without permission.

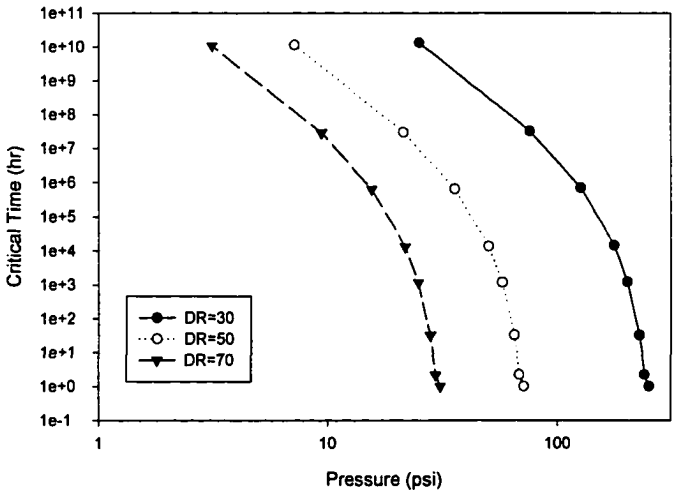

Figure 6.1 Effect of DR on Critical Time as a Function of Pressure

6.2.2 Influence of Gap

The existence of a gap between the liner and its host pipe can reduce the permissible groundwater pressure for a given design life, as shown in Figure 6.2. Notice that he curves become increasingly steep as the groundwater pressure approaches the critical pressure.

6.2.3 Influence of Ovality

It is common for host pipes to become increasingly ovalized as a pipe deteriorates. The effect of ovality on the critical time is shown in Figure 6.3.

Reproduced with permission of the copyright owner. Further reproduction prohibited without permission.

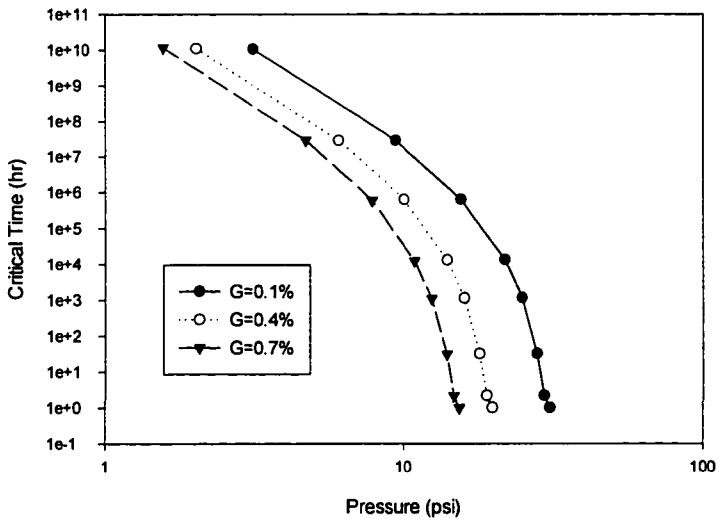

Figure 6.2 Effect of Gap on Critical Time as a Function of Pressure

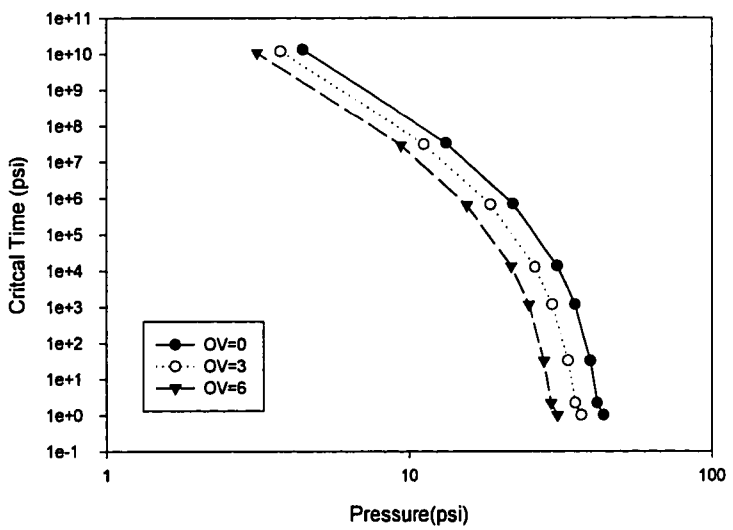

Figure 6.3 Effect of the Ovality on Critical Time as a Function of Pressure

Reproduced with permission of the copyright owner. Further reproduction prohibited without permission.

6.2.4 Influence of Creep Constants

The permissible groundwater pressure for a given design life is a strong function of the resistance of the liner material to creep deformation. Materials that are more creep compliant (deform faster with time for a given stress level) fail more quickly for a given groundwater level. Consequently, the DR of liners for a given lifetime must increase as either A or n is increased. Figures 6.4 and 6.5 show that the creep buckling time is very sensitive to these material properties.

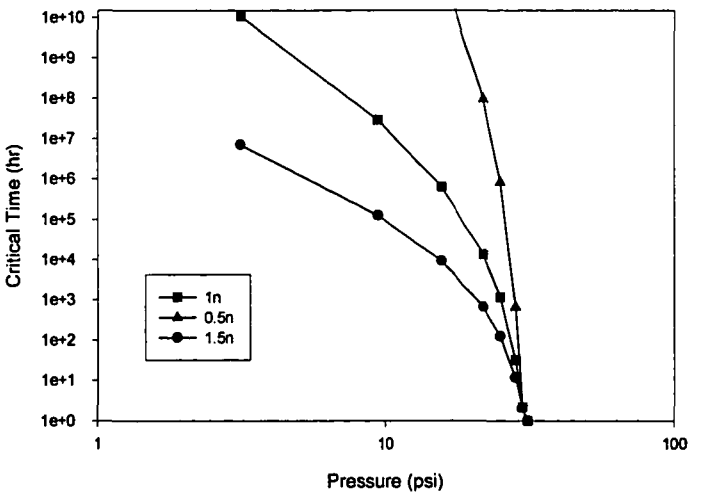

Figure 6.4 Effect of n on Critical Time as a Function of Pressure

Reproduced with permission of the copyright owner. Further reproduction prohibited without permission.

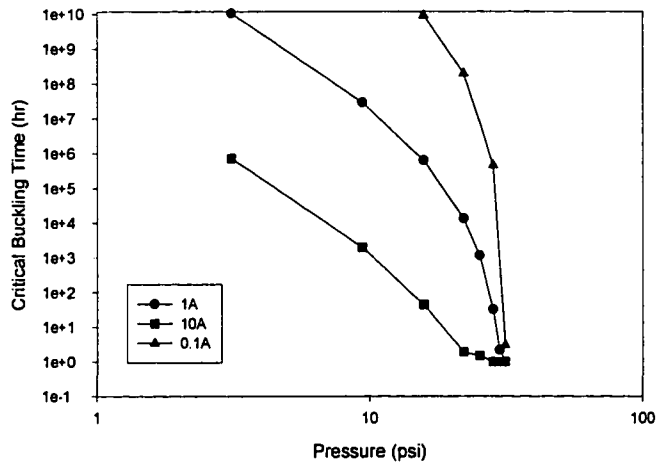

Figure 6.5 Effect of A on Critical Time as a Function of Pressure

6.2.5 Influence of Ground Water Pressure

Higher ground water pressures clearly result in short liner lifetimes. However, the liner lifetime is not linearly related to the pressure ratio, PR (PR = ground water pressure / critical pressure), as shown in Figure 6.6. When PR changes, the entire evolution of stresses and deformations changes due to a different starting point for creep deformation, differences in stress relaxation for different levels of pressure, and different driving forces for eventual elastic instability.

Reproduced with permission of the copyright owner. Further reproduction prohibited without permission.

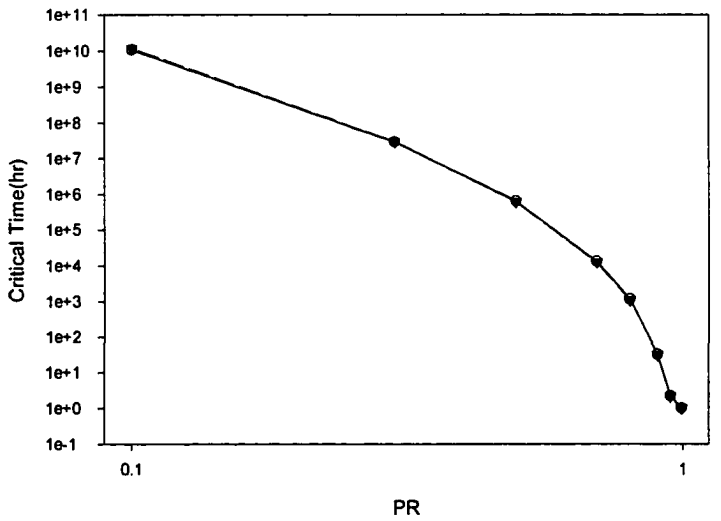

Figure 6.6 Effect of PR on Critical Time as a Function of Pressure

Reproduced with permission of the copyright owner. Further reproduction prohibited without permission.

CHAPTER 7

DETERMINATION OF C^* USING STATISTICAL METHODS

The statistical methods presented in Chapter 3 will be used here to model the finite element results presented in Chapter 6. This modeling will focus on the relationship of C^* with gap, ovality, DR, material properties A and n, and the groundwater pressure. Substituting the groundwater pressure P_g for the long-term P_l in Equation (4-15) leads to

$$P_g = C^* \frac{1}{AEt^n + 1} P_{cr} \tag{7-1}$$

The pressure ratio PR is defined as the ratio of the applied pressure to the critical pressure. For long-term liner applications, the applied pressure is the groundwater pressure. Substituting PR into Equation (7-1) results in

$$PR = C^* \frac{1}{AEt^n + 1} \tag{7-2}$$

Fitting the results of the 729 finite element runs using the SAS statistical software will lead to several equations which can be used to determine C^* for a given set of input parameters. These fitting equations will be embedded into MathCAD, a user-friendly mathematical analysis software package, to allow for the calculation of liner thickness for a given liner lifetime.

Reproduced with permission of the copyright owner. Further reproduction prohibited without permission.

7.1 Statistical Modeling

Recall from Chapter 6 that the finite element runs were carried out to study the effect of six parameters on the buckling time. The parameters studied include three levels of gap (0.1%, 0.4%, 0.7%), ovality (0%, 3%, 6%), DR (30, 50, 70), PR (0.1, 0.3, 0.5), creep coefficient A (0.1A, 1A, 10A), and creep exponent n (0.5n, 1n, 1.5n). Here, PR is defined as the groundwater pressure divided by the critical pressure, and the base value of A and n are 1.21e-7 and 0.24, respectively. The 3 variations of each of the 6 parameters results in 729 ($3^6 = 729$) finite element runs. Using the finite element buckling times in Appendix A along with Equation (7-1) results in a C^* for each set of parameters, as summarized in Appendix B.

7.1.1 C^* as a Function of A, n, Gap, Ovality, PR and DR

The objective of the statistical modeling is to examine the relationships of the six parameters with C^*. Statistical analysis shows that C^* is a function of linear and quadratic combinations of all six of the parameters. For simplicity, let ω= A, q = n, x = gap, y = ovality, z =PR and s = DR, so that C^* can be expressed as

$$C^* = all\ mean\ and\ \text{interaction}\ effect\ \text{of}\ (w, q, x, y, z, s, w^2, q^2, x^2, y^2, z^2, s^2) \qquad (7\text{-}3)$$

In theory, all of the possible arrangements of these linear and quadratic terms could influence C^*.

7.1.2 Simplification by Assuming C^* is a Quadratic Function of PR

To simplify the computations associated with determining which combinations of terms is correlated with C^*, the parameter PR will be removed from Equation (7-3) so that the effect of only five parameters needs to be considered. This removal is accomplished by assuming that C^* is a quadratic function of PR as

Reproduced with permission of the copyright owner. Further reproduction prohibited without permission.

$$C^* = y_0 + y_1 \cdot PR + y_2 \cdot PR^2 \qquad (7\text{-}4)$$

Here, a specific set of y_0, y_1 and y_2 values can be determined by fitting C^* to PR for given values of A, n, gap, DR and ovality. For example, in Table B.1, C^* values of 1.966, 1.617, and 1.359 were fit to PR values of 0.1, 0.3, and 0.5 for the case of DR = 30, gap = 0.1%, ovality = 0%, A = 1.21 e-7($psi^{-1}hr^{-n}$), and n=0.24. This fit resulted in y_0 = 2.1746 (Table C.2), y_1 = -2.2 (Table C.5), and y_2 equal to 1.1375 (Table C.7). Repeating this fitting for each set of DR, gap, ovality, A and n resulted in 243 curve fits. The result of these fits is summarized in Appendix C. For simplicity and speed, this fitting was accomplished using SigmaPlot, a scientific plotting and fitting software package. SigmaPlot is somewhat easier to use than SAS for relatively simple fitting problems. A sample SigmaPlot output screen for these fits is given in Figure 7.1. Notice that R^2 equals to 1.0 in the figure; all of the 243 fits had an R^2 of 1.0.

7.1.3 Determination of Non-negligible Treatment Combinations

The task to determine the relationship between C^* and the geometry, material and loading parameters now boils down to determining the relationships between the 243 sets of y_0, y_1 and y_2 in Appendix C to A, n, gap, DR and ovality. These relationships can be expressed as

$$y_0, y_1, \text{ or } y_2 = \textit{all mean and interaction effct of } (w, q, x, y, s, w^2, q^2, x^2, y^2, s^2) \qquad (7\text{-}5)$$

The dependence of of y_0, y_1 and y_2 on the remaining five parameters still represents a large number of possible combinations of the five linear and five quadratic. There are 3^5, or 243 possible treatment combinations for each y_0, y_1 and y_2 terms. But finding the functional relationships between y_0, y_1 and y_2 and these five parameters is requires much

Reproduced with permission of the copyright owner. Further reproduction prohibited without permission.

less effort than finding the relationship between C^* and all six parameters, as in Equation (7-3).

To determine which of the 243 possible interactions shows significant correlation with y_0, y_1 or y_2, the complete model for each of these three terms was programmed into the SAS software. SAS evaluated the significance of the 243 interaction combinations on y_0, y_1 and y_2, with each term being evaluated separately using the SAS program listed in Appendix E. As described in Chapter 3, in all cases where $P > 0.05$ (Table 3.2), the interaction was determined to be negligible in predicting the value of y_0, y_1 or y_2 (and thus the value of C^*). Any interaction found to be negligible was removed from the potential list of 243 treatment combinations, with the most negligible combination removed during each SAS run. This process was repeated until all negligible terms were removed. A total of 146 treatment combinations of terms were found to be significantly important in the determination of y_0, y_1 and y_2 (and thus C^*). Note that the treatment combinations most important for determining y_0 are not necessarily the most important for determining y_1 and y_2.

After the non-negligible treatment combinations have been determined, SAS was used to fit y_0, y_1 and y_2 as a function of these combinations. The results of this fitting will be presented in the following section.

Reproduced with permission of the copyright owner. Further reproduction prohibited without permission.

Nonlinear Regression

'Automatic Initial Parameter Estimate Functions
F(q)=ape(x,y,2,0,1)
[Parameters]
y0=F(0)[1] "Auto
a=F(0)[2] "Auto
b=F(0)[3] "Auto
[Equations]
f=y0+a*x+b*x^2
fit f to y
[Constraints]
[Options]
tolerance=0.000100
stepsize=100
iterations=100

The regression produces a perfect fit

R = 1.00000000 Rsqr = 1.00000000 Adj Rsqr = >1e20

Standard Error of Estimate = >1e20

	Coefficient
y0	2.1746
a	-2.2000
b	1.1375

Analysis of Variance:

	DF	SS	MS	F	P
Regression	2	0.1856	0.0928	0.0000	>1e20
Residual	0	0.0000	>1e20		
Total	2	0.1856	0.0928		

Figure 7.1 Sigmaplot Regression Output for A=1.21e-7($psi^{-1}hr^{-n}$), n=0.24, DR=30, Ovality=0.0%, and Gap=0.1

Reproduced with permission of the copyright owner. Further reproduction prohibited without permission.

7.2 Formulation of the Long-term Model

The diameter to thickness ratio DR is the dominant design variable for tight fitting pipe liners. The objective of this section is to rewrite the design equations presented earlier in terms of unknown variable DR. Combining Equation (7-2) and (7-4) results in

$$(y_0 + y_1 \cdot PR + y_2 \cdot PR^2)\frac{1}{A \cdot E \cdot t'' + 1} - PR = 0 \tag{7-6}$$

Dividing the equation by PR eliminates the quadratic term on PR, resulting in

$$\frac{y_0}{PR} + y_1 + y_2 \cdot PR - 1 - A \cdot E \cdot t'' = 0 \tag{7-7}$$

The pressure ratio PR is the ratio of the applied pressure to the critical pressure of the liner P_{cr}. Although any short-term buckling model can be embedded into Equation (7-7) to compute P_{cr}, the analysis presented here will employ the short-term buckling model given by Zhu (2000). Using P_{cr} from Equation(2-10) allows PR to be expressed as

$$PR = \frac{P_g}{P_{cr}} = \frac{P_g(1-\nu^2)(DR-1)^m}{a \cdot E} \tag{7-8}$$

where a and m depend on gap, ovality, and longitudinal intrusion imperfections. The coefficient a is computed using Equation (2-11) along with the 27 constants given in Table 2.3. Exponent m is found using Equation (2-12) along with the 27 constants given in Table 2.4.

Reproduced with permission of the copyright owner. Further reproduction prohibited without permission.

Substitution of Equation (7-8) into Equation (7-7) leads to an expression containing a single unknown variable DR as

$$y_1 + \frac{y_0 aE}{P_g(1-\nu^2)(DR-1)^m} + \frac{y_2 \cdot P_g(1-\nu^2)(DR-1)^m}{aE} - 1 - A \cdot E \cdot t'' = 0 \qquad (7\text{-}9)$$

Here, the functions of y_0, y_1 and y_2 depend on gap, ovality, A, and n. They are explicit functions of DR as given below:

$$y_0 = D0 + D1 \cdot DR + D2 \cdot DR^2,$$

$$y_1 = B0 + B1 \cdot DR + B2 \cdot DR^2 \text{ and } y_2 = E0 + E1 \cdot DR + E2 \cdot DR^2 \qquad (7\text{-}10)$$

where *B0*, *B1*, *B2*, *D0*, *D1*, *D2*, *E0*, *E1*, *E2* are coefficients of y_0, y_1 or y_2. These coefficients are functions of gap, ovality, A, and n, as given in Tables 7.1. In this table, gap is *x*, ovality is *y*, A is *w*, and n is *q*.

Substituting Equation (7-10) into Equation (7-9) leads to a single expression by which DR can be determined numerically. This equation was embedded into the MathCAD scientific calculation software to allow the computation of DR and the required thickness of the liner (thickness = OD/DR). The MathCAD file which performs this analysis is given in Figure H.1.

Table 7.1a Constants Used to Compute *D0*

$w^2y^2q^2$	qy^2w^2	x^2y^2	y^2wq	$y\,w^2\,q^2$	ywq	xqy^2	xwq	$w^2\,q^2$
-0.001987	0.00317	0.022254	-0.033594	0.01426	-0.004196	0.020798	0.06072	-0.316604
y^2w^2	x^2y^2	$q\,w^2$	qy^2	wq^2	ψq^2	ωy^2	xy^2	$y\,w^2$
-0.001	-0.007943	0.067729	0.055735	4.098936	-0.890989	0.012275	0.002764	0.003463
ξw	ωq	xq	yq	yw	q^2	w^2	y^2	q
-0.005012	-0.905203	0.251806	0.100385	-0.041971	5.250445	-0.00343	-0.007882	0.171212
w	y	x	1					
0.046288	-0.030546	-0.036573	1.81646					

Table 7.1b Constants Used to Compute *D1*

Reproduced with permission of the copyright owner. Further reproduction prohibited without permission.

xwy^2q	$q^2y^2w^2$	xywq	w^2yq	y w q	$\xi w^2 q^2$	xqy^2	$xw\ y^2$	xyq^2
9.3646e-5	3.496e-6	-0.000336	1.5967e-5	0.00125	5.2204e-5	-8.6757e-5	2.5154e-5	-0.008641
xyw	qy^2	$x\ y^2$	q^2	q	ω	y	1	
1.2393e-5	6.5064e-5	7.4348e-5	-0.052186	0.025041	0.000177	0.000287	-0.005363	

Table 7.1c Constants Used to Compute *D2*

xwy^2q	xwy^2	wq	y w	xy
1.958e-6	-3.55e-7	-1.4642e-5	-4.33e7	1.0688e-5

Table 7.1d Constants Used to Compute *B0*

$x^2y^2w^2q^2$	qy^2w^2	x^2y^2	y^2wq	$y\ w^2\ q^2$	$y\ w^2q$	xqy^2	$qx^2\ y^2$	xyq^2
-0.001454	-0.003941	0.25661	0.076532	-0.004502	-0.011384	-0.658115	0.025661	6.103519
θ^2w^2	ω^2y^2	$q\ w^2$	qy^2	wq^2	ψq^2	$y\ w^2$	xy^2	xwq
1.336916	-17.7277	-0.272074	-0.240348	-17.7277	3.822008	0.008136	0.091319	-0.172437
ξw	yw	xq	q^2	y^2	y	w	q	1
-0.010139	-0.072128	-0.41895	-62.13816	0.013047	0.171701	0.040381	23.48524	-3.831279

Table 7.1e Constants Used to Compute *B1*

$x^2y^2w^2q^2$	$q^2y^2w^2$	$x^2y^2\ w^2$	$y\ w^2q$	$x\ w^2\ q^2$	xqy^2	xyq^2	$qx\ y^2$	ω^2q^2
6.816e-6	0.000131	-1.049e-6	-0.000232	-0.00024	0.009651	-0.07236	0.009651	0.000814
θ^2y^2	ω^2y^2	ξy^2	w^2	q^2	y^2	q	x	1
0.001701	-7.373e-6	-0.001695	-0.000111	0.725935	-7.074e-5	-0.354117	0.000473	0.040129

Table 7.1f Constants Used to Compute *B2*

xwy^2q	$q^2y^2w^2$	wq	y w
2.213e-6	-2.271e-6	8.0412e--5	-0.0000162

Table 7.1g Constants Used to Compute *E0*

qy^2w^2	$qx^2\ y^2$	$y\ w^2\ q^2$	w^2yq	$x\ w^2\ q^2$	$x\ y^2q$	xyq^2	ω^2q^2	ω^2y^2
-0.001079	-0.104203	-0.112635	0.041035	-0.072948	0.316375	1.49439	-0.965618	-4.3306e-5
$q\ w^2$	wq^2	ψq^2	$y\ w^2$	$x\ w^2$	xy	yq	xw	wq
0.196009	15.63413	-5.99158	-0.001089	-0.013146	-0.29653	2.196663	0.289434	-2.76618
q^2	y^2	w	q	y	1			
69.63092	0.028219	-0.124004	-29.20653	-0.363966	3.873929			

Table 7.1h Constants Used to Compute *E1*

Reproduced with permission of the copyright owner. Further reproduction prohibited without permission.

ξyqw^2	$y\,w^2\,q^2$	w^2yq	$x\,w^2q^2$	$x\,y^2q$	$x\,y^2w$	xyq^2	ywq	ω^2q^2
-0.000275	0.002455	-0.000155	0.00432	0.000429	8.436e-5	-0.087623	-0.005643	-0.005905
xy^2	xq	w^2	q^2	x	q	1		
-0.000563	-0.029828	0.000198	-0.681783	0.003796	0.35043	-0.044145		

Table 7.1i Constants Used to Compute *E2*

$xqy^2\,w^2$	$xwqy^2$	$q\,y^2\omega^2$	ξqw^2	xw^2	xy	wq	yw
2.375e-6	-2.66e-5	2.21e-7	-6.253e-6	-2.466e-6	0.000107	8.3122e-5	2.253e-6

7.3 Comparison of the Model with FEA Results

This section compares DR values computed using the MathCAD implementation of the model in Figure H.1 with the finite element results given in Appendix A. To facilitate this comparison, each of the 729 buckling times listed in Appendix A was input into the MathCAD file along with the corresponding values of gap, ovality, A, n and groundwater pressure. The groundwater pressure was chosen for each case such that P_g/P_{cr} would be equal to the PR used in the finite element analysis. The mean error in DR is computed as

$$\text{Mean of Error of DR} = \left(\sum_{i=1}^{N}(\text{DR from MathCAD}_i - \text{DR used in FEA}_i)\right)/N \qquad (7\text{-}11)$$

and the standard deviation in DR was computed as

$$\text{Standard Deviation of DR} = \left(\sum_{i=1}^{N}(\text{DR from MathCAD}_i - \text{DR used in FEA}_i)^2/N\right)^{1/2} \qquad (7\text{-}12)$$

After performing all 729 comparisons, the mean error in DR is 0.305, and the standard deviation is 0.546. For a 12 inch diameter host pipe, this corresponds to a mean error in thickness of 0.001 inches and a standard deviation of 0.003 inches. The maximum difference in DR is 1.965, which corresponds to a maximum difference in thickness of

Reproduced with permission of the copyright owner. Further reproduction prohibited without permission.

0.012 inches. The minimum difference in DR is -1.109, which corresponds to a thickness of -0.014 inches. Table 7.2 presents a portion of the 729 comparisons.

These results show very close agreement between the model presented in this chapter and the finite element results. However, as evidenced by Table 7.1, this model is fairly complex and requires the solution to a nonlinear equation to select liner thicknesses. A simplified version of the model is presented in the next chapter that requires many fewer constants and avoids the requirement of solving a nonlinear equation.

Table 7.2 Comparison of the Results of the Model with the FEA Results

DR	Gap	Ovality	A (psi^{-1} hr^{-n})	n	PR	C*	Time (hrs)	DR model	thickness model (in)	thickness FEA (in)
70	0.1	0	1.21E-07	0.12	0.3	1.394	3.67E+14	69.744	0.172	0.171
70	0.1	3	1.21E-07	0.12	0.3	1.376	3.21E+14	70.065	0.171	0.171
70	0.7	6	1.21E-07	0.12	0.3	1.356	2.73E+14	70.389	0.170	0.171
30	0.4	0	1.21E-07	0.12	0.5	1.261	2.52E+11	29.949	0.401	0.400
30	0.7	0	1.21E-07	0.12	0.5	1.252	2.29E+11	30.011	0.400	0.400
30	0.4	3	1.21E-07	0.12	0.5	1.247	2.16E+11	30.048	0.399	0.400
30	0.7	3	1.21E-07	0.12	0.5	1.245	2.12E+11	30.056	0.399	0.400
50	0.1	0	1.21E-07	0.12	0.5	1.249	2.21E+11	50.071	0.240	0.240
30	0.4	0	1.21E-06	0.24	0.1	1.894	998100	30.142	0.398	0.400
30	0.7	0	1.21E-06	0.24	0.1	2.035	1367000	29.487	0.407	0.400
30	0.1	3	1.21E-06	0.24	0.1	1.847	893000	30.088	0.399	0.400
50	0.1	0	1.21E-06	0.24	0.1	1.884	974000	49.785	0.241	0.240
50	0.4	0	1.21E-06	0.24	0.1	1.889	987000	49.813	0.241	0.240
70	0.1	6	1.21E-06	0.36	0.1	1.979	4.08E+09	69.963	0.172	0.171
70	0.4	6	1.21E-06	0.36	0.1	1.987	4.13E+09	69.845	0.172	0.171
70	0.7	6	1.21E-06	0.36	0.1	2.024	4.36E+09	69.423	0.173	0.171
30	0.1	0	1.21E-06	0.36	0.3	1.73	83990000	30.029	0.400	0.400
30	0.4	0	1.21E-06	0.36	0.3	1.722	88900000	29.944	0.401	0.400
30	0.7	0	1.21E-06	0.36	0.3	1.716	90340000	29.964	0.400	0.400
30	0.1	6	1.21E-06	0.36	0.3	1.659	78500000	29.692	0.404	0.400
30	0.4	6	1.21E-06	0.36	0.3	1.665	79410000	29.922	0.401	0.400

Reproduced with permission of the copyright owner. Further reproduction prohibited without permission.

CHAPTER 8

SIMPLIFICATION OF THE LONG-TERM DESIGN MODEL

8.1 Introduction

The model presented in Chapter 7 accounts for the effects of gap, ovality, DR, groundwater pressure, creep coefficient A, and creep exponent n when determining C^*. The result is a model that contains 146 constants and requires the solution of a nonlinear equation to find DR for long-term liner design. A simplified model with only 18 constants is presented in this chapter. Here, C^* will be assumed to be a function of the long-term material properties, A and n, and the groundwater pressure through PR. The effect of the geometric parameters is modeled by taking the lower-bound solution where the lowest values of C^* for the range of geometric parameters modeled is used. The effect of geometric parameters (gap, ovality, DR, and local imperfections) is assumed to be accounted for in the short-term model by changing the value of P_{cr}.

8.2 Examination of the Influence of Geometrical Parameters on C^*

Before eliminating the dependence of C^* on the geometric parameters, it is prudent to first examine the level of dependence of C^* on these parameters. There are a total of 81 finite element runs corresponding to each pair of A and n values, as tabulated

Reproduced with permission of the copyright owner. Further reproduction prohibited without permission.

in Appendix A. Plotting the 81 C^* values given in Appendix C versus PR for each pair of A and n leads to the nine graphs shown in Figure 8.1. These nine graphs correspond to the nine pairs of A and n values modeled in the finite element test bed. Figure 8.1 shows that there is a relatively small variance in C^* with DR, gap, and ovality.

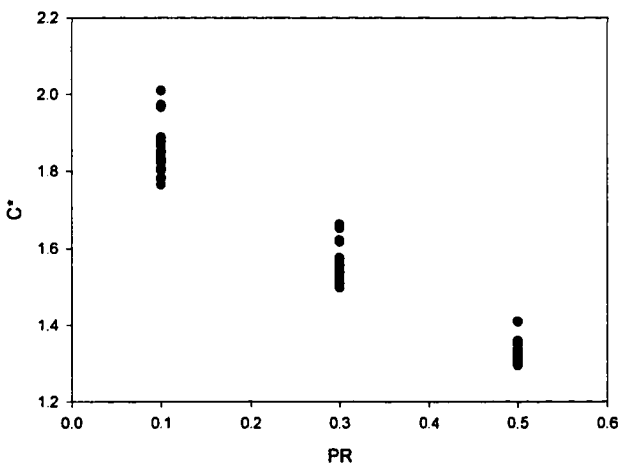

(a) C* verse PR for 81 FEA Runs where A=1.21e-7, n=0.24

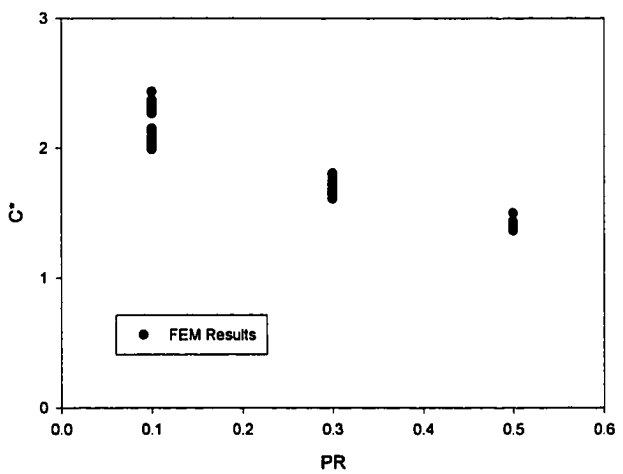

(b) C* verse PR for 81 FEA runs where A=1.21e-7, n=0.36

Reproduced with permission of the copyright owner. Further reproduction prohibited without permission.

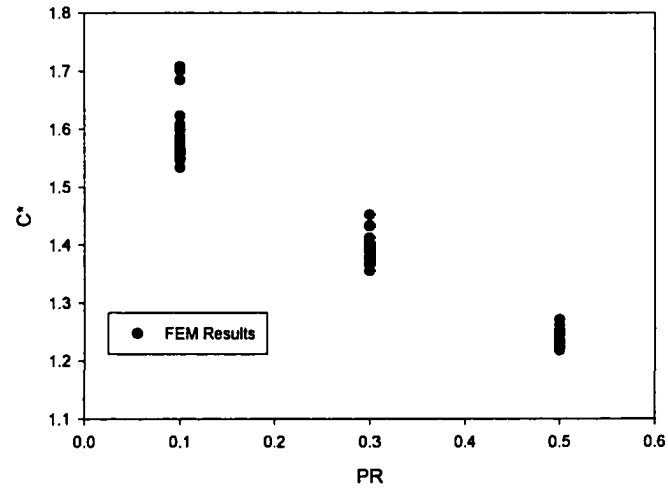

(c) C* verse PR for 81 FEA runs where A=1.21e-7($psi^{-1}hr^{-n}$), n=0.12

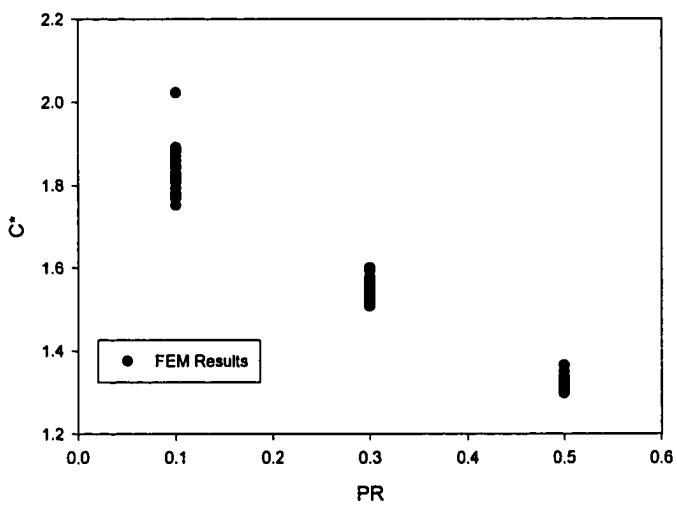

(d) C* verse PR for 81 FEA runs where A=1.21e-8($psi^{-1}hr^{-n}$), n=0.24

Reproduced with permission of the copyright owner. Further reproduction prohibited without permission.

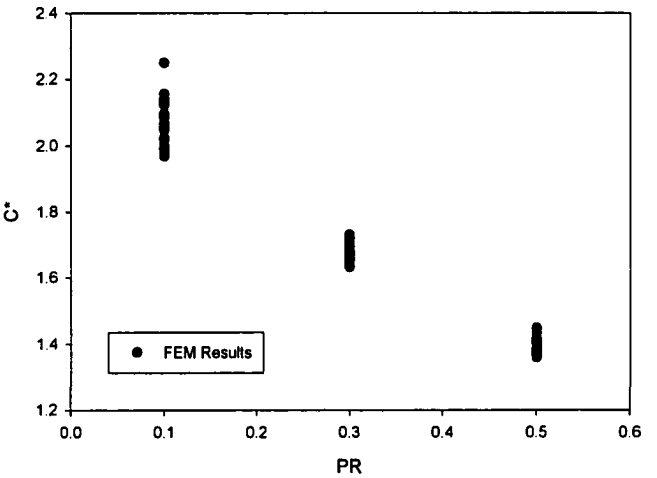

(e) C* verse PR for 81 FEA runs where A=1.21e-8($psi^{-1}hr^{-n}$), n=0.36

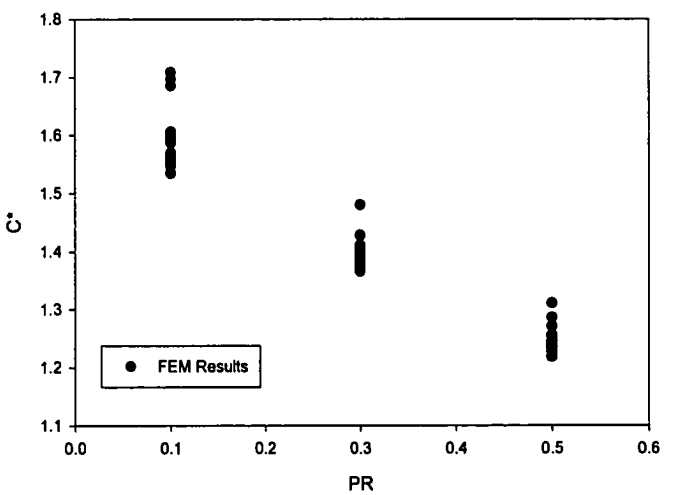

(f) C* verse PR for 81 FEA runs where A=1.21e-8($psi^{-1}hr^{-n}$), n=0.12

Reproduced with permission of the copyright owner. Further reproduction prohibited without permission.

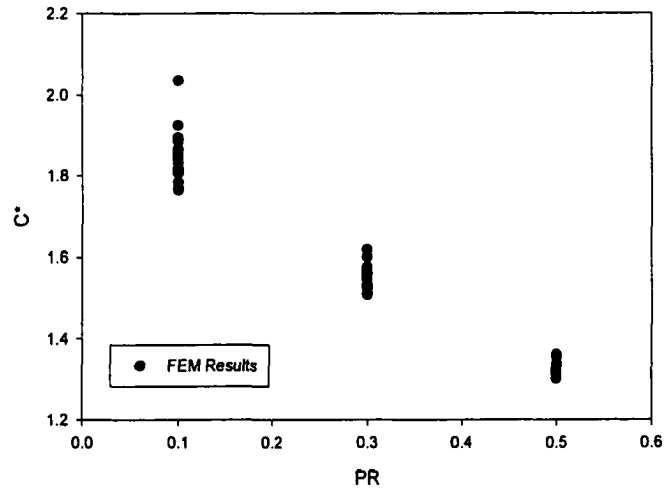

(g) C* verse PR for 81 FEA runs where A=1.21e-6($psi^{-1}hr^{-n}$), n=0.24

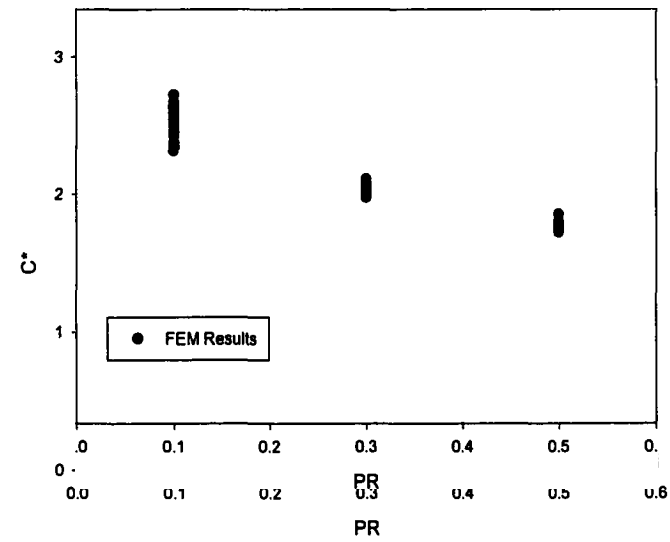

(h) C* verse PR for 81 FEA runs where A=1.21e-6($psi^{-1}hr^{-1}$), n=0.36

Reproduced with permission of the copyright owner. Further reproduction prohibited without permission.

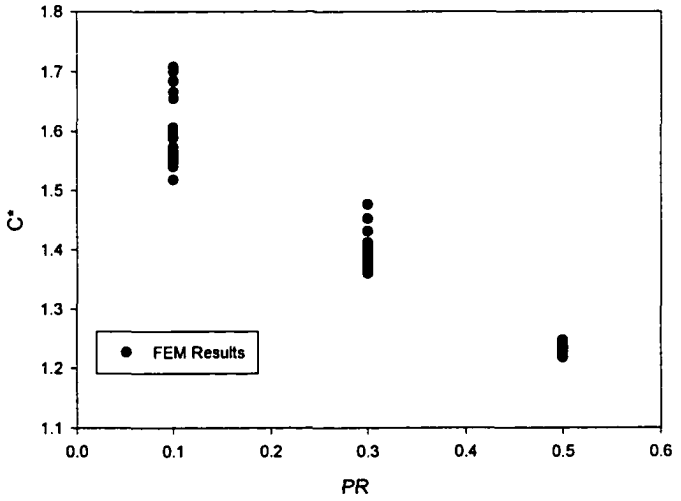

(l) C* verse PR for 81 FEA runs where A=1.21e-6(psi^{-1}hr^{-n}), n=0.12

Figure 8.1 C^* versus PR for Each Combination of A and n
(the Results of 81 FEA Runs are Plotted on Each Graph)

8.3 Simplified Design Model

Due to the relatively small amount of variation in C^* with geometrical parameters, the design model presented in Chapter 7 can be approximated by assuming that C^* is only a function of A, n and PR. Examination of the plots in Figure 8.1 shows that the lower bound for each pair of A and n can be approximated as a straight line. Consequently, the relationship between C* and PR can be given as

$$C^* = y_0 + y_1 \cdot PR \qquad (8\text{-}1)$$

where y_0 and y_1 values can be determined by fitting C^* to PR for given value of A and n. A straight line approximation for A = 1.21e-7 psi^{-1} hr^{-n} and n = 0.24 is shown in Figure 8.2.

Looking carefully at Appendix C shows that the minimum value of C^* for a given pair of A and n most often occurs for an ovality of 6%, a gap of 0.1%, and a DR of 70.

Reproduced with permission of the copyright owner. Further reproduction prohibited without permission.

The original finite element test bed included PR values of 0.1, 0.3 and 0.5. To extend the lower bound model to higher PR levels, additional finite element runs were completed for PR levels of 0.7 and 0.8, as seen Appendix A.10. Although PR values of 0.9 and 0.995 are also included in this table, these values are not used in determining the lower bound solution since the relationship between C^* and PR becomes nonlinear as PR approaches 1.0. Notice that the buckling times approach zero as the pressure approaches P_{cr} (PR approaches 1.0).

SigmaPlot was used to fit y_0 and y_1 in Equation (8-1) for the C^* and PR pairs corresponding to an ovality of 6%, a gap of 0.1%, and a DR of 70. This straight line fit is based on five pairs of C^* and PR, with PR values of 0.1, 0.3, 0.5, 0.7 and 0.8. The fitting results are summarized in Table 8.1.

Table 8.1 SigmaPlot Regression Results for the Lower Bound Model

	y_0	y_1	R^2
1A1n	1.8064	-0.91	0.98804
1A 0.5n	1.5697	-0.6325	0.9918
1A 1.5n	2.0382	-1.19	0.981725
0.1A 1n	1.7985	-0.8985	0.989734
0.1A 1.5n	2.0238	-1.1735	0.984566
0.1A 0.5n	1.5698	-0.632	0.99202
10A 1n	1.8075	-0.8815	0.986752
10A 0.5n	1.4617	-0.44	0.9556
10A 1.5n	2.1273	-1.5175	0.993865

The results of Table 8.1 were embedded into SAS to determine the relationship of y_0 and y_1 to the creep properties A and n. Here, y_0 is assumed to be a quadratic function of material properties A and n and can be expressed as

$$y_0 = c_1 + c_2 \cdot w + c_3 \cdot q + c_4 \cdot w \cdot q + c_5 \cdot w^2 + c_6 \cdot q^2 + c_7 \cdot w^2 \cdot q^2 \qquad (8\text{-}2)$$

Reproduced with permission of the copyright owner. Further reproduction prohibited without permission.

where the coefficients c_i (i = 1,..9) are given in Table 8.2 and w = coefficient A, q = creep exponent n.

Table 8.2 Coefficients Used to Determine y_0

w^2q^2	qw^2	wq^2	wq	q^2	w^2	q	w	1
-1.038e11	2.1624e11	-464451	755578	-0.12421	-1.0648e11	1.9392	-73982	1.338611

The term y_1 can also be expressed as a quadratic function of material properties A and n as

$$y_1 = d_1 + d_2 \cdot w + d_3 \cdot q + d_4 \cdot w \cdot q + d_5 \cdot w^2 + d_6 \cdot q^2 + d_7 \cdot w^2 \cdot q^2 \qquad (8\text{-}3)$$

where d_i (i = 1,..9) are given in Table 8.3.

Table 8.3 Coefficients Used to Determine y_1

w^2q^2	qw^2	wq^2	wq	q^2	w^2	q	w	1
-6.7075e12	2.0698e12	2805836	-1805938	-0.328107	-3.833e8	-2.093035	151566	-0.375834

The simplified model can be formulated by combining Equations (8-1) and (7-2) as

$$\frac{y_0}{PR} + y_1 - 1 - A \cdot E \cdot t^n = 0 \qquad (8\text{-}4)$$

Recall that the pressure ratio PR is the ratio of the applied ground water pressure to the critical pressure P_{cr}. As with the model presented in Chapter 7, the analysis here will employ the short-term buckling model given by Zhu(2000). Substitution of Equation (7-8) into Equation (8-4) leads to an expression where DR is the only unknown variable:

$$DR = 1 + \left[\frac{a \cdot y_0 \cdot E}{P_g \cdot (1 + AEt^n - y_1)(1 - \nu^2)} \right]^{1/m} \qquad (8\text{-}5)$$

A MathCAD implementation of this model is given in Figure H.2. Note that this expression can be used to design liners for any lifetime t.

Reproduced with permission of the copyright owner. Further reproduction prohibited without permission.

8.4 Comparison of the Simply Model with FEA Results

This section compares DR values computed using the MathCAD implementation of the model in Figure H.2 with finite element results given in Appendix A. To facilitate this comparison, each of 729 buckling times listed in Appendix A was input into the MathCAD file along with the corresponding values of gap, ovality, A, n and ground water pressure. The groundwater pressure was chosen for each case such that P_g/P_{cr} would be equal to the PR used in the finite element analysis. The mean error and standard deviation in DR is computed using Equation (7-11) and (7-12).

After performing all 729 comparisons, the mean error in DR is -0.397, and the standard deviation of the error is 0.842. Here, a negative error in the mean DR implies that the model will have a smaller DR than the corresponding FEA result. This means that on average, the model will be conservative relative to the FEA results, since a smaller DR implies a larger thickness for a given host pipe size. This conservative result is expected since the simplified model is a lower-bound model. The difference in DR between the FEA results and the simplified model ranged from -4.453 to 1.085.

For a 12 inch diameter host pipe, the mean error in DR corresponds to a mean error in thickness of 0.003 inches and a standard deviation in error of 0.007 inches. The difference between the thickness computed using FEA and the thickness computed using the simplified model ranges from -0.021 inches to 0.096 inches. Table 8.4 presents a portion of the 729 comparisons.

Thus, the simplified model is able to accurately recreate the finite element results based on the input data. The simplified model is much less complex to implement and is consequently the model put forth in this thesis as an improved liner design model.

Reproduced with permission of the copyright owner. Further reproduction prohibited without permission.

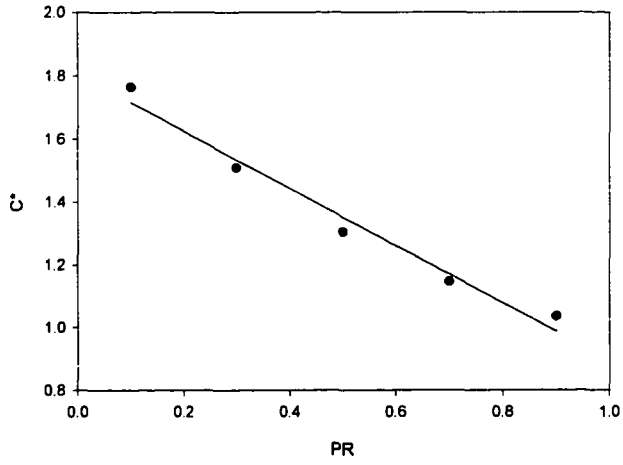

Figure 8 .2 C^* versus PR for A = 1.21e-7(psi^{-1} hr^{-n}) and n = 0.24 with a Linear Fit to the Lower Data Points Shown.

Table 8.4 Comparison of the Results of the Simplified Model with the FEA Results

DR	Gap	Ovality (%)	A (psi^{-1} hr^{-n})	n	PR	Time (hrs)	DR simplified	thickness simplified (in)	thickness FEA (in)
50	0.7	6	1.21E-08	0.24	0.1	1.802E+14	48.949	0.25	0.24
70	0.1	0	1.21E-08	0.24	0.1	1.987E+14	67.674	0.18	0.171
30	0.1	6	1.21E-08	0.24	0.3	4.661E+11	29.960	0.40	0.4
30	0.4	6	1.21E-08	0.24	0.3	4.715E+11	29.945	0.40	0.4
50	0.7	6	1.21E-08	0.24	0.3	4.642E+11	49.954	0.24	0.24
70	0.4	6	1.21E-08	0.24	0.3	4.406E+11	70.155	0.17	0.171
30	0.7	6	1.21E-08	0.24	0.5	9.584E+09	30.231	0.40	0.4
50	0.1	0	1.21E-08	0.24	0.5	1.078E+10	50.193	0.24	0.24
70	0.1	0	1.21E-08	0.24	0.5	1.045E+10	70.361	0.17	0.171
30	0.4	6	1.21E-08	0.36	0.1	4.779E+09	29.070	0.41	0.4
30	0.7	6	1.21E-08	0.36	0.1	4.614E+09	29.224	0.41	0.4
50	0.1	0	1.21E-08	0.36	0.1	5.09E+09	47.844	0.25	0.24
70	0.1	0	1.21E-08	0.36	0.1	5.01E+09	67.095	0.18	0.171
30	0.7	6	1.21E-07	0.12	0.1	4.125E+19	29.574	0.41	0.4
70	0.4	6	1.21E-07	0.12	0.1	3.585E+19	69.330	0.17	0.171
50	0.4	6	1.21E-07	0.12	0.3	3.115E+14	50.088	0.24	0.24
70	0.1	6	1.21E-07	0.12	0.3	2.967E+14	70.254	0.17	0.171
30	0.7	3	1.21E-07	0.12	0.5	2.121E+11	30.056	0.40	0.4
30	0.7	6	1.21E-07	0.12	0.5	1.808E+11	30.152	0.40	0.4
50	0.7	6	1.21E-07	0.12	0.5	1.623E+11	50.365	0.24	0.24
70	0.7	6	1.21E-07	0.12	0.5	1.555E+11	70.574	0.17	0.171
30	0.1	0	1.21E-07	0.24	0.1	1.727E+10	28.447	0.42	0.4
50	0.1	0	1.21E-07	0.24	0.5	733100	50.222	0.24	0.24
50	0.7	6	1.21E-07	0.24	0.5	621900	50.506	0.24	0.24

Reproduced with permission of the copyright owner. Further reproduction prohibited without permission.

CHAPTER 9

EVALUATION OF THE

DESIGN MODEL

The goal when designing liners installed in partially deteriorated host pipes is to choose the appropriate liner thickness so that the liner will be able to resist the applied groundwater pressure for the desired lifetime, which is commonly taken as 50 years. In this chapter, the models presented in Chapters 7 and 8 will be evaluated by comparing them to the results of long-term liner buckling experiments conducted at the Trenchless Technology Center at Louisiana Tech University. The DR values computed using the models will also be compared to DR values computed using ASTM F1216 and to the DR computed by embedding a long-term modulus into a short-term buckling model with no correction factor (that is, for $C^* = 1$).

9.1 Comparison with the Experimental Data

The material properties (E, 1A and 1n) used to simulate the response of the liners in this thesis is based on the CPAR Insituform Enhanced Product. To evaluate the ability of the models in Chapters 7 and 8 to predict the response of liners in the field, the liner buckling data for the CPAR Insituform Enhanced Product (Appendix Table F.3) is plotted alongside the models on a pressure versus time plot in Figure 9.1. The models are evaluated using a DF of 53.2 (the average DR in the experiments), a gap of 0.246%, and an ovality of 0%. The material properties given in Appendix Table F.1 for the polyester

Reproduced with permission of the copyright owner. Further reproduction prohibited without permission.

product are used, since this data corresponds to the Insituform Enhanced Product tested in the CPAR experiments (Lin, 1995). Since the buckling times corresponding to the applied pressure level of the experiments is required for comparison, the models of Chapters 7 and 8 are rewritten to solve for the buckling time as a function of geometry, material properties and pressure level. The MathCAD implementations of these models are given in Appendix Tables H.3, and H.4, respectively.

Figure 9.1 shows that the models accurately represent the experimental data on a log-log plot. Notice that the full model from Chapter 7 and the simplified model from Chapter 8 fall almost exactly on top of one another. This further confirms that the simplified model is an accurate representation of the more complete full model.

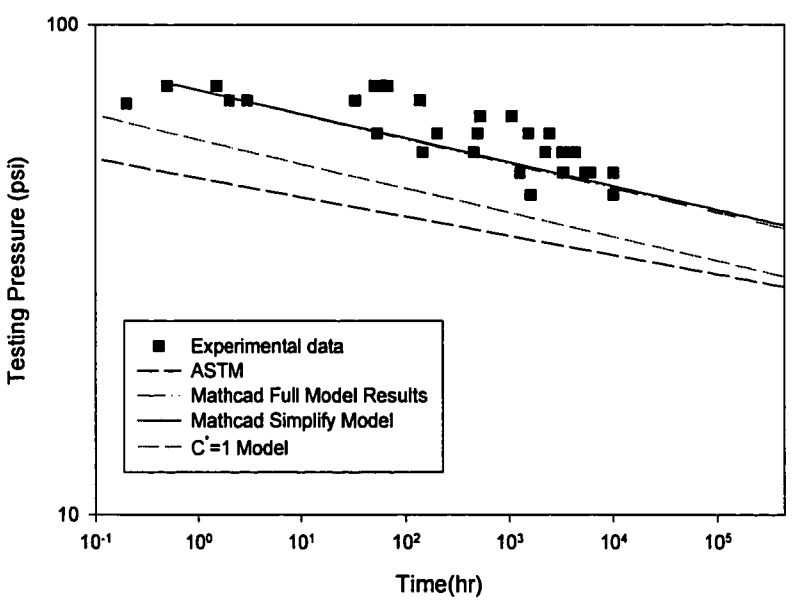

Figure 9.1 Comparison of the Long-term Models with Experimental Data

Reproduced with permission of the copyright owner. Further reproduction prohibited without permission.

9.2 Comparison with Other Models

This thesis focuses on the accurate determination of the C^* parameter which is intended to provide a link between short-term and long-term liner buckling models. The design current practice is to embed a long-term modulus into a short-term liner buckling model to predict long-term response. The long-term modulus is often taken as a fraction of the short-term modulus (such as 0.5 times the short-term modulus) or as a creep modulus that decays with time. The worth of the research performed in this thesis can be quantified by comparing liner designs using the proposed design model (the simplified model) to other models with C^* equal to 1.0. Note that the P_{cr} predicted from any short-term model could be used in Equation (7-1) to predict long-term response, assuming the elastic modulus and the creep constants A and n for the material are known. However, this thesis has employed the short-term model of Zhu (2000) to predict P_{cr}.

Figure 9.1 also shows a plot of the applied pressure versus time for the case of C^* equal to 1.0. It is clear that the proposed design model provides a much closer fit to the experimental data. Notice that both lines have identical slopes, as is expected since the C^* factor acts to produce a vertical shift on a log pressure versus log time. The ASTM F1216 model is also plotted in Figure 9.1. The ASTM line is based on only two points: 1) the 50 year buckling pressure as computed from Equation 2.24, and 2) the short-term pressure which is assumed to occur at a time of 0.1 hours. Notice that the ASTM model very conservative for this combination of geometry and material properties.

Table 9.1 shows the variation in DR with the groundwater pressure for a time of 438,000 hrs (50 years), a gap of 0.4%, an ovality of 3%, a creep coefficient of 0.5A (6.05e-8 psi^{-1} hr^{-n}) and a creep exponent of 0.75n (0.18). The DR decreases with

Reproduced with permission of the copyright owner. Further reproduction prohibited without permission.

increasing pressure, as expected. Also, at low pressure levels, DR values in excess of 70 are predicted. Although these numbers follow the correct trend, the proposed design model may give inaccurate results for DR values less than 30 or greater than 70. The difference between the proposed model and the model with a C^* of 1.0 decreases with increasing groundwater pressure. ASTM F1216 requires DR values 20% to 30% smaller (thickness values 20% to 30% larger) than the proposed model.

Table 9.2 gives the variation in DR with changing creep coefficient for a time of 438,000 hrs (50 years), a gap of 0.4%, an ovality of 3%, a groundwater pressure of 15 psi, and a creep exponent of 1n (0.24). It is clear that the differences between the proposed model and model with a C^* of 1.0 increases as the material becomes more creep compliant (as A increases).

Table 9.3 shows the variation of DR with n for a time of 438,000 hrs (50 years), a gap of 0.4%, an ovality of 3%, a groundwater pressure of 15 psi, and a creep coefficient of 0.5A (6.05e-8 psi^{-1} hr^{-n}). This table shows a similar trend to Table 9.2. As the material becomes more creep compliant, the deviation of the proposed model from the model with a C^* of 1.0 increases.

9.3 Discussion of the Proposed (Simplified) Model

Tables 9.2 and 9.3 show that the difference between the proposed model and ASTM F1216 changes from positive (the proposed model requres a thinner liner) to negative (the proposed model requries a thicker liner) as the material becomes more creep compliant (creeps faster for a given stress level). This is because ASTM F1216 does not directly account for the creep behavior of the material and the same value of the

Reproduced with permission of the copyright owner. Further reproduction prohibited without permission.

short-term modulus is used for all of the comparisons. In many materials, an increase in A would be reflected by a decrease in the short-term modulus of the material, since decreased elastic stiffness is related to decreased bond strength in the polymer. This decrease in bond strength typically results in a corresponding decrease in the resistance to creep deformation. This means that the differences between the proposed model and ASTM F1216 would not increase to the levels shown in Table 9.2 and 9.3. However, long-term properties for materials with identical short-term properties will vary depending on the microstructure of the material. Long-term liner design should be based on long-term properties, not on short-term properties.

Tables 9.4b shows the variation in C^* for the material property combinations listed in Table 9.4a for a 50 year lifetime. Notice that C^* increases with increasing A or n when the elastic modulus is constant, as was noted in earlier when referring to Tables 9.2 and 9.3. Increases in the creep compliance of the material allows for more stress relaxation as the liner deforms. This increased relaxation postpones elastic instability.

A number of different liner design models were analyzed in Chapter 4. These models were based on the extension of short-term liner buckling models to long-term buckling models by incorporating a long-term elastic modulus (See Table 4.1). At a minimum, long-term models should be based on some sort of long-term material or structural testing. While the models of Straughan, Falter, and McAlpine do include (or are capable of including) a time varying elastic modulus, they provide no further correction between the short-term and long-term buckling models. That is, C^* is 1.0 for all of these models. This chapter has clearly shown that C^* values other than 1.0 are typical in liner design. Figure 9.1 shows that the proposed liner design model, which is

Reproduced with permission of the copyright owner. Further reproduction prohibited without permission.

based on a C^* value of 1.30, provides a much closer match to experimental results than a model with C^* equal to 1.0.

Other liner design models, such as the models given by Zhao (1999), require finite element results to derive the constants to be used in liner design. Thus, if a new liner material is developed, short-term material characterization, long-term material characterization, and long-term finite element analysis (or long-term liner buckling experiments) would be required to fit the constants in the model. However, the proposed model only requires short-term and long-term material characterization results.

This chapter has demonstrated that the proposed liner design model offers a significant improvement over other liner design models by providing for an accurate extension from short-term to long-term behavior. This extension is the major contribution of this research. The following chapter summarizes the key points of the proposed models and gives recommendations for future research.

Table 9.1 Comparison of DR Values Computed Using Various Pressures for Time = 438,000 hrs (50 years), Gap = 0.4%, Ovality = 3%, 0.5A (6.05e-8 psi^{-1} hr^{-n}) and 0.75n (0.18)

Groundwater Pressure	DR (Simplified Model)	DR ($C^* = 1$)	Relative Difference	DR (ASTM F1216)	Relative Difference
15 psi	85.58	78.41	8.3%	60.55	29.2%
25 psi	70.27	64.73	7.9%	51.22	27.1%
30 psi	65.50	60.45	7.7%	48.26	26.3%
35 psi	58.56	57.064	2.6%	45.89	21.6%

Reproduced with permission of the copyright owner. Further reproduction prohibited without permission.

Table 9.2 Comparison of DR Values Computed Using Various A Values for Time = 438,000 hrs (50 years), Gap = 0.4%, Ovality = 3%, Pg = 15 psi and 1n (0.24)

A (psi^{-1} hr^{-n})	DR (simplified model)	DR (C* = 1)	Relative Difference	DR (ASTM F1216)	Relative Difference
0.75A (9.07e-8)	72.154	66.144	8.3%	60.55	16.1%
1A (1.21e-7)	69.10	62.27	9.9%	60.55	12.4%
2A (2.42e-7)	60.40	52.28	13.4%	60.55	-0.2%
5A (6.05e-7)	47.53	39.53	16.8%	60.55	-27.4%
10A (1.21e-6)	38.16	31.29	18%	60.55	-58.7%

Table 9.3 Comparison of DR Values Computed Using Various n Values for Time = 438,000 hrs (50 years), Gap = 0.4%, Ovality = 3%, Pg = 15 psi and 1A (1.21e-7 psi^{-1} hr^{-n})

n	DR (simplified model)	DR (C* = 1)	Relative Difference	DR (ASTM F1216)	Relative Difference
0.85n (0.204)	73.59	68.43	7.0%	60.55	17.7%
1n (0.240)	69.10	62.27	9.9%	60.55	12.4%
1.2n (0.288)	61.91	53.30	13.9%	60.55	2.2%
1.5n (0.360)	49.74	40.18	20.0%	60.55	-21.8%

Table 9.4a Matrix of Creep Parameters

0.1A 0.5n	0.1A 1n	0.1A 1.5n
1A 0.5n	1A1n	1A 1.5n
10A 0.5n	10A 1n	10A 1.5n

Table 9.4b C^* for a 50 Year Life for the Material Combinations in Table 9.4a

0.7621	1.032	1.181413
1.064648	1.299242	1.725839
1.307449	1.745243	2.355492

Reproduced with permission of the copyright owner. Further reproduction prohibited without permission.

CHAPTER 10

CONCLUSIONS AND RECOMMENDATIONS

10.1 Conclusions

The ABAQUS finite element software was employed to examine the effect of geometric parameters, material properties and groundwater pressure on the expected lifetime of sewer rehabilitation liners. Factorial analysis of the finite element results was carried out using the SAS and SigmaPlot software programs, leading to the development of two liner design models. These models provide a bridge by which short-term buckling models can be used in long-term liner design. Details of the work performed and of the resulting models developed are given below.

- Most of the existing liner design models, including the recommended ASTM model, are based on extension of short-term liner buckling models to long-term buckling models by using a long-term modulus in place of the short-term elastic modulus.
- Substitution of a long-term (or creep) modulus into a short-term liner buckling model is not theoretically valid, although this has become common practice due to its simplicity. Reasons for these inaccuracies include stress relaxation, evolving stresses, and the continued dominance of the instantaneous elastic modulus (not the decaying creep modulus) as the material property governing buckling.

Reproduced with permission of the copyright owner. Further reproduction prohibited without permission.

- Finite element analysis and statistical methods were used to examine the extension of short-term buckling models to long-term buckling models.
- The ABAQUS finite element software package was used to simulate the long-term response of liners as a function of geometry, material properties, and groundwater pressure.
- The finite element test bed included 729 combinations of DR (30, 50, 70), gap (0.1%, 0.4% and 0.7%), ovality (0%, 3%, and 6%), pressure level (0.1, 0.3, 0.5 times P_{cr}), creep coefficient (0.1A, 1A and 10A where A = 1.21e-7 psi^{-1} hr^{-n}), and creep exponent (0.5n, n, 1.5n where n = 0.24). These material properties correspond to a polyester liner material tested at the TTC.
- A parameter C^*, which is first defined in Equation (4-1), is proposed to extend short-term buckling models to long-term buckling models.
- Using statistical methods, C^* is determined as a function of linear and quadratic combinations of gap, ovality, DR, A, n and groundwater pressure. The expressions for computing C^*, which are given in Equations (7-4) and (7-10), contain 146 constants.
- The model given in Equation (7-9) can be solved numerically to determine DR for any combination of geometry, material properties and groundwater pressure covered by the range of the test bed. This model was shown to agree with the FEA results, with a mean error of 0.305 on DR.
- Due to the large number of terms and the required numerical solution of the full model, a simplified version of the model was given in Equation (8-5). This model only considers the effect of groundwater pressure and creep constants. The C^*

Reproduced with permission of the copyright owner. Further reproduction prohibited without permission.

used in this model is given in Equation (8-1) through (8-3) is based on 18 constants. This model was shown to have good agreement with the FEA results, with a mean error of -0.397 on DR.

- The simplified model was shown in Figure 9.1 to fall on top of the experimental liner buckling results, while a similar model with no correction factor, C^*, fell significantly below the experimental data.
- The correction factor, C^*, is shown to increase with an increase in the creep compliance of the liner material. C^* values were seen to almost always be greater than 1.0, with C^* equal to 1.30 for a polyester material tested at the TTC when a lifetime of 50 years is desired.
- In general, C^* was found to range from about 1.2 to around 2.5. This means that the buckling pressures predicted by using extended short-term design models will be off by a factor ranging from 1.2 to 2.5.
- The simplified model is proposed as a new design model for tight fitting sewer rehabilitation liners.

10.2 Recommendations

The present study indicates that there is a need for the further study of C^* values in the liner buckling design model. Recommendations for future research are given below:

- Further study should be conducted to examine the effect of Young's modulus, E, on both the short-term and long-term design models.

Reproduced with permission of the copyright owner. Further reproduction prohibited without permission.

- The effect of local intrusions and thickness variations should be modeled to determine their effect on C^*. Realistic models of these imperfections would involve three-dimensional finite element analyses.
- Evaluating the influence of additional parameters, as suggested above, would greatly expand the number of terms in a factorial analysis and would increase the complexity of the resulting model. Alternate approaches, such as artificial neural networks to quantify the influence of many parameters on a dependent variable, are available in the literature. New models based on a greater number of geometric and material parameters could be developed based on these approaches.

Reproduced with permission of the copyright owner. Further reproduction prohibited without permission.

APPENDIX A

FINITE ELEMENT RESULTS

Reproduced with permission of the copyright owner. Further reproduction prohibited without permission.

Reproduced with permission of the copyright owner. Further reproduction prohibited without permission.

Table A.1 FEA Results for Material Properties A=1.21e-7($psi^{-1}hr^{-n}$), n=0.24

Buckling times for P/P_{cr} = 0.1 and creep coefficients A = 1A, n=1n									
	OV=0%			OV=3%			OV=6%		
	G=0.1%	G=0.4%	G=0.7%	G=0.1%	G=0.4%	G=0.7%	G=0.1%	G=0.4%	G=0.7%
DR=30	1.727E+10	1.75E+10	1.899E+10	1.307E+10	1.33E+10	1.24E+10	1.312E+10	1.32E+10	1.44E+10
DR=50	1.315E+10	1.372E+10	1.4E+10	1.122E+10	1.256E+10	1.286E+10	1.121E+10	1.17E+10	1.192E+10
DR=70	1.309E+10	1.312E+10	1.415E+10	1.17E+10	1.254E+10	1.267E+10	1.07E+10	1.11E+10	1.171E+10
Buckling times for P/P_{cr} = 0.3 and creep coefficients A = 1A, n=1n									
	OV=0%			OV=3%			OV=6%		
	G=0.1%	G=0.4%	G=0.7%	G=0.1%	G=0.4%	G=0.7%	G=0.1%	G=0.4%	G=0.7%
DR=30	4.153E+07	4.223E+07	4.798E+07	3.467E+07	3.510E+07	4.642E+07	3.175E+07	3.412E+07	4.345E+07
DR=50	3.548E+07	3.583E+07	3.637E+07	3.132E+07	3.21E+07	3.235E+07	2.948E+07	2.951E+07	2.986E+07
DR=70	3.311E+07	3.365E+07	3.481E+07	3.047E+07	3.190E+07	3.138E+07	2.897E+07	2.901E+07	2.941E+07
Buckling times for P/P_{cr} = 0.5 and creep coefficients A = 1A, n=1n									
	OV=0%			OV=3%			OV=6%		
	G=0.1%	G=0.4%	G=0.7%	G=0.1%	G=0.4%	G=0.7%	G=0.1%	G=0.4%	G=0.7%
DR=30	8.341E+05	7.982E+05	1.060E+06	7.387E+05	7.264E+05	7.221E+05	6.920E+05	6.883E+05	6.537E+05
DR=50	7.331E+05	7.391E+05	7.458E+05	6.780E+05	6.77E+05	6.762E+05	6.582E+05	6.420E+05	6.219E+05
DR=70	6.923E+05	7.019E+05	7.030E+05	6.559E+05	6.678E+05	6.453E+05	6.34E+05	6.320E+05	6.044E+05

Reproduced with permission of the copyright owner. Further reproduction prohibited without permission.

Table A.2 FEA Results for Material Properties A=1.21e-7 ($psi^{-1}hr^{-n}$), n=0.36

Buckling times for P/P_{cr} = 0.1 and creep coefficients A = 1A, n=1.5n									
	OV=0%			OV=3%			OV=6%		
	G=0.1%	G=0.4%	G=0.7%	G=0.1%	G=0.4%	G=0.7%	G=0.1%	G=0.4%	G=0.7%
DR=30	1.123E+07	1.152E+07	1.243E+07	8.360E+06	8.543E+06	8.645E+06	7.486E+06	7.789E+06	7.942E+06
DR=50	1.090E+07	1.100E+07	1.120E+07	7.562E+06	7.83E+06	7.912E+06	7.040E+06	7.50E+06	7.780E+06
DR=70	1.012E+07	1.030E+07	1.056E+07	7.260E+06	7.261E+06	7.456E+06	7.030E+06	7.01E+06	6.921E+06
Buckling times for P/P_{cr} = 0.3 and creep coefficients A = 1A, n=1.5n									
	OV=0%			OV=3%			OV=6%		
	G=0.1%	G=0.4%	G=0.7%	G=0.1%	G=0.4%	G=0.7%	G=0.1%	G=0.4%	G=0.7%
DR=30	1.603E+05	1.677E+05	1.723E+05	1.401E+05	1.397E+05	1.387E+05	1.313E+05	1.305E+05	1.293E+05
DR=50	1.441E+05	1.483E+05	1.523E+05	1.308E+05	1.36E+05	1.372E+05	1.245E+05	1.29E+05	1.210E+05
DR=70	1.315E+05	1.450E+05	1.478E+05	1.282E+05	1.282E+05	1.350E+05	1.240E+05	1.29E+05	1.176E+05
Buckling times for P/P_{cr} = 0.5 and creep coefficients A = 1A, n=1.5n									
	OV=0%			OV=3%			OV=6%		
	G=0.1%	G=0.4%	G=0.7%	G=0.1%	G=0.4%	G=0.7%	G=0.1%	G=0.4%	G=0.7%
DR=30	1.114E+04	1.090E+04	1.331E+04	1.012E+04	1.008E+04	1.005E+04	9.598E+03	9.431E+03	9.266E+03
DR=50	1.017E+04	1.040E+04	1.050E+04	9.598E+03	9.66E+03	9.471E+03	9.202E+03	9.285E+03	9.103E+03
DR=70	1.010E+04	1.000E+04	1.015E+04	9.382E+03	9.382E+03	9.353E+03	9.13E+03	9.129E+03	8.984E+03

Reproduced with permission of the copyright owner. Further reproduction prohibited without permission.

Table A.3 FEA Results for Material Properties A=1.21e-7($psi^{-1}hr^{-n}$), n=0.12

Buckling times for P/P_{cr} = 0.1 and creep coefficients A = 1A, n=0.5n									
	OV=0%			OV=3%			OV=6%		
	G=0.1%	G=0.4%	G=0.7%	G=0.1%	G=0.4%	G=0.7%	G=0.1%	G=0.4%	G=0.7%
DR=30	7.645E+19	8.314E+19	8.619E+19	4.256E+19	4.369E+19	4.499E+19	3.890E+19	4.012E+19	4.125E+19
DR=50	5.469E+19	5.055E+19	4.810E+19	3.894E+19	4.02E+19	4.003E+19	3.623E+19	3.741E+19	3.845E+19
DR=70	4.770E+19	4.232E+19	3.920E+19	3.653E+19	3.967E+19	3.810E+19	3.320E+19	3.585E+19	3.612E+19
Buckling times for P/P_{cr} = 0.3 and creep coefficients A = 1A, n=0.5n									
	OV=0%			OV=3%			OV=6%		
	G=0.1%	G=0.4%	G=0.7%	G=0.1%	G=0.4%	G=0.7%	G=0.1%	G=0.4%	G=0.7%
DR=30	5.664E+14	4.872E+14	4.948E+14	4.203E+14	3.845E+14	3.774E+14	3.620E+14	3.431E+14	3.217E+14
DR=50	4.191E+14	3.970E+14	3.960E+14	3.972E+14	3.37E+14	3.324E+14	3.111E+14	3.115E+14	3.072E+14
DR=70	3.669E+14	3.608E+14	3.586E+14	3.211E+14	3.162E+14	3.100E+14	2.967E+14	2.992E+14	2.731E+14
Buckling times for P/P_{cr} = 0.5 and creep coefficients A = 1A, n=0.5n									
	OV=0%			OV=3%			OV=6%		
	G=0.1%	G=0.4%	G=0.7%	G=0.1%	G=0.4%	G=0.7%	G=0.1%	G=0.4%	G=0.7%
DR=30	2.828E+11	2.520E+11	2.286E+11	2.319E+11	2.156E+11	2.121E+11	2.091E+11	1.932E+11	1.808E+11
DR=50	2.211E+11	2.130E+11	1.913E+11	1.962E+11	1.88E+11	1.842E+11	1.810E+11	1.780E+11	1.623E+11
DR=70	1.949E+11	1.900E+11	1.892E+11	1.810E+11	1.810E+11	1.676E+11	1.72E+11	1.707E+11	1.555E+11

Reproduced with permission of the copyright owner. Further reproduction prohibited without permission.

Table A.4 FEA Results for Material Properties A=1.21e-8($psi^{-1}hr^{-n}$), n=0.24

Buckling times for P/P_{cr} = 0.1 and creep coefficients A = 0.1A, n=1n									
	OV=0%			OV=3%			OV=6%		
	G=0.1%	G=0.4%	G=0.7%	G=0.1%	G=0.4%	G=0.7%	G=0.1%	G=0.4%	G=0.7%
DR=30	2.1E+14	2.13E+14	2.87E+14	1.9E+14	1.92E+14	1.98E+14	1.78E+14	1.85E+14	1.93E+14
DR=50	2.1E+14	2.11E+14	2.12E+14	1.82E+14	1.8E+14	1.69E+14	1.59E+14	1.75E+14	1.8E+14
DR=70	1.19E+14	2.03E+14	2.08E+14	1.6E+14	1.69E+14	1.63E+14	1.52E+14	1.65E+14	1.75E+14
Buckling times for P/P_{cr} = 0.3 and creep coefficients A = 0.1A, n=1n									
	OV=0%			OV=3%			OV=6%		
	G=0.1%	G=0.4%	G=0.7%	G=0.1%	G=0.4%	G=0.7%	G=0.1%	G=0.4%	G=0.7%
DR=30	5.65E+11	5.77E+11	5.32E+11	5.09E+11	5.01E+11	5.13E+11	4.66E+11	4.72E+11	4.87E+11
DR=50	5.21E+11	5.26E+11	5.35E+11	4.6E+11	4.71E+11	4.73E+11	4.34E+11	4.46E+11	4.64E+11
DR=70	5.03E+11	5.04E+11	5.11E+11	4.47E+11	4.67E+11	4.6E+11	4.26E+11	4.41E+11	4.58E+11
Buckling times for P/P_{cr} = 0.5 and creep coefficients A = 0.1A, n=1n									
	OV=0%			OV=3%			OV=6%		
	G=0.1%	G=0.4%	G=0.7%	G=0.1%	G=0.4%	G=0.7%	G=0.1%	G=0.4%	G=0.7%
DR=30	1.1E+10	1.17E+10	1.26E+10	1.08E+10	1.06E+10	1.06E+10	1.01E+10	1.01E+10	9.58E+09
DR=50	1.08E+10	1.09E+10	1.1E+10	9.99E+09	1E+10	9.93E+09	9.51E+09	9.57E+09	9.12E+09
DR=70	1.05E+10	1.03E+10	1.03E+10	9.64E+09	9.52E+09	9.47E+09	9.33E+09	9.28E+09	8.99E+09

Reproduced with permission of the copyright owner. Further reproduction prohibited without permission.

Table A.5 FEA Results for Material Properties A=1.21e-8($psi^{-1}hr^{-n}$), n=0.36

Buckling times for P/P_{cr} = 0.1 and creep coefficients A = 0.1A, n=1.5n									
	OV=0%			OV=3%			OV=6%		
	G=0.1%	G=0.4%	G=0.7%	G=0.1%	G=0.4%	G=0.7%	G=0.1%	G=0.4%	G=0.7%
DR=30	4.972E+09	5.130E+09	5.923E+09	4.799E+09	4.831E+09	4.753E+09	4.641E+09	4.779E+09	4.614E+09
DR=50	5.090E+09	5.100E+09	5.120E+09	4.512E+09	5.09E+09	4.320E+09	4.120E+09	4.561E+09	4.781E+09
DR=70	5.010E+09	5.080E+09	5.100E+09	4.012E+09	4.201E+09	4.137E+09	4.078E+09	4.128E+09	4.356E+09
Buckling times for P/P_{cr} = 0.3 and creep coefficients A = 0.1A, n=1.5n									
	OV=0%			OV=3%			OV=6%		
	G=0.1%	G=0.4%	G=0.7%	G=0.1%	G=0.4%	G=0.7%	G=0.1%	G=0.4%	G=0.7%
DR=30	8.399E+07	8.890E+07	9.034E+07	8.399E+07	8.451E+07	8.121E+07	7.850E+07	7.941E+07	7.801E+08
DR=50	8.830E+07	8.860E+07	8.890E+07	7.830E+07	8.01E+07	8.101E+07	7.472E+07	8.030E+07	8.214E+07
DR=70	8.023E+07	8.430E+07	8.862E+07	7.686E+07	8.110E+07	8.097E+07	7.413E+07	7.709E+07	7.891E+07
Buckling times for P/P_{cr} = 0.5 and creep coefficients A = 0.1A, n=1.5n									
	OV=0%			OV=3%			OV=6%		
	G=0.1%	G=0.4%	G=0.7%	G=0.1%	G=0.4%	G=0.7%	G=0.1%	G=0.4%	G=0.7%
DR=30	6.058E+06	6.370E+06	7.946E+06	6.058E+06	6.032E+06	6.015E+06	5.762E+06	5.596E+06	5.557E+06
DR=50	6.200E+06	6.230E+06	6.290E+06	5.775E+06	6.21E+06	5.716E+06	5.532E+06	6.200E+06	5.410E+06
DR=70	6.020E+07	6.160E+06	6.190E+06	5.617E+06	5.736E+06	5.592E+06	5.45E+06	5.520E+06	5.301E+06

Reproduced with permission of the copyright owner. Further reproduction prohibited without permission.

Table A.6 FEA Results for Material Properties A=1.21e-8($psi^{-1}hr^{-n}$), n=0.12

Buckling times for P/P_{cr} = 0.1 and creep coefficients A = 0.1A, n=0.5n									
	OV=0%			OV=3%			OV=6%		
	G=0.1%	G=0.4%	G=0.7%	G=0.1%	G=0.4%	G=0.7%	G=0.1%	G=0.4%	G=0.7%
DR=30	1.648E+28	1.754E+28	1.863E+28	1.074E+28	9.835E+27	9.691E+27	8.268E+27	8.437E+27	8.624E+27
DR=50	1.031E+28	1.058E+28	9.943E+27	8.665E+27	8.58E+27	8.779E+27	7.234E+21	7.758E+21	7.947E+27
DR=70	1.026E+28	9.912E+27	9.763E+27	7.880E+27	8.074E+27	8.211E+27	7.164E+27	7.696E+27	7.867E+27
Buckling times for P/P_{cr} = 0.3 and creep coefficients A = 0.1A, n=0.5n									
	OV=0%			OV=3%			OV=6%		
	G=0.1%	G=0.4%	G=0.7%	G=0.1%	G=0.4%	G=0.7%	G=0.1%	G=0.4%	G=0.7%
DR=30	1.023E+23	9.058E+22	1.490E+23	9.057E+22	8.386E+22	8.130E+22	7.803E+22	7.502E+22	6.904E+22
DR=50	8.932E+22	8.556E+22	8.517E+22	7.380E+22	7.25E+22	6.897E+22	6.692E+22	6.714E+22	6.786E+22
DR=70	7.896E+22	7.804E+22	7.723E+22	6.922E+22	6.754E+22	6.673E+22	6.382E+22	6.439E+22	6.542E+22
Buckling times for P/P_{cr} = 0.5 and creep coefficients A = 0.1A, n=0.5n									
	OV=0%			OV=3%			OV=6%		
	G=0.1%	G=0.4%	G=0.7%	G=0.1%	G=0.4%	G=0.7%	G=0.1%	G=0.4%	G=0.7%
DR=30	6.091E+19	7.145E+19	9.221E+19	5.001E+19	4.689E+19	4.568E+19	4.496E+19	4.338E+19	3.896E+19
DR=50	5.145E+19	4.608E+19	4.562E+19	4.191E+19	3.88E+19	3.702E+19	3.906E+19	4.025E+19	3.520E+19
DR=70	4.209E+19	4.121E+19	4.075E+19	3.920E+19	3.718E+19	3.621E+19	3.72E+19	3.602E+19	3.362E+19

Reproduced with permission of the copyright owner. Further reproduction prohibited without permission.

Table A.7 FEA Results for Material Properties A=1.21e-6($psi^{-1}hr^{-n}$), n=0.24

Buckling times for P/P_{cr} = 0.1 and creep coefficients A =10A, n=1n									
	OV=0%			OV=3%			OV=6%		
	G=0.1%	G=0.4%	G=0.7%	G=0.1%	G=0.4%	G=0.7%	G=0.1%	G=0.4%	G=0.7%
DR=30	9.801E+05	9.981E+05	1.367E+06	8.930E+05	8.857E+05	8.787E+05	8.256E+05	8.567E+05	8.315E+05
DR=50	9.740E+05	9.870E+05	1.070E+06	8.121E+05	8.33E+05	8.631E+05	7.341E+05	8.066E+05	8.000E+05
DR=70	8.954E+05	9.101E+05	9.342E+05	7.342E+05	7.631E+05	7.812E+05	7.283E+05	7.401E+05	7.641E+05
Buckling times for P/P_{cr} = 0.3 and creep coefficients A = 10A, n=1n									
	OV=0%			OV=3%			OV=6%		
	G=0.1%	G=0.4%	G=0.7%	G=0.1%	G=0.4%	G=0.7%	G=0.1%	G=0.4%	G=0.7%
DR=30	2.831E+03	2.677E+03	2.430E+03	2.363E+03	2.278E+03	2.210E+03	2.164E+03	2.205E+03	2.107E+03
DR=50	2.418E+03	2.440E+03	2.480E+03	2.136E+03	2.19E+03	2.178E+03	2.015E+03	2.070E+03	2.101E+03
DR=70	2.257E+03	2.350E+03	2.375E+03	2.079E+03	2.171E+03	2.135E+03	1.976E+03	2.043E+03	2.089E+03
Buckling times for P/P_{cr} = 0.5 and creep coefficients A = 10A, n=1n									
	OV=0%			OV=3%			OV=6%		
	G=0.1%	G=0.4%	G=0.7%	G=0.1%	G=0.4%	G=0.7%	G=0.1%	G=0.4%	G=0.7%
DR=30	5.130E+01	5.540E+01	5.730E+01	5.130E+01	5.050E+01	5.010E+01	4.810E+01	4.780E+01	4.560E+01
DR=50	5.110E+01	5.130E+01	5.180E+01	4.730E+01	4.73E+01	4.720E+01	4.510E+01	4.540E+00	4.360E+01
DR=70	4.820E+01	4.870E+01	4.900E+01	4.560E+01	4.680E+01	4.510E+01	4.42E+01	4.400E+01	4.240E+01

Reproduced with permission of the copyright owner. Further reproduction prohibited without permission.

Table A.8 FEA Results for Material Properties A=1.21e-6($psi^{-1}hr^{-n}$), n=0.36

Buckling times for P/P_{cr} = 0.1 and creep coefficients A =10A, n=1.5n									
	OV=0%			OV=3%			OV=6%		
	G=0.1%	G=0.4%	G=0.7%	G=0.1%	G=0.4%	G=0.7%	G=0.1%	G=0.4%	G=0.7%
DR=30	1.732E+04	1.804E+04	1.932E+04	1.628E+04	1.741E+04	1.369E+04	1.183E+04	1.342E+04	1.701E+04
DR=50	1.592E+04	1.642E+04	1.749E+04	1.327E+04	1.46E+04	1.541E+04	1.178E+04	1.123E+04	1.220E+04
DR=70	1.217E+04	1.356E+04	1.523E+04	1.224E+04	1.371E+04	1.471E+04	1.162E+04	1.210E+04	1.313E+04
Buckling times for P/P_{cr} = 0.3 and creep coefficients A = 10A, n=1.5n									
	OV=0%			OV=3%			OV=6%		
	G=0.1%	G=0.4%	G=0.7%	G=0.1%	G=0.4%	G=0.7%	G=0.1%	G=0.4%	G=0.7%
DR=30	2.680E+02	2.700E+02	2.580E+02	2.310E+02	2.560E+02	2.430E+02	2.200E+02	2.300E+02	2.390E+02
DR=50	2.410E+02	2.490E+02	2.550E+02	2.190E+02	2.28E+02	2.410E+02	2.090E+02	2.170E+02	2.210E+02
DR=70	2.300E+02	2.320E+02	2.480E+02	2.150E+02	2.270E+02	2.340E+02	2.070E+02	2.160E+02	2.180E+02
Buckling times for P/P_{cr} = 0.5 and creep coefficients A = 10A, n=1.5n									
	OV=0%			OV=3%			OV=6%		
	G=0.1%	G=0.4%	G=0.7%	G=0.1%	G=0.4%	G=0.7%	G=0.1%	G=0.4%	G=0.7%
DR=30	1.960E+01	2.020E+01	2.320E+01	1.790E+01	1.780E+01	1.750E+01	1.700E+01	1.680E+01	1.650E+01
DR=50	1.800E+01	1.830E+01	1.850E+01	1.700E+01	1.70E+01	1.710E+01	1.650E+01	1.650E+01	1.600E+01
DR=70	1.730E+01	1.750E+01	1.780E+01	1.660E+01	1.610E+01	1.600E+01	1.62E+01	1.630E+01	1.580E+01

Reproduced with permission of the copyright owner. Further reproduction prohibited without permission.

Table A.9 FEA Results for Material Properties A=1.21e-6 ($psi^{-1}hr^{-n}$), n=0.12

Buckling times for P/P_{cr} = 0.1 and creep coefficients A =10A, n=0.5n									
	OV=0%			OV=3%			OV=6%		
	G=0.1%	G=0.4%	G=0.7%	G=0.1%	G=0.4%	G=0.7%	G=0.1%	G=0.4%	G=0.7%
DR=30	3.548E+11	3.841E+11	4.005E+11	2.316E+11	2.119E+11	2.092E+11	1.876E+11	1.842E+11	1.921E+11
DR=50	3.025E+11	3.214E+11	3.521E+11	1.804E+11	1.85E+11	2.101E+11	1.592E+11	1.712E+11	1.756E+11
DR=70	2.210E+11	2.321E+11	2.099E+11	1.700E+11	1.703E+11	1.79E+11	6.874E+10	1.660E+11	1.704E+11
Buckling times for P/P_{cr} = 0.3 and creep coefficients A = 10A, n=0.5n									
	OV=0%			OV=3%			OV=6%		
	G=0.1%	G=0.4%	G=0.7%	G=0.1%	G=0.4%	G=0.7%	G=0.1%	G=0.4%	G=0.7%
DR=30	2.627E+06	2.256E+06	3.121E+06	1.949E+06	1.812E+06	1.749E+06	1.679E+06	1.523E+06	1.412E+06
DR=50	1.938E+06	1.847E+06	1.748E+06	1.510E+06	1.56E+06	1.574E+06	1.446E+06	1.437E+06	1.312E+06
DR=70	1.692E+06	1.678E+06	1.659E+06	1.483E+06	1.453E+06	1.432E+06	1.326E+06	1.383E+06	1.432E+06
Buckling times for P/P_{cr} = 0.5 and creep coefficients A = 10A, n=0.5n									
	OV=0%			OV=3%			OV=6%		
	G=0.1%	G=0.4%	G=0.7%	G=0.1%	G=0.4%	G=0.7%	G=0.1%	G=0.4%	G=0.7%
DR=30	1.010E+03	9.480E+02	9.040E+02	8.980E+02	8.870E+02	8.620E+02	8.980E+02	8.630E+02	8.420E+02
DR=50	9.560E+02	9.020E+02	8.870E+02	8.710E+02	8.68E+02	8.530E+02	8.370E+02	8.230E+02	8.010E+02
DR=70	9.020E+02	8.840E+02	8.710E+02	8.420E+02	8.020E+02	7.740E+02	7.96E+02	7.740E+02	7.190E+02

Reproduced with permission of the copyright owner. Further reproduction prohibited without permission.

Table A.10 FEA Results for Ovality=6%, Gap=0.1%, DR=70

PR	P	Buckling time (hr)								
		1A1n	1A 1.5n	1A 0.5n	10A 1n	10A 1.5n	10A 0.5n	0.1A 1n	0.1A 0.5n	0.1A 1.5n
0.995	31.14	1	1	1	1	1	1	3.03	1	2.67
0.90	28.17	3.21E+01	1.17E+01	6.61E+02	1.01E+00	1.02E+00	1.00E+00	4.56E+05	1.44E+11	6.25E+03
0.8	25.04	1.15E+03	1.24E+02	8.11E+05	1.07E+00	1.10E+00	1.03E+00	1.60E+07	1.60E+14	6.70E+04
0.7	21.91	1.33E+04	6.54E+02	9.49E+07	1.91E+00	2.10E+00	1.43E+00	1.98E+08	2.05E+16	3.92E+05
0.5	15.65	6.34E+05	9.13E+03	1.72E+11	4.42E+01	1.62E+01	7.96E+02	9.33E+09	3.72E+19	5.45E+06
0.3	9.39	2.90E+07	1.24E+05	2.97E+14	1.98E+03	2.07E+02	1.33E+06	4.26E+11	6.38E+22	7.41E+07
0.1	3.13	1.07E+10	7.03E+06	3.32E+19	7.28E+05	1.16E+04	6.87E+10	1.52E+14	7.16E+27	4.08E+09

APPENDIX B

C^* VALUES BASED ON THE FINITE ELEMENT RESULTS IN APPENDIX A

Reproduced with permission of the copyright owner. Further reproduction prohibited without permission.

Reproduced with permission of the copyright owner. Further reproduction prohibited without permission.

Table B.1 FEA C^* Value for Material Properties A= 1.21e-7($psi^{-1}hr^{-n}$), n=0.24

Buckling times for P/P_{cr} = 0.1 and creep coefficients A = 1A, n=1n									
	OV=0%			OV=3%			OV=6%		
	G=0.1%	G=0.4%	G=0.7%	G=0.1%	G=0.4%	G=0.7%	G=0.1%	G=0.4%	G=0.7%
DR=30	1.966	1.972	2.009	1.846	1.853	1.824	1.847	1.850	1.887
DR=50	1.848	1.866	1.875	1.783	1.829	1.839	1.783	1.800	1.808
DR=70	1.846	1.847	1.879	1.800	1.828	1.833	1.764	1.779	1.800
Buckling times for P/P_{cr} = 0.3 and creep coefficients A = 1A, n=1n									
	OV=0%			OV=3%			OV=6%		
	G=0.1%	G=0.4%	G=0.7%	G=0.1%	G=0.4%	G=0.7%	G=0.1%	G=0.4%	G=0.7%
DR=30	1.617	1.622	1.663	1.561	1.565	1.653	1.535	1.556	1.631
DR=50	1.568	1.571	1.576	1.531	1.538	1.540	1.513	1.513	1.517
DR=70	1.547	1.552	1.562	1.523	1.536	1.531	1.508	1.508	1.512
Buckling times for P/P_{cr} = 0.5 and creep coefficients A = 1A, n=1n									
	OV=0%			OV=3%			OV=6%		
	G=0.1%	G=0.4%	G=0.7%	G=0.1%	G=0.4%	G=0.7%	G=0.1%	G=0.4%	G=0.7%
DR=30	1.359	1.350	1.410	1.335	1.331	1.330	1.322	1.321	1.310
DR=50	1.333	1.335	1.337	1.318	1.317	1.317	1.312	1.307	1.301
DR=70	1.322	1.324	1.325	1.311	1.315	1.308	1.304	1.304	1.295

Reproduced with permission of the copyright owner. Further reproduction prohibited without permission.

Table B.2 FEA C^* Value for Material Properties A= 1.21e-7($psi^{-1}hr^{-n}$), n=0.36

Buckling times for P/P_{cr} = 0.1 and creep coefficients A = 1A, n=1.5n									
	OV=0%			OV=3%			OV=6%		
	G=0.1%	G=0.4%	G=0.7%	G=0.1%	G=0.4%	G=0.7%	G=0.1%	G=0.4%	G=0.7%
DR=30	2.350	2.371	2.434	2.123	2.139	2.148	2.044	2.072	2.086
DR=50	2.326	2.333	2.348	2.052	2.076	2.084	2.002	2.045	2.072
DR=70	2.267	2.281	2.301	2.009	2.023	2.042	2.001	1.999	1.990
Buckling times for P/P_{cr} = 0.3 and creep coefficients A = 1A, n=1.5n									
	OV=0%			OV=3%			OV=6%		
	G=0.1%	G=0.4%	G=0.7%	G=0.1%	G=0.4%	G=0.7%	G=0.1%	G=0.4%	G=0.7%
DR=30	1.762	1.786	1.801	1.693	1.691	1.688	1.661	1.658	1.653
DR=50	1.707	1.722	1.735	1.659	1.676	1.682	1.635	1.654	1.621
DR=70	1.661	1.710	1.720	1.649	1.649	1.674	1.633	1.652	1.608
Buckling times for P/P_{cr} = 0.5 and creep coefficients A = 1A, n=1.5n									
	OV=0%			OV=3%			OV=6%		
	G=0.1%	G=0.4%	G=0.7%	G=0.1%	G=0.4%	G=0.7%	G=0.1%	G=0.4%	G=0.7%
DR=30	1.433	1.426	1.495	1.401	1.400	1.399	1.384	1.379	1.373
DR=50	1.403	1.410	1.413	1.384	1.386	1.380	1.371	1.374	1.368
DR=70	1.401	1.398	1.402	1.377	1.377	1.376	1.369	1.369	1.364

Reproduced with permission of the copyright owner. Further reproduction prohibited without permission.

Table B.3 FEA C^* Value for Material Properties A= 1.21e-7($psi^{-1}hr^{-n}$), n=0.12

Buckling times for P/P_{cr} = 0.1 and creep coefficients A = 1A, n=0.5n									
	OV=0%			OV=3%			OV=6%		
	G=0.1%	G=0.4%	G=0.7%	G=0.1%	G=0.4%	G=0.7%	G=0.1%	G=0.4%	G=0.7%
DR=30	1.685	1.701	1.708	1.578	1.582	1.587	1.562	1.567	1.572
DR=50	1.623	1.608	1.599	1.562	1.567	1.567	1.549	1.555	1.560
DR=70	1.598	1.577	1.563	1.551	1.565	1.558	1.534	1.547	1.549
Buckling times for P/P_{cr} = 0.3 and creep coefficients A = 1A, n=0.5n									
	OV=0%			OV=3%			OV=6%		
	G=0.1%	G=0.4%	G=0.7%	G=0.1%	G=0.4%	G=0.7%	G=0.1%	G=0.4%	G=0.7%
DR=30	1.452	1.432	1.434	1.412	1.400	1.398	1.392	1.385	1.377
DR=50	1.411	1.404	1.404	1.404	1.383	1.381	1.372	1.373	1.371
DR=70	1.394	1.392	1.391	1.376	1.374	1.372	1.366	1.367	1.356
Buckling times for P/P_{cr} = 0.5 and creep coefficients A = 1A, n=0.5n									
	OV=0%			OV=3%			OV=6%		
	G=0.1%	G=0.4%	G=0.7%	G=0.1%	G=0.4%	G=0.7%	G=0.1%	G=0.4%	G=0.7%
DR=30	1.271	1.261	1.252	1.253	1.247	1.245	1.244	1.237	1.231
DR=50	1.249	1.245	1.236	1.238	1.234	1.233	1.231	1.230	1.222
DR=70	1.238	1.235	1.235	1.231	1.231	1.224	1.226	1.226	1.218

Reproduced with permission of the copyright owner. Further reproduction prohibited without permission.

Table B.4 FEA C^* Value for Material Properties A= 1.21e-6($psi^{-1}hr^{-n}$), n=0.24

Buckling times for P/P_{cr} = 0.1 and creep coefficients A = 0.1A, n=1n									
	OV=0%			OV=3%			OV=6%		
	G=0.1%	G=0.4%	G=0.7%	G=0.1%	G=0.4%	G=0.7%	G=0.1%	G=0.4%	G=0.7%
DR=30	1.884	1.891	2.022	1.843	1.846	1.858	1.815	1.830	1.849
DR=50	1.883	1.886	1.888	1.823	1.820	1.794	1.768	1.807	1.820
DR=70	1.861	1.870	1.880	1.770	1.793	1.779	1.752	1.782	1.808
Buckling times for P/P_{cr} = 0.3 and creep coefficients A = 0.1A, n=1n									
	OV=0%			OV=3%			OV=6%		
	G=0.1%	G=0.4%	G=0.7%	G=0.1%	G=0.4%	G=0.7%	G=0.1%	G=0.4%	G=0.7%
DR=30	1.593	1.600	1.575	1.561	1.557	1.564	1.535	1.538	1.548
DR=50	1.568	1.571	1.576	1.531	1.538	1.539	1.514	1.522	1.534
DR=70	1.558	1.559	1.563	1.522	1.536	1.531	1.508	1.518	1.530
Buckling times for P/P_{cr} = 0.5 and creep coefficients A = 0.1A, n=1n									
	OV=0%			OV=3%			OV=6%		
	G=0.1%	G=0.4%	G=0.7%	G=0.1%	G=0.4%	G=0.7%	G=0.1%	G=0.4%	G=0.7%
DR=30	1.338	1.350	1.365	1.335	1.331	1.330	1.321	1.320	1.310
DR=50	1.333	1.335	1.337	1.318	1.319	1.317	1.309	1.310	1.301
DR=70	1.327	1.324	1.325	1.311	1.309	1.308	1.305	1.304	1.298

Reproduced with permission of the copyright owner. Further reproduction prohibited without permission.

Table B.5 FEA C^* Value for Material Properties A= 1.21e-6 ($psi^{-1}hr^{-n}$), n=0.36

Buckling times for P/P_{cr} = 0.1 and creep coefficients A = 0.1A, n=1.5n									
	OV=0%			OV=3%			OV=6%		
	G=0.1%	G=0.4%	G=0.7%	G=0.1%	G=0.4%	G=0.7%	G=0.1%	G=0.4%	G=0.7%
DR=30	2.155	2.140	2.249	2.092	2.097	2.085	2.068	2.089	2.064
DR=50	2.135	2.136	2.139	2.048	2.135	2.018	1.986	2.056	2.089
DR=70	2.123	2.133	2.136	1.968	1.999	1.988	1.979	1.987	2.024
Buckling times for P/P_{cr} = 0.3 and creep coefficients A = 0.1A, n=1.5n									
	OV=0%			OV=3%			OV=6%		
	G=0.1%	G=0.4%	G=0.7%	G=0.1%	G=0.4%	G=0.7%	G=0.1%	G=0.4%	G=0.7%
DR=30	1.730	1.722	1.716	1.693	1.696	1.676	1.659	1.665	1.670
DR=50	1.712	1.720	1.722	1.658	1.669	1.675	1.635	1.671	1.682
DR=70	1.670	1.695	1.720	1.649	1.675	1.675	1.632	1.651	1.662
Buckling times for P/P_{cr} = 0.5 and creep coefficients A = 0.1A, n=1.5n									
	OV=0%			OV=3%			OV=6%		
	G=0.1%	G=0.4%	G=0.7%	G=0.1%	G=0.4%	G=0.7%	G=0.1%	G=0.4%	G=0.7%
DR=30	1.432	1.417	1.446	1.401	1.400	1.399	1.385	1.376	1.373
DR=50	1.408	1.410	1.408	1.386	1.409	1.382	1.372	1.408	1.365
DR=70	1.408	1.406	1.401	1.377	1.383	1.375	1.367	1.371	1.359

Reproduced with permission of the copyright owner. Further reproduction prohibited without permission.

Table B.6 FEA C^* Value for Material Properties A= 1.21e-6 ($psi^{-1}hr^{-n}$), n=0.12

Buckling times for P/P_{cr} = 0.1 and creep coefficients A = 0.1A, n=0.5n									
	OV=0%			OV=3%			OV=6%		
	G=0.1%	G=0.4%	G=0.7%	G=0.1%	G=0.4%	G=0.7%	G=0.1%	G=0.4%	G=0.7%
DR=30	1.685	1.697	1.709	1.606	1.590	1.587	1.559	1.563	1.567
DR=50	1.599	1.603	1.592	1.568	1.566	1.570	1.536	1.548	1.552
DR=70	1.598	1.591	1.589	1.551	1.555	1.558	1.534	1.547	1.551
Buckling times for P/P_{cr} = 0.3 and creep coefficients A = 0.1A, n=0.5n									
	OV=0%			OV=3%			OV=6%		
	G=0.1%	G=0.4%	G=0.7%	G=0.1%	G=0.4%	G=0.7%	G=0.1%	G=0.4%	G=0.7%
DR=30	1.428	1.412	1.480	1.412	1.402	1.397	1.392	1.387	1.376
DR=50	1.410	1.404	1.404	1.385	1.382	1.376	1.372	1.373	1.374
DR=70	1.394	1.392	1.391	1.377	1.373	1.372	1.366	1.367	1.369
Buckling times for P/P_{cr} = 0.5 and creep coefficients A = 0.1A, n=0.5n									
	OV=0%			OV=3%			OV=6%		
	G=0.1%	G=0.4%	G=0.7%	G=0.1%	G=0.4%	G=0.7%	G=0.1%	G=0.4%	G=0.7%
DR=30	1.271	1.286	1.311	1.253	1.247	1.245	1.244	1.240	1.231
DR=50	1.256	1.246	1.245	1.237	1.231	1.227	1.231	1.234	1.222
DR=70	1.238	1.236	1.235	1.232	1.227	1.225	1.227	1.224	1.218

Reproduced with permission of the copyright owner. Further reproduction prohibited without permission.

Table B.7 FEA C^* Value for Material Properties A= 1.21e-8 ($psi^{-1}hr^{-n}$), n=0.24

Buckling times for P/P_{cr} = 0.1 and creep coefficients A =10A, n=1n									
	OV=0%			OV=3%			OV=6%		
	G=0.1%	G=0.4%	G=0.7%	G=0.1%	G=0.4%	G=0.7%	G=0.1%	G=0.4%	G=0.7%
DR=30	1.886	1.894	2.035	1.847	1.843	1.840	1.814	1.830	1.817
DR=50	1.884	1.889	1.924	1.808	1.818	1.833	1.767	1.805	1.801
DR=70	1.848	1.855	1.866	1.767	1.782	1.792	1.764	1.770	1.783
Buckling times for P/P_{cr} = 0.3 and creep coefficients A = 10A, n=1n									
	OV=0%			OV=3%			OV=6%		
	G=0.1%	G=0.4%	G=0.7%	G=0.1%	G=0.4%	G=0.7%	G=0.1%	G=0.4%	G=0.7%
DR=30	1.617	1.600	1.570	1.561	1.550	1.541	1.535	1.541	1.527
DR=50	1.568	1.571	1.576	1.531	1.538	1.537	1.514	1.522	1.526
DR=70	1.547	1.560	1.563	1.523	1.536	1.531	1.508	1.518	1.525
Buckling times for P/P_{cr} = 0.5 and creep coefficients A = 10A, n=1n									
	OV=0%			OV=3%			OV=6%		
	G=0.1%	G=0.4%	G=0.7%	G=0.1%	G=0.4%	G=0.7%	G=0.1%	G=0.4%	G=0.7%
DR=30	1.338	1.354	1.361	1.338	1.335	1.334	1.326	1.324	1.315
DR=50	1.338	1.338	1.340	1.322	1.322	1.322	1.313	1.314	1.306
DR=70	1.326	1.328	1.329	1.315	1.320	1.313	1.309	1.308	1.301

Reproduced with permission of the copyright owner. Further reproduction prohibited without permission.

Table B.8 FEA C^* Value for Material Properties A= 1.21e-8 ($psi^{-1}hr^{-n}$), n=0.36

Buckling times for P/P_{cr} = 0.1 and creep coefficients A =10A, n=1.5n									
	OV=0%			OV=3%			OV=6%		
	G=0.1%	G=0.4%	G=0.7%	G=0.1%	G=0.4%	G=0.7%	G=0.1%	G=0.4%	G=0.7%
DR=30	2.287	2.320	2.375	2.239	2.292	2.110	2.007	2.096	2.273
DR=50	2.222	2.246	2.295	2.087	2.155	2.197	2.004	1.972	2.028
DR=70	2.027	2.103	2.189	2.031	2.111	2.163	1.995	2.023	2.080
Buckling times for P/P_{cr} = 0.3 and creep coefficients A = 10A, n=1.5n									
	OV=0%			OV=3%			OV=6%		
	G=0.1%	G=0.4%	G=0.7%	G=0.1%	G=0.4%	G=0.7%	G=0.1%	G=0.4%	G=0.7%
DR=30	1.763	1.767	1.743	1.687	1.739	1.713	1.663	1.685	1.704
DR=50	1.708	1.725	1.737	1.661	1.681	1.708	1.638	1.656	1.665
DR=70	1.685	1.689	1.723	1.652	1.678	1.694	1.633	1.654	1.658
Buckling times for P/P_{cr} = 0.5 and creep coefficients A = 10A, n=1.5n									
	OV=0%			OV=3%			OV=6%		
	G=0.1%	G=0.4%	G=0.7%	G=0.1%	G=0.4%	G=0.7%	G=0.1%	G=0.4%	G=0.7%
DR=30	1.451	1.462	1.511	1.421	1.419	1.413	1.404	1.400	1.394
DR=50	1.422	1.428	1.432	1.404	1.404	1.406	1.394	1.394	1.384
DR=70	1.409	1.413	1.419	1.396	1.386	1.384	1.388	1.390	1.380

Reproduced with permission of the copyright owner. Further reproduction prohibited without permission.

Table B.9 FEA C^* Value for Material Properties A= 1.21e-8 ($psi^{-1}hr^{-n}$), n=0.12

Buckling times for P/P_{cr} = 0.1 and creep coefficients A =10A, n=0.5n									
	OV=0%			OV=3%			OV=6%		
	G=0.1%	G=0.4%	G=0.7%	G=0.1%	G=0.4%	G=0.7%	G=0.1%	G=0.4%	G=0.7%
DR=30	1.685	1.700	1.708	1.606	1.590	1.588	1.568	1.565	1.573
DR=50	1.655	1.666	1.684	1.562	1.566	1.589	1.540	1.552	1.557
DR=70	1.598	1.606	1.588	1.551	1.551	1.560	1.402	1.547	1.552
Buckling times for P/P_{cr} = 0.3 and creep coefficients A = 10A, n=0.5n									
	OV=0%			OV=3%			OV=6%		
	G=0.1%	G=0.4%	G=0.7%	G=0.1%	G=0.4%	G=0.7%	G=0.1%	G=0.4%	G=0.7%
DR=30	1.452	1.431	1.476	1.412	1.402	1.397	1.392	1.379	1.369
DR=50	1.411	1.405	1.397	1.378	1.382	1.384	1.373	1.372	1.360
DR=70	1.393	1.392	1.390	1.376	1.373	1.371	1.361	1.367	1.371
Buckling times for P/P_{cr} = 0.5 and creep coefficients A = 10A, n=0.5n									
	OV=0%			OV=3%			OV=6%		
	G=0.1%	G=0.4%	G=0.7%	G=0.1%	G=0.4%	G=0.7%	G=0.1%	G=0.4%	G=0.7%
DR=30	1.247	1.242	1.238	1.237	1.236	1.233	1.237	1.233	1.231
DR=50	1.242	1.237	1.236	1.234	1.234	1.232	1.231	1.229	1.227
DR=70	1.237	1.236	1.234	1.231	1.227	1.224	1.226	1.224	1.218

APPENDIX C

LISTING OF y_0, y_1, y_2 VALUES

CORRESPONDING TO APPENDIX B

Reproduced with permission of the copyright owner. Further reproduction prohibited without permission.

Table C.1 Values of y_0 for A=1.21e-8 ($psi^{-1}hr^{-n}$) and Three Levels of n

y_0 value with creep coefficients A =0.1A, n=1n									
	OV=0%			OV=3%			OV=6%		
	G=0.1 %	G=0.4 %	G=0.7 %	G=0.1 %	G=0.4 %	G=0.7 %	G=0.1 %	G=0.4 %	G=0.7 %
DR=30	2.043	2.0519	2.3344	2.005	2.0141	2.0275	1.9983	2.0038	2.0231
DR=50	2.0705	2.0731	2.0714	1.9986	1.9846	1.9339	1.9134	1.9769	1.9829
DR=70	2.0395	2.054	2.0681	1.9079	1.9327	1.9124	1.8894	1.9327	1.9643
y_0 value with creep coefficients A = 0.1A, n=1.5n									
	OV=0%			OV=3%			OV=6%		
	G=0.1 %	G=0.4 %	G=0.7 %	G=0.1 %	G=0.4 %	G=0.7 %	G=0.1 %	G=0.4 %	G=0.7 %
DR=30	2.4151	2.3914	2.5966	2.3316	2.3369	2.339	2.3231	2.3516	2.2974
DR=50	2.3911	2.3838	2.3861	2.2872	2.4452	2.2082	2.1945	2.2943	2.3262
DR=70	2.4211	2.4079	2.3804	2.1451	2.173	2.1494	2.1833	2.176	2.2271
y_0 value with creep coefficients A = 0.1A, n=0.5n									
	OV=0%			OV=3%			OV=6%		
	G=0.1 %	G=0.4 %	G=0.7 %	G=0.1 %	G=0.4 %	G=0.7 %	G=0.1 %	G=0.4 %	G=0.7 %
DR=30	1.851	1.8991	1.846	1.7161	1.6964	1.6962	1.6496	1.6619	1.6798
DR=50	1.7066	1.7179	1.6969	1.6726	1.6704	1.6839	1.6266	1.649	1.6507
DR=70	1.718	1.7066	1.7038	1.6489	1.6595	1.6656	1.6289	1.6509	1.6536

Reproduced with permission of the copyright owner. Further reproduction prohibited without permission.

Table C.2 Values of y_0 for A=1.21e-7 ($psi^{-1}hr^{-n}$) and Three Levels of n

y_0 value with creep coefficients A =1A, n=1n									
	OV=0%			OV=3%			OV=6%		
	G=0.1 %	G=0.4 %	G=0.7 %	G=0.1 %	G=0.4 %	G=0.7 %	G=0.1 %	G=0.4 %	G=0.7 %
DR=30	2.1746	2.1763	2.2169	2.0106	2.0172	1.8525	2.0401	2.0191	1.9906
DR=50	2.0049	2.0356	2.047	1.9236	2.0007	2.017	1.9439	1.9739	1.9816
DR=70	2.0233	2.0196	2.0675	1.9629	2.0006	2.0136	1.9115	1.9396	1.9706
y_0 value with creep coefficients A = 1A, n=0.5n									
	OV=0%			OV=3%			OV=6%		
	G=0.1 %	G=0.4 %	G=0.7 %	G=0.1 %	G=0.4 %	G=0.7 %	G=0.1 %	G=0.4 %	G=0.7 %
DR=30	1.821	1.8723	1.8795	1.6636	1.6839	1.695	1.6553	1.6708	1.6879
DR=50	1.7477	1.7269	1.7066	1.638	1.6721	1.6743	1.651	1.6606	1.6695
DR=70	1.718	1.68	1.655	1.6497	1.6785	1.6652	1.6285	1.6516	1.6661
y_0 value with creep coefficients A = 1A, n=1.5n									
	OV=0%			OV=3%			OV=6%		
	G=0.1 %	G=0.4 %	G=0.7 %	G=0.1 %	G=0.4 %	G=0.7 %	G=0.1 %	G=0.4 %	G=0.7 %
DR=30	2.7411	2.7479	2.8731	2.3897	2.4219	2.442	2.2753	2.3296	2.3599
DR=50	2.7536	2.7506	2.7636	2.2928	2.3173	2.3225	2.2241	2.2821	2.3718
DR=70	2.6998	2.6636	2.6901	2.222	2.2482	2.2522	2.224	2.1965	2.128

Reproduced with permission of the copyright owner. Further reproduction prohibited without permission.

Table C.3 Values of y_0 for A=1.21e-6 ($psi^{-1}hr^{-n}$) and Three Levels of n

y_0 value with creep coefficients A =10A, n=1n									
	OV=0%			OV=3%			OV=6%		
	G=0.1 %	G=0.4 %	G=0.7 %	G=0.1 %	G=0.4 %	G=0.7 %	G=0.1 %	G=0.4 %	G=0.7 %
DR=30	2.0167	2.059	2.3635	2.0136	2.0187	2.024	1.9797	2.0015	1.9912
DR=50	2.0742	2.0799	2.14	1.972	1.982	2.0114	1.913	1.9746	1.9591
DR=70	2.0285	2.0261	2.0434	1.9025	1.9163	1.9386	1.9134	1.9118	1.9247
y_0 value with creep coefficients A = 10A, n=0.5n									
	OV=0%			OV=3%			OV=6%		
	G=0.1 %	G=0.4 %	G=0.7 %	G=0.1 %	G=0.4 %	G=0.7 %	G=0.1 %	G=0.4 %	G=0.7 %
DR=30	1.812	1.8645	1.8218	1.7101	1.6923	1.6936	1.6639	1.673	1.6997
DR=50	1.8051	1.8314	1.8748	1.669	1.6715	1.7114	1.6329	1.6559	1.6795
DR=70	1.7189	1.7348	1.7028	1.6497	1.652	1.6702	1.3872	1.6509	1.653
y_0 value with creep coefficients A = 10A, n=1.5n									
	OV=0%			OV=3%			OV=6%		
	G=0.1 %	G=0.4 %	G=0.7 %	G=0.1 %	G=0.4 %	G=0.7 %	G=0.1 %	G=0.4 %	G=0.7 %
DR=30	2.6285	2.6895	2.841	2.6222	2.6559	2.3449	2.2109	2.3488	2.6546
DR=50	2.5645	2.5905	2.6689	2.3634	2.4659	2.5116	2.2327	2.1503	2.2403
DR=70	2.2228	2.3618	2.4828	2.2666	2.3804	2.4571	2.2199	2.2469	2.345

Reproduced with permission of the copyright owner. Further reproduction prohibited without permission.

Table C.4 Values of y_1 for A=1.21e-8 ($psi^{-1}hr^{-n}$) and Three Levels of n

y_1 value with creep coefficients A =0.1A, n=1n									
	OV=0%			OV=3%			OV=6%		
	G=0.1 %	G=0.4 %	G=0.7 %	G=0.1 %	G=0.4 %	G=0.7 %	G=0.1%	G=0.4 %	G=0.7 %
DR=30	-1.635	-1.66	-3.42	-1.69	-1.76	-1.77	-1.9767	-1.83	-1.82
DR=50	-1.975	-1.97	-1.925	-1.855	-1.725	-1.44	-1.515	-1.79	-1.695
DR=70	-1.875	-1.935	-1.98	-1.425	-1.435	-1.365	-1.425	-1.57	-1.62
y_1 value with creep coefficients A = 0.1A, n=1.5n									
	OV=0%			OV=3%			OV=6%		
	G=0.1 %	G=0.4 %	G=0.7 %	G=0.1 %	G=0.4 %	G=0.7 %	G=0.1%	G=0.4 %	G=0.7 %
DR=30	-2.76	-2.655	-3.77	-2.53	-2.53	-2.075	-2.72	-2.795	-2.455
DR=50	-2.71	-2.61	-2.6	-2.54	-3.36	-1.965	-2.195	-2.535	-2.485
DR=70	-3.22	-2.935	-2.565	-1.83	-1.78	-1.63	-2.145	-1.96	-2.105
y_1 value with creep coefficients A = 0.1A, n=0.5n									
	OV=0%			OV=3%			OV=6%		
	G=0.1 %	G=0.4 %	G=0.7 %	G=0.1 %	G=0.4 %	G=0.7 %	G=0.1%	G=0.4 %	G=0.7 %
DR=30	-1.785	-2.22	-1.445	-1.145	-1.105	-1.14	-0.93	-1.025	-1.185
DR=50	-1.12	-1.2	-1.085	-1.09	-1.085	-1.195	-0.935	-1.055	-1.02
DR=70	-1.26	-1.21	-1.2	-1.015	-1.09	-1.125	-0.985	-1.085	-1.065

Reproduced with permission of the copyright owner. Further reproduction prohibited without permission.

Table C.5 Values of y_1 for A=1.21e-7 ($psi^{-1}hr^{-n}$) and Three Levels of n

y_1 value with creep coefficients A =1A, n=1n									
	OV=0%			OV=3%			OV=6%		
	G=0.1 %	G=0.4 %	G=0.7 %	G=0.1 %	G=0.4 %	G=0.7 %	G=0.1 %	G=0.4 %	G=0.7%
DR=30	-2.2	-2.14	-2.195	-1.72	-1.71	-0.095	-2.055	-1.765	-0.955
DR=50	-1.625	-1.77	-1.795	-1.455	-1.805	-1.875	-1.695	-1.84	-1.83
DR=70	-1.865	-1.81	-1.985	-1.71	-1.815	-1.905	-1.54	-1.69	-1.795
y_1 value with creep coefficients A = 1A, n=0.5n									
	OV=0%			OV=3%			OV=6%		
	G=0.1 %	G=0.4 %	G=0.7 %	G=0.1 %	G=0.4 %	G=0.7 %	G=0.1 %	G=0.4 %	G=0.7%
DR=30	-1.425	-1.835	-1.83	-0.865	-1.055	-1.125	-0.96	-1.08	-1.22
DR=50	-1.31	-1.245	-1.11	-0.75	-1.095	-1.12	-1.065	-1.105	-1.145
DR=70	-1.26	-1.065	-0.94	-1.025	-1.195	-1.12	-0.98	-1.095	-1.24
y_1 value with creep coefficients A = 1A, n=1.5n									
	OV=0%			OV=3%			OV=6%		
	G=0.1 %	G=0.4 %	G=0.7 %	G=0.1 %	G=0.4 %	G=0.7 %	G=0.1 %	G=0.4 %	G=0.7%
DR=30	-4.235	-4.05	-4.8	-2.84	-3.025	-3.155	-2.445	-2.745	-2.93
DR=50	-4.67	-4.55	-4.52	-2.555	-2.55	-2.51	-2.35	-2.51	-3.245
DR=70	-4.76	-4.15	-4.22	-2.24	-2.38	-2.19	-2.36	-2.055	-1.2033

Reproduced with permission of the copyright owner. Further reproduction prohibited without permission.

Table C.6 Values of y_1 for A=1.21e-6 ($psi^{-1}hr^{-n}$) and Three Levels of n

y_1 value with creep coefficients A =10A, n=1n									
	OV=0%			OV=3%			OV=6%		
	G=0.1 %	G=0.4 %	G=0.7 %	G=0.1 %	G=0.4 %	G=0.7 %	G=0.1 %	G=0.4 %	G=0.7 %
DR=30	-1.295	-1.71	-3.605	-1.745	-1.855	-1.955	-1.745	-1.805	-1.84
DR=50	-2.01	-2.015	-2.3	-1.725	-1.72	-1.885	-1.525	-1.79	-1.65
DR=70	-1.905	-1.79	-1.86	-1.4	-1.38	-1.52	-1.565	-1.47	-1.46
y_1 value with creep coefficients A = 10A, n=0.5n									
	OV=0%			OV=3%			OV=6%		
	G=0.1 %	G=0.4 %	G=0.7 %	G=0.1 %	G=0.4 %	G=0.7 %	G=0.1 %	G=0.4 %	G=0.7 %
DR=30	-1.305	-1.745	-1.13	-1.065	-1.05	-1.09	-0.985	-1.13	-1.35
DR=50	-1.595	-1.77	-2.065	-1.12	-1.1	-1.29	-0.96	-1.085	-1.305
DR=70	-1.27	-1.36	-1.2	-1.025	-1.05	-1.155	0.265	-1.085	-1.045
y_1 value with creep coefficients A = 10A, n=1.5n									
	OV=0%			OV=3%			OV=6%		
	G=0.1 %	G=0.4 %	G=0.7 %	G=0.1 %	G=0.4%	G=0.7 %	G=0.1 %	G=0.4 %	G=0.7 %
DR=30	-3.68	-4.005	-5.16	-4.19	-3.93	-2.47	-2.145	-2.685	-4.14
DR=50	-3.71	-3.725	-4.055	-2.975	-3.355	-3.38	-2.44	-1.85	-2.225
DR=70	-2.04	-2.76	-3.14	-2.51	-2.87	-3.14	-2.395	-2.37	-2.83

Reproduced with permission of the copyright owner. Further reproduction prohibited without permission.

Table C.7 Values of y_2 for A=1.21e-8 ($psi^{-1}hr^{-n}$) and Three Levels of n

y_2 value with creep coefficients A =0.1A, n=1n									
	OV=0%			OV=3%			OV=6%		
	G=0.1 %	G=0.4 %	G=0.7 %	G=0.1 %	G=0.4 %	G=0.7 %	G=0.1 %	G=0.4 %	G=0.7 %
DR=30	0.45	0.5125	2.9625	0.7	0.7875	0.75	1.4417	0.925	0.7875
DR=50	1	0.9875	0.9125	0.9875	0.7875	0.4125	0.6125	0.9125	0.6625
DR=70	0.9	0.95	0.9875	0.4625	0.375	0.3125	0.5125	0.625	0.575
y_2 value with creep coefficients A = 0.1A, n=1.5n									
	OV=0%			OV=3%			OV=6%		
	G=0.1 %	G=0.4 %	G=0.7 %	G=0.1 %	G=0.4 %	G=0.7 %	G=0.1 %	G=0.4 %	G=0.7 %
DR=30	1.5875	1.4125	2.9375	1.3375	1.3125	1.65	1.6875	1.6875	1.2125
DR=50	1.4875	1.325	1.2875	1.475	2.575	0.625	1.1	1.525	1.125
DR=70	2.3875	1.8625	1.2125	0.5875	0.4	0.1625	1.025	0.7	0.7375
y_2 value with creep coefficients A = 0.1A, n=0.5n									
	OV=0%			OV=3%			OV=6%		
	G=0.1 %	G=0.4 %	G=0.7 %	G=0.1 %	G=0.4 %	G=0.7 %	G=0.1 %	G=0.4 %	G=0.7 %
DR=30	1.25	1.9875	0.75	0.4375	0.4125	0.475	0.2375	0.3625	0.575
DR=50	0.4375	0.5125	0.3625	0.4375	0.4125	0.5625	0.2875	0.45	0.325
DR=70	0.6	0.5375	0.525	0.3625	0.45	0.4875	0.3625	0.4625	0.3875

Reproduced with permission of the copyright owner. Further reproduction prohibited without permission.

Table C.8 Values of y_2 for A=1.21e-7 ($psi^{-1}hr^{-n}$) and Three Levels of n

y_2 value with creep coefficients A =1A, n=1n									
	OV=0%			OV=3%			OV=6%		
	G=0.1 %	G=0.4 %	G=0.7 %	G=0.1 %	G=0.4 %	G=0.7 %	G=0.1 %	G=0.4 %	G=0.7%
DR=30	1.1375	0.975	1.1625	0.7375	0.675	-1.9	1.2375	0.7375	-0.8125
DR=50	0.5625	0.7375	0.75	0.4875	0.875	0.95	0.8625	1.0125	0.9375
DR=70	0.925	0.8375	1	0.8125	0.8875	0.9875	0.65	0.8375	0.8875
y_2 value with creep coefficients A = 1A, n=0.5n									
	OV=0%			OV=3%			OV=6%		
	G=0.1 %	G=0.4 %	G=0.7 %	G=0.1 %	G=0.4 %	G=0.7 %	G=0.1 %	G=0.4 %	G=0.7%
DR=30	0.65	1.225	1.15	0.0528	0.3625	0.45	0.275	0.425	0.6125
DR=50	0.625	0.5625	0.3375	-0.1	0.4375	0.475	0.45	0.4875	0.5
DR=70	0.6	0.35	0.2	0.375	0.6	0.475	0.35	0.4875	0.6875
y_2 value with creep coefficients A = 1A, n=1.5n									
	OV=0%			OV=3%			OV=6%		
	G=0.1 %	G=0.4 %	G=0.7 %	G=0.1 %	G=0.4 %	G=0.7 %	G=0.1 %	G=0.4 %	G=0.7%
DR=30	3.2375	2.8125	4.0875	1.725	1.9625	2.138	1.325	1.6875	1.9125
DR=50	3.9375	3.7375	3.6375	1.475	1.375	1.25	1.2875	1.3875	2.475
DR=70	4.325	3.2375	3.2875	1.1	1.275	0.875	1.3	0.8	-1.7667

Reproduced with permission of the copyright owner. Further reproduction prohibited without permission.

Table C.9 Values of y_2 for A=1.21e-6 ($psi^{-1}hr^{-n}$) and Three Levels of n

y_2 value with creep coefficients A =10A, n=1n									
	OV=0%			OV=3%			OV=6%		
	G=0.1 %	G=0.4 %	G=0.7 %	G=0.1 %	G=0.4 %	G=0.7 %	G=0.1 %	G=0.4 %	G=0.7 %
DR=30	-0.125	0.6	3.2	0.7875	0.975	1.15	0.875	0.9	0.975
DR=50	1.075	1.0625	1.4	0.85	0.8	1.0125	0.65	0.9375	0.6875
DR=70	1	0.7875	0.8625	0.45	0.375	0.5375	0.7125	0.525	0.425
y_2 value with creep coefficients A = 10A, n=0.5n									
	OV=0%			OV=3%			OV=6%		
	G=0.1 %	G=0.4 %	G=0.7 %	G=0.1 %	G=0.4 %	G=0.7 %	G=0.1 %	G=0.4 %	G=0.7 %
DR=30	0.35	1	-0.075	0.2375	0.275	0.3375	0.2625	0.5	0.825
DR=50	0.9375	1.1625	1.575	0.5	0.45	0.6625	0.3125	0.4625	0.8
DR=70	0.6125	0.725	0.525	0.375	0.4	0.525	-1.175	0.4625	0.35
y_2 value with creep coefficients A = 10A, n=1.5n									
	OV=0%			OV=3%			OV=6%		
	G=0.1 %	G=0.4 %	G=0.7 %	G=0.1 %	G=0.4 %	G=0.7 %	G=0.1 %	G=0.4 %	G=0.7 %
DR=30	2.65	3.1	5	3.575	2.9125	1.2125	1.0625	1.575	3.2375
DR=50	2.85	2.8	3.1625	2.1125	2.4625	2.3375	1.525	0.675	1.025
DR=70	0.825	1.725	2.025	1.5375	1.7625	1.9875	1.4625	1.3125	1.8

Reproduced with permission of the copyright owner. Further reproduction prohibited without permission.

APPENDIX D

PORTION OF SAS INPUT DATA

Reproduced with permission of the copyright owner. Further reproduction prohibited without permission.

Table D.1 Portion of SAS Factorial Input Data Set for y_0

A(DR)	A2	B(Gap)	B2	C(OV)	C2	D(A)	D2	E(n)	E2	Y_0
-1	1	-1	1	-1	1	-1	1	-1	1	1.851
-1	1	0	-2	-1	1	-1	1	-1	1	1.8991
-1	1	1	1	-1	1	-1	1	-1	1	1.846
-1	1	-1	1	0	-2	-1	1	-1	1	1.7161
-1	1	0	-2	0	-2	-1	1	-1	1	1.6964
-1	1	1	1	0	-2	-1	1	-1	1	1.6962
-1	1	-1	1	1	1	-1	1	-1	1	1.6496
-1	1	0	-2	1	1	-1	1	-1	1	1.6619
-1	1	1	1	1	1	-1	1	-1	1	1.6798
0	-2	-1	1	-1	1	-1	1	-1	1	1.7066
0	-2	0	-2	-1	1	-1	1	-1	1	1.7179
0	-2	1	1	-1	1	-1	1	-1	1	1.6969
0	-2	-1	1	0	-2	-1	1	-1	1	1.6726
0	-2	0	-2	0	-2	-1	1	-1	1	1.6704
0	-2	1	1	0	-2	-1	1	-1	1	1.6839
0	-2	-1	1	1	1	-1	1	-1	1	1.6266
0	-2	0	-2	1	1	-1	1	-1	1	1.649
0	-2	1	1	1	1	-1	1	-1	1	1.6507
1	1	-1	1	-1	1	-1	1	-1	1	1.718
1	1	0	-2	-1	1	-1	1	-1	1	1.7066
1	1	1	1	-1	1	-1	1	-1	1	1.7038
1	1	-1	1	0	-2	-1	1	-1	1	1.6489
1	1	0	-2	0	-2	-1	1	-1	1	1.6595
1	1	1	1	0	-2	-1	1	-1	1	1.6656
1	1	-1	1	1	1	-1	1	-1	1	1.6289
1	1	0	-2	1	1	-1	1	-1	1	1.6509
1	1	1	1	1	1	-1	1	-1	1	1.6536
-1	1	-1	1	-1	1	-1	1	0	-2	2.043
-1	1	0	-2	-1	1	-1	1	0	-2	2.0519
-1	1	1	1	-1	1	-1	1	0	-2	2.3344
-1	1	-1	1	0	-2	-1	1	0	-2	2.005
-1	1	0	-2	0	-2	-1	1	0	-2	2.0141
-1	1	1	1	0	-2	-1	1	0	-2	2.0275
...	...	...	...	...	...	...	...	...	...	...
-1	1	0	-2	1	1	-1	1	0	-2	2.0038
-1	1	1	1	1	1	-1	1	0	-2	2.0231
0	-2	-1	1	-1	1	-1	1	0	-2	2.0705
0	-2	0	-2	-1	1	-1	1	0	-2	2.0731
0	-2	1	1	-1	1	-1	1	0	-2	2.0714
0	-2	-1	1	0	-2	-1	1	0	-2	1.9986
0	-2	0	-2	0	-2	-1	1	0	-2	1.9846
0	-2	1	1	0	-2	-1	1	0	-2	1.9339

Reproduced with permission of the copyright owner. Further reproduction prohibited without permission.

Table D.2 Portion of SAS factorial Input Data Set for y_1

A(DR)	A2	B(G)	B2	C(OV)	C2	D(A)	D2	E(n)	E2	Y_1
-1	1	-1	1	-1	1	-1	1	-1	1	-1.785
-1	1	0	-2	-1	1	-1	1	-1	1	-2.22
-1	1	1	1	-1	1	-1	1	-1	1	-1.445
-1	1	-1	1	0	-2	-1	1	-1	1	-1.145
-1	1	0	-2	0	-2	-1	1	-1	1	-1.105
-1	1	1	1	0	-2	-1	1	-1	1	-1.14
-1	1	-1	1	1	1	-1	1	-1	1	-0.93
-1	1	0	-2	1	1	-1	1	-1	1	-1.025
-1	1	1	1	1	1	-1	1	-1	1	-1.185
0	-2	-1	1	-1	1	-1	1	-1	1	-1.12
0	-2	0	-2	-1	1	-1	1	-1	1	-1.2
0	-2	1	1	-1	1	-1	1	-1	1	-1.085
0	-2	-1	1	0	-2	-1	1	-1	1	-1.09
0	-2	0	-2	0	-2	-1	1	-1	1	-1.085
0	-2	1	1	0	-2	-1	1	-1	1	-1.195
0	-2	-1	1	1	1	-1	1	-1	1	-0.935
0	-2	0	-2	1	1	-1	1	-1	1	-1.055
0	-2	1	1	1	1	-1	1	-1	1	-1.02
1	1	-1	1	-1	1	-1	1	-1	1	-1.26
1	1	0	-2	-1	1	-1	1	-1	1	-1.21
1	1	1	1	-1	1	-1	1	-1	1	-1.2
1	1	-1	1	0	-2	-1	1	-1	1	-1.015
1	1	0	-2	0	-2	-1	1	-1	1	-1.09
1	1	1	1	0	-2	-1	1	-1	1	-1.125
1	1	-1	1	1	1	-1	1	-1	1	-0.985
1	1	0	-2	1	1	-1	1	-1	1	-1.085
1	1	1	1	1	1	-1	1	-1	1	-1.065
-1	1	-1	1	-1	1	-1	1	0	-2	-1.635
-1	1	0	-2	-1	1	-1	1	0	-2	-1.66
-1	1	1	1	-1	1	-1	1	0	-2	-3.42
-1	1	-1	1	0	-2	-1	1	0	-2	-1.69
-1	1	0	-2	0	-2	-1	1	0	-2	-1.76
-1	1	1	1	0	-2	-1	1	0	-2	-1.77
-1	1	-1	1	1	1	-1	1	0	-2	-1.9767
-1	1	0	-2	1	1	-1	1	0	-2	-1.83
-1	1	1	1	1	1	-1	1	0	-2	-1.82
...	...	...	...	...	...	...	...	...	...	...
0	-2	0	-2	-1	1	-1	1	0	-2	-1.97
0	-2	1	1	-1	1	-1	1	0	-2	-1.925
0	-2	-1	1	0	-2	-1	1	0	-2	-1.855
0	-2	0	-2	0	-2	-1	1	0	-2	-1.725
0	-2	1	1	0	-2	-1	1	0	-2	-1.44

Reproduced with permission of the copyright owner. Further reproduction prohibited without permission.

Table D.3 Portion of SAS factorial Input Data Set for y_2

A(DR)	A2	B(G)	B2	C(OV)	C2	D(A)	D2	E(n)	E2	Y_2
-1	1	-1	1	-1	1	-1	1	-1	1	1.25
-1	1	0	-2	-1	1	-1	1	-1	1	1.9875
-1	1	1	1	-1	1	-1	1	-1	1	0.75
-1	1	-1	1	0	-2	-1	1	-1	1	0.4375
-1	1	0	-2	0	-2	-1	1	-1	1	0.4125
-1	1	1	1	0	-2	-1	1	-1	1	0.475
-1	1	-1	1	1	1	-1	1	-1	1	0.2375
-1	1	0	-2	1	1	-1	1	-1	1	0.3625
-1	1	1	1	1	1	-1	1	-1	1	0.575
0	-2	-1	1	-1	1	-1	1	-1	1	0.4375
0	-2	0	-2	-1	1	-1	1	-1	1	0.5125
0	-2	1	1	-1	1	-1	1	-1	1	0.3625
0	-2	-1	1	0	-2	-1	1	-1	1	0.4375
0	-2	0	-2	0	-2	-1	1	-1	1	0.4125
0	-2	1	1	0	-2	-1	1	-1	1	0.5625
0	-2	-1	1	1	1	-1	1	-1	1	0.2875
0	-2	0	-2	1	1	-1	1	-1	1	0.45
0	-2	1	1	1	1	-1	1	-1	1	0.325
1	1	-1	1	-1	1	-1	1	-1	1	0.6
1	1	0	-2	-1	1	-1	1	-1	1	0.5375
1	1	1	1	-1	1	-1	1	-1	1	0.525
1	1	-1	1	0	-2	-1	1	-1	1	0.3625
1	1	0	-2	0	-2	-1	1	-1	1	0.45
1	1	1	1	0	-2	-1	1	-1	1	0.4875
1	1	-1	1	1	1	-1	1	-1	1	0.3625
1	1	0	-2	1	1	-1	1	-1	1	0.4625
1	1	1	1	1	1	-1	1	-1	1	0.3875
-1	1	-1	1	-1	1	-1	1	0	-2	0.45
-1	1	0	-2	-1	1	-1	1	0	-2	0.5125
-1	1	1	1	-1	1	-1	1	0	-2	2.9625
-1	1	-1	1	0	-2	-1	1	0	-2	0.7
-1	1	0	-2	0	-2	-1	1	0	-2	0.7875
-1	1	1	1	0	-2	-1	1	0	-2	0.75
-1	1	-1	1	1	1	-1	1	0	-2	1.4417
-1	1	0	-2	1	1	-1	1	0	-2	0.925
-1	1	1	1	1	1	-1	1	0	-2	0.7875
...	...	...	...	...	...	...	...	...	...	...
0	-2	0	-2	-1	1	-1	1	0	-2	0.9875
0	-2	1	1	-1	1	-1	1	0	-2	0.9125
0	-2	-1	1	0	-2	-1	1	0	-2	0.9875
0	-2	0	-2	0	-2	-1	1	0	-2	0.7875
0	-2	1	1	0	-2	-1	1	0	-2	0.4125

Reproduced with permission of the copyright owner. Further reproduction prohibited without permission.

APPENDIX E

SAS PROGRAM

Reproduced with permission of the copyright owner. Further reproduction prohibited without permission.

```
// EXEC SAS
//SAS.SYSIN DD *
DATA LONGFIRTC;
INPUT A  B  C  D  E  Y;
AB=A*B;
A2=A*A;
B2=B*B;
C2=C*C;
D2=D*D;
E2=E*E;
AC=A*C;
AD=A*D;
AE=A*E;
AB2=A*B2;
AC2=A*C2;
AD2=A*D2;
AE2=A*E2;
BC=B*C;
BD=B*D;
BE=B*E;
BA2=B*A2;
BC2=B*C2;
BD2=B*D2;
BE2=B*E2;
CD=C*D;
CE=C*E;
CA2=C*A2;
CB2=C*B2;
CD2=C*D2;
CE2=C*E2;
DE=D*E;
DA2=D*A2;
DB2=D*B2;
DC2=D*C2;
DE2=D*E2;
EA2=E*A2;
EB2=E*B2;
EC2=E*C2;
ED2=E*D2;
A2B2=A2*B2;
A2C2=A2*C2;
A2D2=A2*D2;
A2E2=A2*E2;
B2C2=B2*C2;
B2D2=B2*D2;
```

Reproduced with permission of the copyright owner. Further reproduction prohibited without permission.

```
B2E2=B2*E2;
C2D2=C2*D2;
C2E2=C2*E2;
D2E2=D2*E2;
ABC=AB*C;
ABD=AB*D;
ABE=AB*E;
ABC2=AB*C2;
ABD2=AB*D2;
ABE2=AB*E2;
ACD=AC*D;
ACE=AC*E;
ACB2=AC*B2;
ACD2=AC*D2;
ACE2=AC*E2;
ADE=AD*E;
ADB2=AD*B2;
ADC2=AD*C2;
ADE2=AD*E2;
AEB2=AE*B2;
AEC2=AE*C2;
AED2=AE*D2;
AB2C2=AB2*C2;
AB2D2=AB2*D2;
AB2E2=AB2*E2;
AC2D2=AC2*D2;
AC2E2=AC2*E2;
AD2E2=AD2*E2;
BCD=BC*D;
BCE=BC*E;
BCA2=BC*A2;
BCD2=BC*D2;
BCE2=BC*E2;
BDE=BD*E;
BDA2=BD*A2;
BDC2=BD*C2;
BDE2=BD*E2;
BEA2=BE*A2;
BEC2=BE*C2;
BED2=BE*D2;
BA2C2=BA2*C2;
BA2D2=BA2*D2;
BA2E2=BA2*E2;
BC2D2=BC2*D2;
BC2E2=BC2*E2;
BD2E2=BD2*E2;
```

Reproduced with permission of the copyright owner. Further reproduction prohibited without permission.

```
CDE=CD*E;
CDA2=CD*A2;
CDB2=CD*B2;
CDE2=CD*E2;
CEA2=CE*A2;
CEB2=CE*B2;
CED2=CE*D2;
CA2B2=CA2*B2;
CA2D2=CA2*D2;
CA2E2=CA2*E2;
CB2D2=CB2*D2;
CB2E2=CB2*E2;
CD2E2=CD2*E2;
DEA2=DE*A2;
DEB2=DE*B2;
DEC2=DE*C2;
DA2B2=DA2*B2;
DA2C2=DA2*C2;
DA2E2=DA2*E2;
DB2C2=DB2*C2;
DB2E2=DB2*E2;
DC2E2=DC2*E2;
EA2B2=EA2*B2;
EA2C2=EA2*C2;
EA2D2=EA2*D2;
EB2C2=EB2*C2;
EB2D2=EB2*D2;
EC2D2=EC2*D2;
A2B2C2=A2B2*C2;
A2B2D2=A2B2*D2;
A2B2E2=A2B2*E2;
A2C2D2=A2C2*D2;
A2C2E2=A2C2*E2;
A2D2E2=A2D2*E2;
B2C2D2=B2C2*D2;
B2C2E2=B2C2*E2;
B2D2E2=B2D2*E2;
C2D2E2=C2D2*E2;
ABCD=ABC*D;
ABCE=ABC*E;
ABCD2=ABC*D2;
ABCE2=ABC*E2;
ABDE=ABD*E;
ABDC2=ABD*C2;
ABDE2=ABD*E2;
ABEC2=ABE*C2;
```

Reproduced with permission of the copyright owner. Further reproduction prohibited without permission.

```
ABED2=ABE*D2;
ABC2D2=ABC2*D2;
ABC2E2=ABC2*E2;
ABD2E2=ABD2*E2;
ACDE=ACD*E;
ACDB2=ACD*B2;
ACDE2=ACD*E2;
ACEB2=ACE*B2;
ACED2=ACE*D2;
ACB2D2=ACB2*D2;
ACB2E2=ACB2*E2;
ACD2E2=ACD2*E2;
ADEB2=ADE*B2;
ADEC2=ADE*C2;
ADB2C2=ADB2*C2;
ADB2E2=ADB2*E2;
ADC2E2=ADC2*E2;
AEB2C2=AEB2*C2;
AEB2D2=AEB2*D2;
AEC2D2=AEC2*D2;
AB2C2D2=AB2C2*D2;
AB2C2E2=AB2C2*E2;
AB2D2E2=AB2D2*E2;
AC2D2E2=AC2D2*E2;
BCDE=BCD*E;
BCDA2=BCD*A2;
BCDE2=BCD*E2;
BCEA2=BCE*A2;
BCED2=BCE*D2;
BCA2D2=BCA2*D2;
BCA2E2=BCA2*E2;
BCD2E2=BCD2*E2;
BDEA2=BDE*A2;
BDEC2=BDE*C2;
BDA2C2=BDA2*C2;
BDA2E2=BDA2*E2;
BDC2E2=BDC2*E2;
BEA2C2=BEA2*C2;
BEA2D2=BEA2*D2;
BEC2D2=BEC2*D2;
BA2C2D2=BA2C2*D2;
BA2C2E2=BA2C2*E2;
BA2D2E2=BA2D2*E2;
BC2D2E2=BC2D2*E2;
CDEA2=CDE*A2;
CDEB2=CDE*B2;
```

Reproduced with permission of the copyright owner. Further reproduction prohibited without permission.

```
CDA2B2=CDA2*B2;
CDA2E2=CDA2*E2;
CDB2E2=CDB2*E2;
CEA2B2=CEA2*B2;
CEA2D2=CEA2*D2;
CEB2D2=CEB2*D2;
CA2B2D2=CA2B2*D2;
CA2B2E2=CA2B2*E2;
CA2D2E2=CA2D2*E2;
CB2D2E2=CB2D2*E2;
DEA2B2=DEA2*B2;
DEA2C2=DEA2*C2;
DEB2C2=DEB2*C2;
DA2B2C2=DA2B2*C2;
DA2B2E2=DA2B2*E2;
DA2C2E2=DA2C2*E2;
DB2C2E2=DB2C2*E2;
EA2B2C2=EA2B2*C2;
EA2B2D2=EA2B2*D2;
EA2C2D2=EA2C2*D2;
EA2C2D2=EA2C2*D2;
EB2C2D2=EB2C2*D2;
A2B2C2D2=A2B2C2*D2;
A2B2C2E2=A2B2C2*E2;
A2B2D2E2=A2B2D2*E2;
B2C2D2E2=B2C2D2*E2;
A2C2D2E2=A2C2D2*E2;
A2B2C2FG=A2B2C2*D2E2;
ABCDE=ABCD*E;
ABCDE2=ABCD*E2;
ABCED2=ABCE*D2;
ABCD2E2=ABCD2*E2;
ABDEC2=ABDE*C2;
ABDC2E2=ABDC2*E2;
ABEC2D2=ABEC2*D2;
ABC2D2E2=ABC2D2*E2;
ACDEB2=ACDE*B2;
ACDB2E2=ACDB2*E2;
ACEB2D2=ACEB2*D2;
ACB2D2E2=ACB2D2*E2;
ADEB2C2=ADEB2*C2;
ADB2C2E2=ADB2C2*E2;
AEB2C2D2=AEB2C2*D2;
AB2C2D2G=AB2C2D2*E2;
BCDA2E2=BCDA2*E2;
BCDEA2=BCDE*A2;
```

Reproduced with permission of the copyright owner. Further reproduction prohibited without permission.

```
BCEA2D2=BCEA2*D2;
BCA2D2E2=BCA2D2*E2;
BDEA2C2=BDEA2*C2;
BDA2C2E2=BDA2C2*E2;
BEA2C2D2=BEA2C2*D2;
BA2C2FG=BA2C2D2*E2;
CDEA2B2=CDEA2*B2;
CDA2B2E2=CDA2B2*E2;
CEA2B2D2=CEA2B2*D2;
CA2B2D2G=CA2B2D2*E2;
DEA2B2C2=DEA2B2*C2;
DA2B2C2G=DA2B2C2*E2;
EA2B2C2F=EA2B2C2*D2;
LINES;
/*data input from Appendix D
;
PROC REG;
MODEL Y= A  A2 B  B2  C  C2 D D2 E E2 AB AC
      AD  AE  AB2 AC2 AD2 AE2 BC BE BA2 BC2
      BD2 BE2 CD CE CA2 CB2 BD
     CD2 CE2 DE DA2 DB2 DC2 DE2 EA2 EB2 EC2
     ED2 A2B2 A2C2 A2D2 A2E2 B2C2 B2D2 B2E2 C2D2
     C2E2 D2E2
     ABC ABD ABE ABC2 ABD2 ABE2 ACD ACE ACB2 ACD2
     ACE2 ADE ADB2 ADC2 ADE2 AEB2 AEC2 AED2 AB2C2
     AB2D2 AB2E2 AC2D2 AC2E2 AD2E2 BCD BCE BCA2
     BCD2 BCE2 BDE BDA2 BDC2 BDE2 BEA2 BEC2 BED2
     BA2C2 BA2D2 BA2E2 BC2D2 BC2E2 BD2E2
     CDE CDA2 CDB2 CDE2 CEA2 CEB2 CED2 CA2B2 CA2D2
     CA2E2 CB2D2 CB2E2 CD2E2 DEA2 DEB2 DEC2 DA2B2
     DA2C2 DA2E2 DB2C2 DB2E2 DC2E2 EA2B2 EA2C2 EA2D2
     EB2C2 EB2D2 EC2D2 A2B2C2 A2B2D2 A2B2E2 A2C2D2
     A2C2E2 A2D2E2 B2C2D2 B2C2E2 B2D2E2 C2D2E2
     ABCD ABCE ABCD2 ABCE2 ABDE ABDC2 ABDE2 ABEC2
     ABED2 ABC2D2 ABC2E2 ABD2E2 ACDE ACDB2 ACDE2
     ACEB2 ACED2 ACB2D2 ACB2E2 ACD2E2 ADEB2 ADEC2
     ADB2C2 ADB2E2 ADC2E2 AEB2C2 AEB2D2 AEC2D2 AB2C2D2
     AB2C2E2 AB2D2E2 AC2D2E2 BCDE BCDA2 BCDE2 BCEA2
     BCED2 BCA2D2 BCA2E2 BCD2E2 BDEA2 BDEC2 BDA2C2
     BDA2E2 BDC2E2 BEA2C2 BEA2D2 BEC2D2 BA2C2D2 BA2D2E2
     BA2C2E2
     BC2D2E2 CDEA2 CDEB2 CDA2B2 CDA2E2 CDB2E2 CEA2B2
     CEA2D2  CEB2D2 CA2B2D2 CA2B2E2 CA2D2E2 CB2D2E2
     DEA2B2 DEA2C2 DEB2C2 DA2B2C2 DA2B2E2 DA2C2E2
     DB2C2E2 EA2B2C2 EA2B2D2 EA2C2D2 EB2C2D2 A2B2C2D2
     A2B2C2E2 A2B2D2E2 B2C2D2E2 A2C2D2E2
```

Reproduced with permission of the copyright owner. Further reproduction prohibited without permission.

```
      ABCDE ABCDE2 ABCED2 ABCD2E2 ABDEC2 ABDC2E2 ABEC2D2
      ABC2D2E2  ACDEB2 ACDB2E2 ACEB2D2 ACB2D2E2 ADEB2C2
      ADB2C2E2 AEB2C2D2 AB2C2D2G BCDA2E2 BCDEA2 BCEA2D2
      BCA2D2E2 BDEA2C2 BDA2C2E2 BEA2C2D2 BA2C2FG CDEA2B2
      CDA2B2E2 CEA2B2D2 CA2B2D2G DEA2B2C2 DA2B2C2G
      EA2B2C2F /SS1;
run;
//
```

Reproduced with permission of the copyright owner. Further reproduction prohibited without permission.

APPENDIX F

MATERIAL PROPERTIES AND LINER BUCKLING EXPERIMENT RESULTS

Reproduced with permission of the copyright owner. Further reproduction prohibited without permission.

Table F.1 Creep Properties of Various Polymers

Plastic	n	$A_{(psi^{-1}\ hr^{-n})}$	E (psi)
Polyvinyl chloride*	0.305	1.15E-07	493827
Polyethylene*	0.154	1.05E-05	21666.7
Polyester **	0.24	1.21E-07	652400

* Data selected from Findley (1987)

** Curve fitting results on Lin's data

Table F.2 Material Properties for Insituform Enhanced Product (Lin, 1994)

Coefficients for Compression					
Stress (psi)	ε_0	ε_t	n	$A_{(psi^{-1}\ hr^{-n})}$	m+1
1000	0.001567	0.000115	0.2389	2.74735E-08	0.2389
2000	0.00298	0.00026	0.23771	3.09023E-08	0.23771
3000	0.004667	0.000407	0.218	2.95753E-08	0.218
4000	0.005838	0.000563	0.22663	3.18982E-08	0.22663
Coefficients for Tension					
Stress (psi)	ε_0	ε_t	n	$A_{(psi^{-1}\ hr^{-n})}$	m+1
1000	1.33E-03	6.43E-04	0.173	1.11239E-07	0.173
1500	2.94E-03	8.76E-04	0.1624	9.48416E-08	0.1624
2000	4.45E-03	1.02E-03	0.1623	8.30165E-08	0.1623
2500	6.67E-03	7.42E-04	0.2028	6.0191E-08	0.2028
Coefficients for Bending					
Stress (psi)	ε_0	ε_t	n	$A_{(psi^{-1}\ hr^{-n})}$	m+1
1000	2.05E-03	1.75E-04	0.2648	4.634E-08	0.2648
1500	4.11E-03	3.90E-04	0.2823	7.3398E-08	0.2823
2000	6.54E-03	6.45E-04	0.2878	9.28155E-08	0.2878
2500	8.83E-03	8.95E-04	0.3356	1.20145E-07	0.3356

Reproduced with permission of the copyright owner. Further reproduction prohibited without permission.

Table F.3 Long-Term Buckling Test Results for the Insituform Enhanced Product (Guice et. al, 1994)

Test No.	DR	P(psi)	Tcr(hr)	G(%)	PR
1	51.27	75	0.5	0.2087	0.990
2	51.09	75	51	0.12765	0.990
4	52.87	75	68	0.1704	0.990
5	52.44	75	1.5	0.17455	0.990
6	49.34	70	33	0.2993	0.924
7	52.96	75	54	0.1361	0.990
8	52.24	69	0.2	0.3403	0.911
9	53.82	70	3	0.34095	0.924
11	51.27	70	2	0.1661	0.924
12	52.39	65	521	0.2471	0.858
13	54.07	70	136	0.21305	0.924
14	52.3	65	1056	0.2774	0.858
15	53.27	65	528	0.27305	0.858
16	54.72	60	2455	0.2295	0.792
17	52.83	60	200	0.2302	0.792
18	52.44	60	54	0.14945	0.792
19	51.78	60	2455	0.3361	0.792
21	53.23	60	494	0.29895	0.792
22	52.3	55	3272	0.25605	0.726
23	54.02	60	1536	0.26	0.792
24	53.43	55	4349	0.34185	0.726
25	55.1	55	3384	0.213	0.726
26	53.82	55	455	0.2131	0.726
27	55.71	55	144	0.3846	0.726
28	55.9	55	2236	0.21295	0.726
29	54.02	50	5379	0.2559	0.660
31	53.57	50	6013	0.2216	0.660
32	53.86	50	10000	0.17035	0.660
33	54.02	50	1272	0.2559	0.660
34	53.32	50	3302	0.21315	0.660
35	52.83	50	3338	0.21315	0.660
36	52.98	45	10000	0.2989	0.594
37	53.77	45	10000	0.25595	0.594
38	53.18	45	10000	0.3675	0.594
39	54.58	45	1616	0.26415	0.594
Ave	53.164	59.686	2411.663	0.246	0.788

* P(short-term for average) = 75.769 psi

Reproduced with permission of the copyright owner. Further reproduction prohibited without permission.

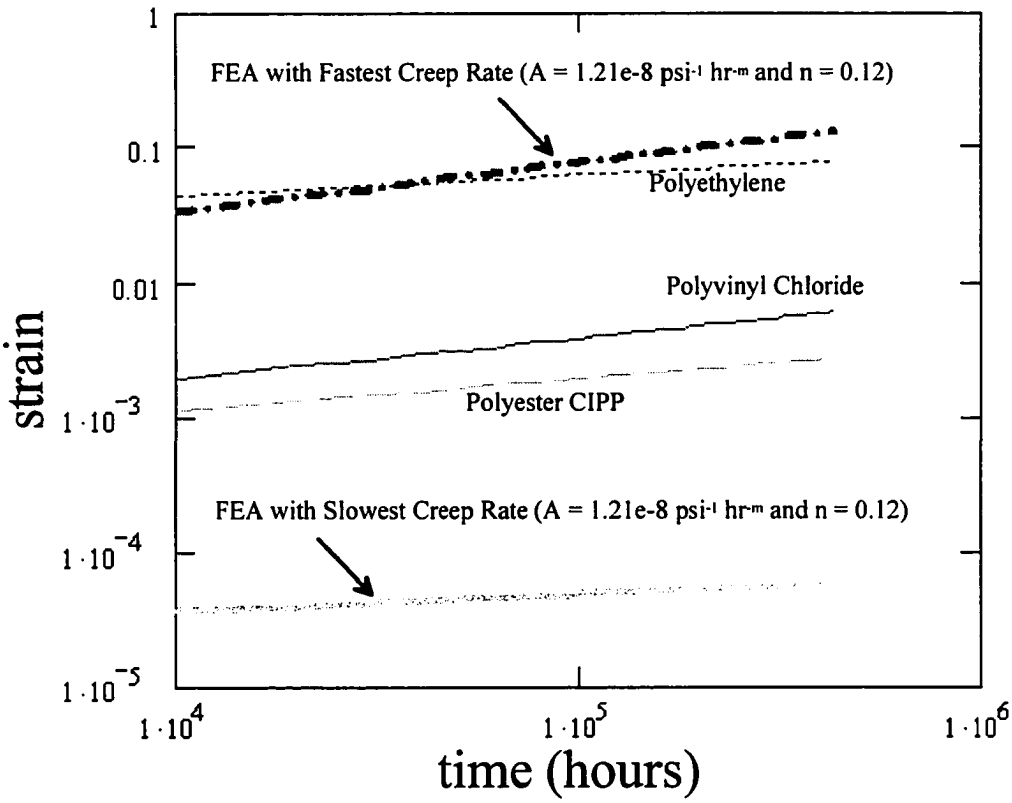

Figure F.1 Strain Verse Time for the Material in Table F.1 and for the Extreme Values of A and n Simulated in the Finite Element Analysis

Reproduced with permission of the copyright owner. Further reproduction prohibited without permission.

APPENDIX G

ABAQUS INPUT FILE

Reproduced with permission of the copyright owner. Further reproduction prohibited without permission.

```
*HEADING
 oval(=6%)gap(=0.1%)DR(30)RING BUCKLING ANALYSIS, CPE4, 4*320 MESH
1-1-6-SM
*NODE,INPUT=layer1.inp
*NODE,INPUT=layer2.inp
*NODE,INPUT=layer3.inp
*NODE,INPUT=layer4.inp
*NODE,INPUT=layer5.inp
*Ngen,NSET=SYM1
1,4001,1000
*NGEN,NSET=sym2
321,4321,1000
*NSET,NSET=MID,GEN
2001,2321,1
*ELEMENT,TYPE=CPE4
1,1,1001,1002,2
*ELGEN,ELSET=EALL
1,4,1000,1000,320,1,1
*ELSET,GENERATE,ELSET=LOAD
3001,3320
*orientation,name=or,system=cylindrical
 0.,0.,0.,0.,0.,10.
 3,0.
*MATERIAL ,NAME=A1
*ELASTIC
538621,0.3
 creep,law=strain
 1.00788e-8,1.14585,-.76
*SOLID SECTION,MATERIAL=A1,ELSET=EALL,orientation=or
*NODE,input=hostpipe.inp
*ELEMENT,TYPE=R2D2
 10001,50001,50002
*ELGEN,ELSET=HOSTPIPE
 10001,320
*RIGID BODY,ELSET=HOSTPIPE,REF NODE=50001
*SURFACE DEFINITION,NAME=ASURF
 load,S2
*SURFACE DEFINITION,NAME=BSURF
 HOSTPIPE,spos
*CONTACT PAIR,INTERACTION=smooth
 ASURF,BSURF
*SURFACE INTERACTION,NAME=smooth
*BOUNDARY
 50001,ENCASTRE
 Sym1,1
```

Reproduced with permission of the copyright owner. Further reproduction prohibited without permission.

```
 sym1,6
 sym1,2
 sym2,6
 sym2,1
*RESTART,WRITE,FREQ=5
*STEP,NLGEOM,INC=1000
*STATIC
 0.2,2.,1.E-15,1.E-1
*DLOAD
 load,P2,200
*NODE PRINT,nset=mid,FREQ=500
 U
*EL PRINT,ELSET=eall,FREQ=500
 S
*contact print,slave=asurf,master=bsurf,freq=500
*contact print,slave=asurf,freq=500
 CFN
*END STEP
*step,nlgeom,inc=500
*visco,cetol=1.e-4
 1.e-7,26280000,1.e-30
*node print,freq=500
 u
*el print,elset=eall,freq=500
 s
*contact print,slave=asurf,master=bsurf,freq=500
*contact print,slave=asurf,freq=500
CFN
*end step
```

Reproduced with permission of the copyright owner. Further reproduction prohibited without permission.

APPENDIX H

MATHCAD IMPLEMENTATION OF

THE DESIGN MODEL

Reproduced with permission of the copyright owner. Further reproduction prohibited without permission.

MATHCAD IMPLEMENTATION OF THE PROPOSED DESIGN MODEL

Calculation of Long Term Buckling Linear Thickness

Definition of Constants Based on Finite Element Runs and SAS Factorial Analysis Results

Definition of Liner Geometry and Material Properties:

$E := 538621$	**Elastic Modulus**
$v := 0.3$	**Poisson's Ratio**
$w := 1.21 \cdot 10^{-7}$	**Creep Coefficient A (Range = 1.21*10-6 to 1.21*10-8)**
$q := 0.24$	**Creep Exponent n (q = 0.12 to 0.36)**
$x := 0.1$	**Gap Ratio (range = 0.1 to 0.7)**
$y := 0$	**Ovality (range = 0% to 6%)**
$z := 0.0$	**Local Intrusion Ratio (range = 0% to 2.25%)**
DR	**Outer Liner Diameter / Liner Thickness** **Outside Diameter**
$Pg := 34.8058$	**External Groundwater Pressure**
$s := 30$	**Outer Liner Diameter / Liner Thickness** **Outside Diameter**
PR	**Pressure Ratio (External Groundwater Pressure/Short-term Critical Pressure)**

continued on the next page

Reproduced with permission of the copyright owner. Further reproduction prohibited without permission.

Definition of Constants Based on Finite Element Runs:

Constant A:

$$A1(x,y,z) := -0.0124981x^2\cdot y^2\cdot z^2 - 0.00720165x^2\cdot y^2\cdot z + (-0.0135185)\cdot x^2\cdot y^2 - (-0.0616369)\cdot x^2\cdot z^2\cdot y \ldots + 0.107695x^2\cdot y\cdot z - (-0.0433333)\,x^2\cdot y$$

$$A2(x,y,z) := 0.616516x^2\cdot z^2 - 0.851605x^2\cdot z - 2.73111x^2 - (-0.00867063)\cdot x\cdot y^2\cdot z^2 \ldots + (-0.0046214)\cdot x\cdot y^2\cdot z - (-0.0119815)\cdot x\cdot y^2$$

$$A3(x,y,z) := 0.00756836x\cdot y\cdot z^2 - 0.0861687x\cdot y\cdot z - 0.191778x\cdot y - 0.802743x\cdot z^2 \ldots + 0.0564691x\cdot z + 6.49522x - 0.0046488y^2\cdot z^2$$

$$A4(x,y,z) := 0.00992675y^2\cdot z + (-0.00297963)\cdot y^2 + 0.0245297y\cdot z^2 - 0.0953193y\cdot z \ldots + 0.0301722y + 0.0286771z^2 \ldots + 1.0946z + 1.06019$$

$$A(x,y,z) := A1(x,y,z) + A2(x,y,z) + A3(x,y,z) + A4(x,y,z)$$

Constant M:

$$M1(x,y,z) := -0.00118275x^2\cdot y^2\cdot z^2 - (-0.00179698)\cdot x^2\cdot y^2\cdot z - 0.00290123x^2\cdot y^2 - (-0.00501143)\cdot x^2\cdot z^2\cdot y \ldots + (-0.000123457)\cdot x^2\cdot y\cdot z - 0.0012963x^2\cdot y$$

$$M2(x,y,z) := -0.0215089x^2\cdot z^2 + 0.271605x^2\cdot z - 0.66x^2 + 0.0011986x\cdot y^2\cdot z^2 \ldots + 0.00306311x\cdot y^2\cdot z + 0.00274691x\cdot y^2$$

$$M3(x,y,z) := -0.00296662x\cdot y\cdot z^2 - (-0.0038395)\cdot x\cdot y\cdot z + 0.000537037x\cdot y + 0.03538x\cdot z^2 \ldots + (0.441728x)\cdot z + 1.14667x - 0.000474562y^2\cdot z^2$$

$$M4(x,y,z) := 0.00128834y^2\cdot z - 0.000673457y^2 + 0.00259717y\cdot z^2 - 0.00739753y\cdot z + 0.00610926y \ldots + 0.0284093z^2 + 0.255457z + 2.25553$$

$$M(x,y,z) := M1(x,y,z) + M2(x,y,z) + M3(x,y,z) + M4(x,y,z)$$

$$P := \frac{A(x,y,z)\cdot E}{1-\nu^2}\cdot\left(\frac{1}{s-1}\right)^{M(x,y,z)}$$

$$PR := \frac{Pg}{P}$$

$$KK := \frac{Pg\cdot(1-\nu^2)}{A(x,y,z)\cdot E}$$

$$K := \frac{1}{KK}$$

continued on the next page

Reproduced with permission of the copyright owner. Further reproduction prohibited without permission.

LONG - TERM MODEL

$$D0 := 1.81646 + (-0.036573)\cdot x + (-0.030546)\cdot y + (-0.007882)\cdot y^2 \ldots$$
$$+ 0.046288w + (-0.00343)\cdot w^2 + 0.171212q \ldots$$
$$+ 5.250445q^2 + 0.251806x\cdot q + 0.002764x\cdot y^2 + (-0.041971)\cdot y\cdot w \ldots$$
$$+ (0.100385)\cdot y\cdot q + (-0.005012)\cdot x\cdot w \ldots$$
$$+ 0.003463y\cdot w^2 + (-0.890989)\cdot y\cdot q^2 + (-0.905203)\cdot w\cdot q + 0.012275w\cdot y^2 \ldots$$
$$+ 4.098936w\cdot q^2 + 0.055735q\cdot y^2 \ldots$$
$$+ 0.067729q\cdot w^2 + (-0.007943)\cdot x^2\cdot y^2 + (-0.001)\cdot y^2\cdot w^2 + (-0.316604)\cdot w^2\cdot q^2 \ldots$$
$$+ 0.060726x\cdot w\cdot q + 0.020798x\cdot q\cdot y^2 \ldots$$
$$+ (-0.004196)\cdot y\cdot w\cdot q + 0.01426y\cdot w^2\cdot q^2 + (-0.033594)\cdot w\cdot q\cdot y^2 + 0.022254q\cdot x^2\cdot y^2 \ldots$$
$$+ 0.00317q\cdot y^2\cdot w^2 + (-0.001987)\cdot y^2\cdot w^2\cdot q^2$$

$$D1 := (-0.005363) + (0.000287)\cdot y + 0.000177w + 0.025041q + (-0.052186)\cdot q^2 \ldots$$
$$+ (-0.000074348)\cdot x\cdot y^2 + (-0.000065064)\cdot q\cdot y^2 \ldots$$
$$+ 0.000012393x\cdot y\cdot w + (-0.008641)\cdot x\cdot y\cdot q^2 + 0.000025154x\cdot w\cdot y^2 \ldots$$
$$+ (-0.000086757)\cdot x\cdot q\cdot y^2 + 0.000052204x\cdot w^2\cdot q^2 \ldots$$
$$+ 0.000125y\cdot w\cdot q + 0.000015967y\cdot q\cdot w^2 + (-0.000003496)\cdot y^2\cdot w^2\cdot q^2 \ldots$$
$$+ (-0.000336)\cdot x\cdot y\cdot w\cdot q + (-0.000093646)\cdot x\cdot w\cdot q\cdot y^2$$

$$D2 := 0.000010688x\cdot y + (-0.000000433)\cdot y\cdot w + (-0.000014642)\cdot w\cdot q \ldots$$
$$+ (-0.000000355)\cdot x\cdot w\cdot y^2 + 0.000001958w\cdot q\cdot y^2\cdot x$$

$$B0 := -3.831279 + 0.171701y + 0.013047y^2 + 0.040381w + 23.485241q \ldots$$
$$+ -62.138158q^2 + 0.091319x\cdot y^2 + (-0.072128)\cdot y\cdot w \ldots$$
$$+ (-0.418949)\cdot y\cdot q + (-0.010139)\cdot x\cdot w + 0.008136y\cdot w^2 + 3.822008y\cdot q^2 \ldots$$
$$+ 3.50497w\cdot q + (-17.727698)\cdot w\cdot q^2 \ldots$$
$$+ (-0.240348)\cdot q\cdot y^2 + (-0.272074)\cdot q\cdot w^2 + (-0.000647)\cdot y^2\cdot w^2 \ldots$$
$$+ 1.336916w^2\cdot q^2 + 6.103519x\cdot y\cdot q^2 + (-0.172437)\cdot x\cdot w\cdot q \ldots$$
$$+ (-0.658115)\cdot x\cdot q\cdot y^2 + (-0.011384)\cdot y\cdot q\cdot w^2 + (-0.004502)\cdot y\cdot w^2\cdot q^2 \ldots$$
$$+ 0.076532w\cdot q\cdot y^2 + 0.025661q\cdot x^2\cdot y^2 \ldots$$
$$+ (-0.003941)\cdot q\cdot y^2\cdot w^2 + (-0.001454)\cdot x^2\cdot y^2\cdot w^2\cdot q^2$$

$$B1 := (0.040129) + 0.000473x + (-0.354117)\cdot q + (-0.000070737)\cdot y^2 \ldots$$
$$+ -0.000111w^2 + 0.725935q^2 \ldots$$
$$+ (-0.001695)\cdot x\cdot y^2 + 0.000007373y^2\cdot w^2 + 0.001701y^2\cdot q^2 \ldots$$
$$+ 0.000814w^2\cdot q^2 + (-0.072361)\cdot x\cdot y\cdot q^2 \ldots$$
$$+ (0.009651)\cdot x\cdot q\cdot y^2 + (-0.00024)\cdot x\cdot w^2\cdot q^2 + 0.002339y\cdot q\cdot w \ldots$$
$$+ (-0.000232)\cdot w^2\cdot q\cdot y + (-0.000001049)\cdot x^2\cdot y^2\cdot w^2 \ldots$$
$$+ 0.000131y^2\cdot w^2\cdot q^2 + 0.000006816x^2\cdot y^2\cdot w^2\cdot q^2$$

continued on the next page

Reproduced with permission of the copyright owner. Further reproduction prohibited without permission.

$$B2 := (-0.00000162)\cdot y\cdot w + 0.000080412\cdot w\cdot q + (-0.00000227)\cdot y^2\cdot w^2\cdot q^2 \ldots$$
$$+ 0.000002213\cdot x\cdot w\cdot q\cdot y^2$$

$$E0 := 3.873929 + (-0.363966)\cdot y + 0.028219\cdot y^2 + (-0.124004)\cdot w \ldots$$
$$+ -29.206532\cdot q + 69.630926\cdot q^2 + (-0.296528)\cdot x\cdot y \ldots$$
$$+ (-0.013146)\cdot x\cdot w^2 + 2.196663\cdot y\cdot q + 0.289434\cdot x\cdot w \ldots$$
$$+ (-0.001089)\cdot y\cdot w^2 + (-5.991578)\cdot y\cdot q^2 + (-2.766178)\cdot w\cdot q \ldots$$
$$+ 15.634132\cdot w\cdot q^2 + 0.196009\cdot q\cdot w^2 + (-0.000043306)\cdot y^2\cdot w^2 \ldots$$
$$+ (-0.965618)\cdot w^2\cdot q^2 + 1.49439\cdot x\cdot y\cdot q^2 + 0.316375\cdot x\cdot q\cdot y^2 \ldots$$
$$+ (-0.072948)\cdot x\cdot w^2\cdot q^2 + 0.041035\cdot y\cdot q\cdot w^2 + (-0.112635)\cdot y\cdot w^2\cdot q^2 \ldots$$
$$+ (-0.104203)\cdot q\cdot x^2\cdot y^2 + (-0.001079)\cdot q\cdot y^2\cdot w^2$$

$$E1 := (-0.044145) + 0.003796\cdot x + 0.350425\cdot q + 0.000198\cdot w^2 + (-0.681783)\cdot q^2 \ldots$$
$$+ (-0.029828)\cdot x\cdot q + (-0.000563)\cdot x\cdot y^2 \ldots$$
$$+ (-0.005905)\cdot w^2\cdot q^2 + (-0.087623)\cdot x\cdot y\cdot q^2 + 0.000084355\cdot x\cdot w\cdot y^2 \ldots$$
$$+ 0.000429\cdot x\cdot q\cdot y^2 + 0.00432\cdot x\cdot w^2\cdot q^2 \ldots$$
$$+ (-0.005643)\cdot y\cdot w\cdot q + (-0.000155)\cdot y\cdot q\cdot w^2 + 0.002455\cdot y\cdot w^2\cdot q^2 + (-0.000275)\cdot x\cdot y\cdot q\cdot w^2$$

$$E2 := 0.000107\cdot x\cdot y + (-0.000002466)\cdot x\cdot w^2 + 0.000002253\cdot y\cdot w + 0.000083122\cdot w\cdot q + (-0.000006253)\cdot x\cdot q\cdot w^2 \ldots$$
$$+ (-0.000000221)\cdot q\cdot y^2\cdot w^2 + (-0.000026)\cdot x\cdot w\cdot q\cdot y^2 + 0.000002375\cdot x\cdot q\cdot y^2\cdot w^2$$

$$D0a := D0\cdot K \qquad E0a := E0\cdot KK$$

$$D1a := D1\cdot K \qquad E1a := E1\cdot KK$$

$$D2a := D2\cdot K \qquad E2a := E2\cdot KK$$

$$DR := \mathrm{root}\left[\begin{bmatrix} B0 - 1 + B1\cdot s + B2\cdot s^2 + D2a\cdot s^2\cdot(s-1)^{-M(x,y,z)} \ldots \\ + D1a\cdot s\cdot(s-1)^{-M(x,y,z)} + D0a\cdot(s-1)^{-M(x,y,z)} \ldots \\ + E0a\cdot(s-1)^{M(x,y,z)} + E1a\cdot s\cdot(s-1)^{M(x,y,z)} \ldots \\ + E2a\cdot s\cdot(s-1)^{M(x,y,z)} - w\cdot E\cdot Time^q \end{bmatrix}, s\right]$$

$$DR = 56.334$$

$$Thickness := \frac{12}{DR}$$

$$Thickness = 0.213$$

Figure H.1 MathCAD Implementation of the Long-term Liner Design Model for DR

Reproduced with permission of the copyright owner. Further reproduction prohibited without permission.

...Same as the full model (except long-term part)

...

LONG - TERM SIMPLIFY MODEL

Definition of Constants Based on Finite Element Runs and Regression Analysis:

$$y0 := (1.338611) + (-73982)\cdot w + -1.06476510^{11}\cdot w^2 + 1.939159q + (-0.112421)\cdot q^2 \ldots + (755578)\cdot w\cdot q + (-464451)\cdot w\cdot q^2 + (21623648963)\cdot w^2\cdot q + -1.03806310^{11}\cdot w^2\cdot q^2$$

$$y1 := (-0.375834) + 151566w + (-383284769)\cdot w^2 + (-2.093035)\cdot q + (-0.328107)\cdot q^2 \ldots + (-1805938)\cdot w\cdot q + (2805836)\cdot w\cdot q^2 + 2.069737710^{12}\cdot w^2\cdot q + -6.70748310^{12}\cdot w^2\cdot q^2$$

$$DR := 1 + \left[\frac{(A\cdot y0\cdot E)}{Pg\cdot(1 + w\cdot E\cdot T^q - y1\cdot(1 - v^2))}\right]^{\frac{1}{M}}$$

DR = 34.75

$$Thickness := \frac{12}{DR}$$

Thickness = 0.345

Figure H.2 Mathcad Implementation of the Simplified Long-term Liner Design Model for DR

Reproduced with permission of the copyright owner. Further reproduction prohibited without permission.

...Same as the Figure H.1 (except the implementation is about the time)

$$TT := \left(\frac{1}{w \cdot E}\right)^{\frac{1}{q}} \left(B0 - 1 + B1 \cdot s + B2 \cdot s^2 + E0 \cdot PR + E1 \cdot PR \cdot s + E2 \cdot s^2 \cdot PR + D2 \cdot \frac{s^2}{PR} + D1 \cdot \frac{s}{PR} + \frac{D0}{PR}\right)^{\frac{1}{q}}$$

$$TT = 1.575 \cdot 10^{10}$$

Notice: TT represent time (hours) in this equation

Figure H.3 Mathcad Implementation of the Long-term Liner Design Model for Buckling Time

....Same as the Figure H.2 (except the implementation is about time)

$$TT := \left(\frac{1}{w \cdot E}\right)^{\frac{1}{q}} \cdot \left(y1 - 1 + \frac{y0}{PR}\right)^{\frac{1}{q}}$$

$$TT = 8.026 \cdot 10^{5}$$

Notice: TT represent time(hours) in this equation

Figure H.4 Mathcad Implementation of the Simplfied Long-term Liner Design Model for Buckling Time

Reproduced with permission of the copyright owner. Further reproduction prohibited without permission.

REFERENCES

Aalders, A.C., Bakeer, R.M. and Barber, M.E. (1998). "Deformation Measurement of Liners During Buckling Tests." *Proceeding of NO-DIG ENGINEERING 1st&2nd* Quarters, 12-15.

Aggarwal, S.C. and Cooper, M.J. (1984). "External Pressure Testing of Insituform Lining." Internal Report.

Amstutz, E. (1969). "Das Einbeulen von Schacht- und Stollenpanzerungen." Schweizerische Bauzeitung, Vol. 68, No. 9, 102-105.

ASTM, (1995). "Standard Practice for Rehabilitation of Existing Pipelines and Conduits by the Inversion and Curing of a Resin-Impregnated Tube." *ASTM Designation F1216-95*. Philadelphia, PA.

ASTM, (1998). "Standard Test Method for Obtaining Hydrostatic Design Basis for Thermoplastic Pipe Materials." *ASTM Designation D2837-98*. Philadelphia, PA.

ASTM, (1996). "Standard Practice for Obtaining Hydrostatic or Pressure Design Basis for 'Fiberglass' (Glass-Fiber-Reinforced Thermosetting-Resin) Pipe and Fittings." *ASTM Designation D2992-96*. Philadelphia, PA.

ASTM, (1993). "Standard Test Method for Determination for External Loading Characteristics of Plastic Pipe by Parallel-Plate Loading." *ASTM Designation D2412-93*. Philadelphia, PA.

ASTM, (1993). "Standard Practice for rehabilitation of existing Pipelines and Conduits by the Inversion and Curing of a Resin-Impregnated Tube." *ASTM Designation F1216-93*. Philadelphia, PA.

Bates, D. M. and Donald G.W. (1988). *Nonlinear Regression Analysis and Its Applications*. John Wiley & Sons.

Bakeer, R.M., and Barber, M.E. (1996). "Effect of Welding on a High Density Polyethylene Liner." *Journal of Materials in Civil Engineering*, ASCE, Vol. 8, No. 2, May, 94-99.

Reproduced with permission of the copyright owner. Further reproduction prohibited without permission.

Boot, J. C., and Welch, A. J. (1996). "Creep Buckling of Thin-walled Polymeric Pipe Linings Subject to External Groundwater Pressure." *Thin-Walled Structures*, Vol. 24, 191-210.

Boot, J. C., and Javadi, A. A. (1998). "The Structural Behavior of Cured-In-Place Pipe." *Bradford Reports and Revised PPX Paper*. University of Bradford, UK.

Boot, J.C. and Gumbel, J.E. (1998). "Discussion by Boot and Gumbel on Structural Analysis of Sewer Linings by B. Falter."

Boot, J.C. (1998). "Elastic buckling of cylindrical pipe linings with small imperfections subject to external pressure." *Trenchless Technology Research*, Vol. 12, 3-15.

Bryan, G. H. (1888). "Application of the Energy Test to the Collapse of a Long Pipe Under External Pressure." *Proceeding of the Cambridge Philosophical Society*, Vol. 6, 287-292.

Cohen, A. and Arends, C. B. (1988). "Application of a Concept of Distributed Damage to Creep Induced Buckling of High Density Polyethylene Specimens." *Polymer Engineering and Science*, Vol. 28, No. 15, 1066-1070.

Cohen, A. and Arends, C. B. (1988). "Creep Induced Buckling of Plastic Materials." *Polymer Engineering and Science*, Vol. 28, No. 8, 506-509.

Chicurel, R. (1968). "Shrink Buckling of Thin Circular Rings." *Journal of Applied Mechanics,* ASME, Vol. 35, No. 3, 608-610.

Cheney, J. A. (1968). "Pressure Buckling of Ring Encased in a Cavity." *Journal of Applied Mechanics*, ASME, 608-610.

El-Sawy, K., and Moore, I. D. (1997). "Parametric Study for Buckling of Liners: Effect of Liner Geometry and Imperfections." *Proceeding of 1997 ASCE Conference on Trenchless Pipeline Projects*. Boston, MA.

Fairbairn, W. (1858). "On the Resistance of Tubes to Collapse." *Phil. Trans. Royal Soc.*, London, UK.

Falter, B. (1996). "Structural Analysis of Sewer Linings." *Trenchless Technology. Res.*, Vol. 11, No. 2, 27-41.

Findley, W. (1987). "26-Year Creep and Recovery of Poly(Vinyl Chloride) and Polyethylene." *Polymer Engineering and Science, April,* Vol. 27, No. 8, 582-585.

Reproduced with permission of the copyright owner. Further reproduction prohibited without permission.

Glock, D. (1977). "Critical Behavior of Liners of Rigid Pipeline Under External Water Pressure and Thermal Expansion." *Der Stahlbau*, Vol. 7, 212-217.

Guice, L. K., Straughan, W. T., Norris, C. R., and Bennett, R. D. (1994). "Long-Term Structural Behavior of Pipeline Rehabilitation Systems." *Technical Report No. 302*. Trenchless Technology Center, Louisiana Tech University.

Guice, Leslie K. and Li, J. Y. (1994). "Buckling Models and Influencing Factors for Pipe Rehabilitation Design." *North American No-Dig'94*, Dallas, Texas.

Guice, L.R. (1995). "Guideline for Trenchless Technology: Cured-in Pipe (CIPP), Fold and Formed Pipe (FFP) Mini-Horizontal Directional Drilling (mini-HDD) Microtunneling." *TTC Technical report # 400.*

Gumbel, J. E. (1983). "Analysis and Design of Buried Flexible Pipes." Submitted to the Survey for the Degree of Doctor of Philosophy in the Department of Civil Engineering.

Gumbel, J. E. (1997). "Structural Design of Pipe Linings–Review of Principles, Practice and Current Developments Worldwide." *Proceeding of the International No-Dig'97.*,Taipei.

Hayter, A. J. *Probability and Statistics for Engineers and Scientists*. PWS Publishing Company.

Hsu, P.T., Elkon, J. and Pian, T.H.H. (1964). "Note on the instability of circular Rings Confined to a rigid Boundary." Journal of Applied Mechanics, Vol. 31,. No. 3, Trans. ASME, Series E, 559-562.

Hucks, R. T., Jr. (1972). "Design of PVC Water-Distribution Pipe." Civil Engineering ASCE, Vol. 42, No. 6.

Graybill, F. A. and Hariharan K. Iyer, (1975). *Regression Analysis: Concepts and Applications*. An Alexander Kugushev Book.

Insituform, (1991). "Insituform Engineering Design Guide." Insituform of North America, Inc., Memphis, Tennessee.

Jaeger, J.C. and Cook, N.C. W. (1976). "Foundationals of Rock Mechanics." New York: John Wiley.

Kleweno, Doug. "Long Term Performance Comparison of Pipe Lining Systems using Traditional Methodologies." InLiner U.S.A., Inc.

Reproduced with permission of the copyright owner. Further reproduction prohibited without permission.

Kleweno, Doug. (1998). "Analysis of Thermosetting and Thermoplastic Materials Used for CIPP and Fold-and-Form Pipe Liners." *Proceedings of International No-DIG'98.*, 333-342.

Kramer, S. R., McDonald, W.J., and Thomson, J.G. (1992). *An Introduction to Trenchless Technology.* Van Nostrand Reinhold, N.Y.

Levy, M. (1884). "Memoir on a new integrable case of the problem of elasticity and one of its applications." *J. Math Pure et Appl.*, Series 3, Vol. 10, 5-42.

Linhart, H., and Zucchini, W. (1986). *Model Selection.* John Wiley &Sons.

Li, J. Y., and Guice, L. K. (1995). "Buckling of Encased Elliptic Thin Rings." *Journal of Engineering Mechanics*, ASCE, Vol. 121, No. 12, 1325-1329.

Li, J. Y. (1994). "Design Criterion Analysis for Cured-In-Place Pipe." *MS Thesis.* Department of Civil Engineering, Louisiana Tech University, Ruston, LA.

Lin, H. (1995). "Creep Characterization of CIPP Material Under Tension, Compression, and Bending." *MS Thesis.* Department of Civil Engineering, Louisiana Tech University, Ruston, LA.

Lo, K. H., and Zhang, J. Q. (1994). "Collapse Resistance Modeling of Encased Pipes." *Buried Plastic Pipe Technology*: Vol. 2, ASTM STP1222, Dave Eckstein, Ed. ASTM, Philadelphia.

Lo. Hsu, (1962). "A Buckling Problem of a Circular Ring." *Proceeding of 4th U.S. national Congress of Applied Mechanics*, ASME, 691-695.

McAlphine, G. A. (1996). "Statistical Analysis and Implications or Test Data from 'Long-Term Structural Behavior of Pipeline Rehabilitation Systems'." *Proceedings of the Water Environment Federation 69th Annual conf. & Expo.*, Dallas, TX.

Mengers, G. and Gaube, E. (1969) "Failure by Buckling." *Modern Plastics*, Vol. 9, No.7, 96-110.

Moore, I.D. (1998). "Tests for Pipe Liner Stability: What We Can And Cannot Learn." *North American NO-Dig'98* , Albuquerquie.

Moore, I. D., and El-Sway, K. (1996). "Buckling Strength of Polymer Liners Used in Sewer Rehabilitation." *Transportation Research Record 1541*, 127-132.

Norton, F.H. (1929). *Creep of Steel at High Temperature*, New York: McGraw-Hill.

Reproduced with permission of the copyright owner. Further reproduction prohibited without permission.

Omara, A. M. (1996). "Analysis of Cure-In-Place-Pipe Installed in Circular and Oval Deteriorated Host Pipes." *DE Dissertation.* Department of Civil Engineering, Louisiana Tech University, Ruston, LA.

Osborn, L. E. (1993). *CIPP Design Theory.* Insituform Technologies, Memphis, TN.

Ostle, B. and Linda c. Malone, (1987). *Statistics in Research : Basic concepts and Techniques for Research Workers.* Iowa State University Press.

Pao, Y. and Martin, J. (1952). "Deflection and Stressed in Beams Subjected to Bending and Creep." Acta. Tech. Acadamic Scientiarum hungariae.

Pian. T.H.H. and Bucciarelli, l. L., Jr. (1965). "Symmetric Deformation of a Radially constrained Thin Circular Ring under Inertia Loading." AFOSR 65-1619, ASRL TR 127-1, Air force Research Grant No. AFOSR-347-64.

Seber, G. A. F., and Wild C. J. (1988). *Nonlinear Regression,* John Wiley & Sons Inc.

Sigmaplot, (1997). *User's Manual.* SPSS Inc.

Slocum, S.E. (1909). "The Cooapse of Tubes Under External Pressure." *Engineering, Jan.8,* 35-37.

Soong, T. C., and Choi, I. (1985). "Buckling of an Elastic Elliptical Ring Inside a Rigid Boundary." *Journal of Applied Mechanics,* Vol. 52, No. 3, 523-528.

Straughan, W.T., Tantirungrojchai, N., Guice, L. K. and Lin, Y. (1998). " Creep Test of Cured-In-Place Pipe Material Under Tension, Compression, and Bending." *Journal of Testing and Evaluation,* Vol. 26, No. 6, 594-601.

Timoshenko, S. P., and Gere, J. M. (1961). *Theory of Elastic Stability, 2nd ed.,* New York: McGraw-Hill

TTC (1998). *Preliminary Short-Term Buckling Results.* The Trenchless Technology Center, Louisiana Tech University, Ruston, LA.

TTC (1998) *Internal test data on long-term buckling tests.* The Trenchless Technology Center, Louisiana Tech University, Ruston, LA.

Th pot (2001) "The Structural Design of Non-Circular Linings." *Underground Infrastructure research: Municipal, Industrial and environmental Applications.* Swets&Zeitlinger, Lisse, 65-74.

Watkins, Reynold K. (1989). "Structural Performance of Nupipe." Report to Insituform of North America Inc., Memphis, Tennessee.

Reproduced with permission of the copyright owner. Further reproduction prohibited without permission.

Welch, A. J. (1989). "Creep Buckling of Infinitely Long Constrained Cylinders under Hydrostatic Loading." Submitted for the degree of Doctor of Philosophy, Postgraduate School of Studies in Civil Engineering, University of Bradford.

Yamamoto, Y. & Matsubara, N. (1981). "Buckling Strength of Steel Cylindrical Liners for Waterway Tunnels." *Theoretical and Applied Mechanics*, Vol. 30, 225-235, University of Tokyo Press, Japan.

Yi, H. (1996). "Finite Element Analysis for Cured-In-Place-Pipe." *MS Thesis.* Department of Civil Engineering, Louisiana Tech University, Ruston, LA.

Zagustin, E.Q, and Herrmann, G. (1967). "Stability of an Elastic Ring in a Rigid Cavity." *Journal of Applied Mechanics*, Vol. 34, No. 2, Trans., ASME, Series E. Vol. 89, 263-270.

Zhao, J. (1998). "Finite Element Analysis of Creep Buckling for Cured-In-Place Pipe." *MS Thesis.* Department of Civil Engineering, Louisiana Tech University.

Zhao, Q. (1999). "Finite Element Simulation of Creep Buckling of CIPP Liners Under External Pressure." *Ph.D. Dissertation.* Department of Computation Analysis and Modeling, Louisiana Tech University.

Zhao, Q., Hall, D.E. and Nassar, R.F. "Deflection Evolution of Thin Walled Pipe Liners Under External Pressure." Louisiana Tech University.

Zhu, M. (2000). "Computational Investigation of Stress, contact Conditions, and Buckling of Thin-walled Pipe Liners." *Ph.D. Dissertation.* Department of Civil Engineering, Louisiana Tech University.

Zhu, M., and Hall, D.E. (2001) "Creep Induced Contact and Stress Evolution in Thin-walled pipe Liners." *Thin-walled Structures*, Vol. 39, 939-959.

Reproduced with permission of the copyright owner. Further reproduction prohibited without permission.